THEORETICAL STUDIES OF

THREE-BODY ION-ION RECOMBINATION

AND

ION-ATOM ASSOCIATION

A THESIS

Presented to

The Faculty of the Division of Graduate

Studies and Research

By

Ting-Pin Yang

In Partial Fulfillment

of the Requirements for the degree

Doctor of Philosophy

in the School of Physics

Georgia Institute of Technology

December, 1978

THEORETICAL STUDIES OF

THREE-BODY ION-ION RECOMBINATION

AND

ION-ATOM ASSOCIATION

Approved:

M. R. Flannery, Chairman

E. W. McDaniel

T. F. Moran

Date Approved by Chairman: 9/29/1978

ACKNOWLEDGEMENTS

I would like to express my deep appreciation to my adviser, Dr. M. R. Flannery, for providing me the environment to finish my graduate study. Without his continuing interest, assistance and guidance the present investigation would be impossible.

It is also a pleasure to thank Dr. E. W. McDaniel, Dr. I. R. Gatland, Dr. T. F. Moran and Dr. K. J. McCann for serving the reading committe.

The friendship, enthusiatic help and strong moral support from Dr. H. Tai is also acknowledged.

In addition, I thank the Graduate Division for waiving certain format requirements so that this dissertation could be produced by means of the CYBER 70 system.

Finally, and most importantly, for the care , understanding, encouragement and help she provided throughout my graduate career, I reserve my deepest appreciation for my fellow physicist wife, Jo-Lien.

TABLE OF CONTENTS

Table of Contents (continued)

LIST OF TABLES

LIST OF ILLUSTRATIONS

SUMMARY

A theoretical description of the three-body ion-ion recombination process, $X^+ + Y^- + X \dashrightarrow (XY)^* + X$, is developed and various approximations such as the 'Bottleneck Model' to the full treatment are proposed. The formalism is then applied to the reaction $Rg^+ + F^- + Rg \dashrightarrow RgF^* + Rg$ (where Rg= rare gas, such as He, Ne, Ar, Kr and Xe) which is a basic mechanism in the kinetics of the rare gas-halide lasers feasible for laser fusion. The rate coefficient is also determined as a function of the neutral gas density and temperature.

In addition, the ion-atom association process $X^+ + 2X \dashrightarrow X_2^+ + X$, in which atomic ions are converted to molecular ions in a dense plasma, is also investigated for rare gas systems.

CHAPTER I

INTRODUCTION

Remarkable progress has occurred during the past few years in the research and development of electronically-excited molecular lasers (excimer lasers) with high efficiency and high power (J. Ewing, 1978; C. Werner and E. George, 1976; D. Lorents, 1976, 1977), especially for the rare-gas halide systems (EW, 1978). An excimer is an aggregate, composed of two atoms or molecules, that is repulsive or slightly bound in the ground state and bound in the excited states. The excited states of the excimer can radiate in a broad band which can easily be observed when rare gases or mercury at high pressure are electrically excited. The radiation is from the diatomic molecular excimer which is favorably formed under high pressure which enhances the recombination of

the neutral atoms. With higher pressure the rare-gas halide laser will instead have a narrow band with an order of magnitude higher stimulated emission coefficient than that of rare gas molecules or rare-gas halide at low pressure. The excimer emissions are useful as lasers because the lower levels dissociate rapidly (about 10^{-12} sec compared with the radiative life time 10^{-9} to 10^{-6} sec of the upper molecular level) implying that the population inversion can be readily achieved and maintained. The rare-gas halide laser produces an ultra-violet radiation band with high efficiency and tunability. They are apparently capable of being scaled to high averaged power. They are therefore expected to be very useful in applications as laser isotope separation, laser fusion and selected photochemical processes.

The physical conditions depend strongly on the class of laser under consideration. In the case of the bound-bound transitions of the form

$$(XY)^* \longrightarrow (XY) + h\nu \qquad (1\text{-}1)$$

pumping is generally direct from the ground state of the parent molecule, and may be carried out at low pressure by conventional electric discharges, e-beams etc.

In contrast, most bound-free systems (like most of the rare-gas halide lasers) represented by the general reaction

$$(XY)^* \longrightarrow X + Y + h\nu \qquad (1\text{-}2)$$

can not be operated at low pressures, since the excited state $(XY)^*$ must be generated in situ from its atomic constituents. Because of the chemical inertness of the noble gas, systems involving them generally have only repulsive or very weakly bound ground states. This precludes the possibility of direct channel pumping from a stable ground state. In order to generate the desired excited molecular state, three-body reactions of the form

$$X^+ + Y^- + Z \longrightarrow (XY)^* + Z \qquad (1\text{-}3)$$

must be employed. Here the third body is required to drain away as translational motion excess energy of recombination, i.e., the difference between the free and bound relative energy of the ion-pair $(X^+\text{-}Y^-)$. In practice, this third body is often identical to or lighter than one of the participating atoms (i.e., in the former case Z=X or even Z=X=Y). To achieve sufficiently high densities of the excited molecules so that the three-body reaction rate overcomes the radiation loss rate, these system must be operated at high pressures, where the molecular formation becomes rapid. As an example, the

kinetic sequence in the production of KrF* excited states is

$$e(fast) + Kr \longrightarrow Kr^+ + e(slow) + e \qquad (1\text{-}4a)$$

$$e(slow) + F_2 \longrightarrow F^- + F \qquad (1\text{-}4b)$$

$$F^- + Kr^+ + M \longrightarrow (KrF)^* + M \qquad (1\text{-}4c)$$

$$KrF^* \longrightarrow Kr + F + h\nu \qquad (1\text{-}4d)$$

where M is any third body, typically a lighter rare-gas buffer. Process (1-4c) is a three-body ion-ion recombination, a subject with long history, important not only in excimer laser pumping but also of fundamental importance. Recently it has been quite extensively reviewed by Flannery (FM1, 1972; FM2, 1976).

In the rare-gas molecular excimer laser, another important process is the three-body ion-atom association

$$X_2^+ + 2X \longrightarrow X_2^+ + X \qquad (1\text{-}5a)$$

which converts atomic ions into molecular ions which in turn undergo the following sequence of reactions:

dissociative recombination

$$X_2^+ + e \longrightarrow X^{**} + X \qquad (1\text{-}5b)$$

three-body recombination

$$X^{**} + 2X \longrightarrow X_2^{**} + X \qquad (1\text{-}5c)$$

$$X_2^{**} + (X) \longrightarrow X_2^{*} + X + (X) \qquad (1\text{-}5d)$$

$$X^{*} + 2X \longrightarrow X_2^{*} + X \qquad (1\text{-}5e)$$

$$X_2^{*} \longrightarrow 2X + h\nu \qquad (1\text{-}5f)$$

Process (1-5a) is in itself an important basic reaction, and theoretically is an even more difficult problem than (1.4c) because of the short-range forces involved as will be discussed in CHAPTER VII.

Thus in this study we will concentrate on the collisional aspects of the two important three-body reactions (1-4c) and (1-5a), all involving ions only.

We shall devote CHAPTER II through CHAPTER V to the discussion of three-body ion-ion recombination. Beginning with a brief review of the Thomson treatment (low gas density), the Langevin treatment (high density), we shall present a detailed account of the accurate low-density Quasi-Equilibrium Statistical Distribution Treatment (QEST) and its application to the rare gas systems. An approximation, the Bottleneck Model (BTL) is also presented. CHAPTER VI will include the discussion and application to the rare-gas halide systems of the revised Natanson's model treatment to cover the full range of gas densities.

To conclude this study we shall discuss the three-body ion-atom association problem in CHAPTER VII. We follow the approaches presented in the recombination part, apply the QEST and the Bottleneck Model to the problem. Results are discussed and comparisons are made for different approximations and for the two processes.

CHAPTER II

THREE-BODY ION-ION RECOMBINATION

-EARLY TREATMENTS

2.1 Introduction

Ionic recombination is a general term used to denote various processes that contribute to the overall neutralization in a plasma containing positive ions X^+ and negative ions Y^- in a background neutral gas Z. The rate of the ion loss depends naturally on the capability of each ion-pair to dispose of sufficient internal energy so that mutual neutralization proceeds. The mechanisms, at least at low density, causing this energy reduction are

the following

(i) radiative recombination :

$$X^+ + Y^- \longrightarrow XY + h\nu \qquad (2\text{-}1)$$

with emission of a photon of frequency ν, or

(ii) mutual neutralization :

$$X^+ + Y^- \longrightarrow X^* + Y^* + \Delta E \qquad (2\text{-}2)$$

where the asterisk (*) denotes possible excited states of the neutralized products, ΔE the final relative K.E. of the end products, or

(iii) three-body recombination

$$X^+ + Y^- + Z \longrightarrow [XY]^* + Z \qquad (2\text{-}3)$$

where the internal energy has been transfered to the third body Z and the bracket denotes that the molecule XY may not be bound.

The probability of recombination is conveniently described by the recombination coefficient α (in units of cm^3/sec) defined in terms of the rate of the ions loss by the relationship

$$R = dN_1/dt = dN_2/dt = -\alpha N_1 N_2 \qquad (2\text{-}4)$$

where N_1, N_2 denote the concentration(in unit of cm^{-3}) of positive and negative ions respectively at time t such that $\alpha N_1 N_2$ is the number of recombination events that occurs per unit volume per second. α depends, in general, on the temperature θ and the third body number density N_3 .

Two body processes like radiative recombination and mutual neutralization are important only in the limit of vanishing gas pressure. As the pressure increases to tens of torr , three-body process (2-3) becomes dominant, where a series of individual collisions (not just a single collision!) of the ion-pair with the neutral drains away the excess energy of recombination. At sufficiently high pressure the collisions become so frequent that the ionic approach is limited by the speed of random diffusion and by the speed of the attractive drift of the ions in an increasingly dense medium. The recombination rate can then be explained in terms of macroscopic quantities such as ionic mobilities and diffusion coefficients. A unified description of recombination to couple the individual microscopic collisional events ((2-1) to (2-3)) in the low density region with the macroscopic phenomena in the high density region is very difficult and still unsettled, though recently some progress has been made in the middle pressure regime (Bates and Mendas, 1978). Still one could

understand the behavior of the ionized gas by the physics of each mechanism individually.

Since the three microscopic mechanisms have been exhaustively reviewed (FM1, FM2) and we are mainly interested in the application to the excimer laser we will confine our study in this part to the three-body recombination.

First consider some historical aspects. At room temperature, as the gas pressure of neutral gas density N_3 increases, the recombination rate α initially increases linearly as N_3 from the two body, zero pressure limits ($\approx 10^{-7}$ cm^3/sec) to a maximum of 2×10^{-6} cm^3/sec, decreases and approaches a variation of N_3^{-1}. While the linear increase of α in N_3 at low pressure region was first theoretically established in Thomson's work of three-body recombination (Thomson, 1924), the N_3^{-1} dependence was predicted even earlier by Langevin (LA, 1903).

2.2 Thomson's Treatment: low density region

In this treatment and in all modifications of it, a trapping radius r_T is assumed. According to Thomson, recombination proceeds when a single collision with the neutral gas atom reduces the internal energy of the ion-pair to such an extent that its total internal energy becomes negative so that it is no longer separable into ionic constituents. Eventual electron transfer between the ions within the closed orbit just formed completes the recombination. The radius r_T can be found by equating the gain of K.E. to e^2/r at r_T, because of Coulombic attraction, to its initial thermal energy $3k\theta/2$ at temperature θ :

$$r_T = 2e^2/3k\theta \qquad (2\text{-}5)$$

where k is the Boltzmann constant. For collisions occurring at $r < r_T$, the ions will recombine. Assuming equal mass of the species, the reduced recombination coefficient is thus

$$\alpha_T = \pi r_T^2 \bar{V} P(r_T, N_3) \qquad (2\text{-}6)$$

where $\bar{V}$ is the mean relative speed of the ion-pair, $P(r_T, N_3)$ the density-dependent probability of a collision between the ion-pair and a neutral within ion-ion separation r . Probability $P(r_T, N_3)$ is expressed in terms

of $W^{\pm}$, the probability of a single positive (negative) ion colliding with a neutral, as

$$P(r_T,N_3)=W^{+}+W^{-}-W^{+}W^{-} \tag{2-7}$$

where for a straight line trajectory (Loeb, 1955)

$$W^{\pm}= 1- \frac{1}{2}\left(\frac{\lambda_{\pm}}{r_T}\right)^2 \left(1-(1+2r_T/\lambda_{\pm})\exp(-2r_T/\lambda_{\pm})\right). \tag{2-8}$$

In (2-7), the presence of the third term is due to double counting of the simultaneous collision of both ions with the neutral in the sum $W^{+}+W^{-}$. In the low and high density limits, we have

$$P(r_T,N_3)\rightarrow\begin{cases} \frac{4}{3}\left(\frac{1}{\lambda_{+}}+\frac{1}{\lambda_{-}}\right)r_T & \text{low } N_3 \\ 1 & \text{high } N_3 \end{cases} \tag{2-9}$$

Note that the mean free paths $\lambda_{\pm}$ of the ion are conveniently expressed in terms of the diffusion cross section Q_D

$$\lambda_{\pm}=1/N_3Q_D \tag{2-10}$$

Thomson's expression (2-6) coupled with the first of (2-9) gives a correct linear dependence in N_3 of α in the low density region (r_T,V independent of N_3). But at high density it gives saturation behavior, in contrast to the

experimental fact that the relative approach speed of the ions are then limited by random diffusion and attractive drift so α should decrease with increasing N_3 (in fact $\sim N_3^{-1}$). As previously discussed (FM1) there are some other obvious inadequcies in this model (i) recombination can well take place even at $r > r_T$, (ii) simultaneous multiple collisions with two or more bodies may not be neglected, (iii) masses of the species are not necessarily equal and (iv) bound-bound transition can not be neglected.

As pointed out earlier (FM1, FM2; Bates and Moffett, 1966) much effort, though ineffective, was put into refining the model to cover several deficiencies, including those mentioned above, while retaining the trapping radius concept in which r_T has to be carefully determined. In fact before one can realistically assign r_T, the detailed history of the ions must first be established. This consideration led to the Quasi-Equilibrium Distribution of the bound ion-pair Treatment of Bates and Moffett (1966) for ions in parent gases and that of Bates and Flannery (1968) for general third body case. Before a more detailed account of this treatment is presented in CHAPTER III and CHAPTER IV we will look at the situation in the high density region.

2.3 Langevin's Theory: high density limit

The earliest study of ionic recombination was done in 1903, from the point of view of attractive drift of ions, by Langevin. He assumed that the positive and negative ions, separated by a distance r, drift toward each other in a medium of neutral gas 3 by the Coulomb attraction with field intensity $\xi = e/r^2$.

The attractive drift is essentially achieved by a balance of the energy gained by each ion-pair from the mutual Coulomb field, with the energy loss by the numerous collisions with many gaseous particles present at high densities. The speed of the relative drift V_A is then determined by the mobilities of the ions K_{i3} (i=1,2) of each ion in the electrostatic field ξ ,

$$V_A = (K_{13}+K_{23})\,\xi = K(e/r^2)\,. \qquad (2\text{-}11)$$

Under the assumption that recombination is assured when ions have radially drifted to within r_x of each other, the recombination rate coefficient is therefore

$$\alpha_L = 4\pi r_x^2\, V_A(r_x) = 4\pi\, e\, K \qquad (2\text{-}12)$$

with the aid of (2-11). Note this α_L is independent of r_x unless K depends on it. With the zero-field mobility, which is proportional to N_3^{-1} (and independent of r_x), α_L

in (2-12) gives the correct variation of N_3 at high density. The studies initiated by Bates and Massey (1943) suggest the range of r_x from 10Å to 50Å, a range in which many pseudo-crossing of the molecular potential energy curves are provided to ensure mutual neutralization for free ion-pairs and electron tranfer for bound ion-pairs.

As is discussed in McDaniel's book (1964, Chap 9) the mobility K and diffusion coefficient D are independent of ξ/N_3 only when the electrostatic field energy is negligible compared with the thermal energy, i.e., when

$$(M/m_{\pm}+m_{\pm}/M)\, e\, \xi \lambda_{\pm} << k\theta \simeq P/N_3 , \qquad (2\text{-}13)$$

where N_3 is the number density and M the mass of the neutral gas, $m_{\pm}$ the mass of either ion and $\lambda_{\pm}$ the ionic mean free paths. The expression $e\,\xi\lambda_{\pm}$ is then the energy gained by an ion in moving a mean free path $\lambda_{\pm}$ along the field through the gas at pressure P. Putting in the mean free path for the ion-neutral collision $\lambda_{\pm} = (N_3 Q_D)^{-1}$ with typical cross section $Q_D \approx 5\times10^{-15}$ cm^2, (2-13) becomes,

$$\xi/P(\text{atm}) << 5.3 \qquad (2\text{-}14)$$

for equal masses of ions and neutral gas, ξ is in c.g.s. units. This criterion depends on P as well as the ion-ion separation r_x. For r_x at 10Å, 50Å and 500Å, the criterion is satisfied for P much greater than 10^4 atm, 400 atm and

4 atm respectively. Thus with $r_x = 50\text{Å}$, the validity range of α_L is at pressures of $10^2 \sim 10^3$ atm. Yet the experimental results show that α_L of (2-12), holds true not only in 5-25 atm (Mächler, 1936) but also in 2-5 atm (LA, 1903), a region much lower than required.

In deriving α_L of (2-12) Langevin completely ignored diffusion which is important when the ion-ion separation is large. As the neutral gas density N_3 is increasing, ion-neutral collisions with cross section Q_D become more frequent, and the ionic mean free path $\lambda_\pm$ decreases as $(N_3 Q_D)^{-1}$. The rate of approach of oppositly charged ions eventually become limited not only by the speed of attractive drift V_A at small separation but also by the speed of diffuson, or Brownian movement at large r. The mean speed of random diffusion of ions in the gas is, in terms of total diffusion coefficient D,

$$V_D \approx D/r \qquad (2\text{-}15)$$

The ratio of V_A to V_D, which gives a measure of the relative importance of each process is

$$V_A/V_D = Ke/Dr = e^2/rk\theta \qquad (2\text{-}16)$$

where the last equality follows from using Einstein relation

$$De = Kk\theta \qquad (2\text{-}17)$$

Thus the condition

$$r < e^2/k\theta = r_E \qquad (2\text{-}18)$$

implies that attractive drift processes are favored, while for $r > r_E$, diffusion is dominant.

Indeed both Harper (1932, 1935) and Jeffé (1940) did derive the rate coefficient including only diffusion. Here it was assumed that recombination occurred once the oppositely charged ions diffused by Brownian movement to within a separation r_x of each other. Thus the recombination rate coefficient is

$$\alpha_{HJ} = 4\pi r_x^2 V_D(r_x) \ . \qquad (2\text{-}19)$$

The detailed form of Harper's and Jeffé's results were different, a technical point we will not discuss here. With the aid of v_D in (2-15) and arbitrarily putting $r_x = r_E$, one has

$$\alpha_{HJ} = 4\pi r_x D = 4\pi De^2/k\theta \qquad (2\text{-}20)$$

which is identical to Langevin's expression α_L when the Einstein relation (2-17) is used. Though $r \approx 500\text{Å}$ at room temperature is too far from 50Å to ensure recombination, nonetheless it is the region favoring diffusion and ensuring validity of the Einstein relation at pressures as low as 4 atm.

Thus the physics is that when the ion separation is large, diffusion by random motion dominates the process. When the ions of opposite charge come closer to less than r_E the attractive drift process begins to catch up and come even closer to a point that r is so small to favor mutual neutralization or electron-transfer so that the recombination is stabilized. In fact Bates (1975) recently gave a unified treatment to combine the two distinct effects of electrostic attraction and diffusion by explicitly assuming a mutual neutralization sink at r_x. His expression of rate coefficient

$$\alpha_B = 4\pi \, Ke(1-\exp(-Ke/Dr_o)) \quad r \geq r_o, \qquad (2\text{-}21)$$

reduces to $4\pi r_o D$ when the diffusion controls the process, i.e., when $r_o >> Ke/D$ (where r_o is the radius of the absorbing sphere characterizing the electron-transfer). When r_o is associated with mutual neutralizations and electron-transfer that $r_x << r_E$ (also $r_o << r_E$) where the macroscopic diffusion is no longer important, and the Einstein relation applies $Ke/D = r_E$, thus

$$\exp(-r_E/r_o) \dashrightarrow 0$$

and α_B approaches the Langevin expression : $4\pi Ke$.

CHAPTER III

THREE-BODY RECOMBINATION : QUASI-EQUILIBRIUM STATISTICAL TREATMENT (QEST) AT LOW DENSITIES

3.1 General Picture

As the gas is introduced at low pressure (a few torr), the reduction of the internal energy E of the ion pairs in the recombination process

$$X^+ + Y^- + Z \longrightarrow [X^+ Y^-]^* + Z \qquad (3\text{-}1)$$

is accomplished through collisions with the neutral gas Z at ion-ion separation r much larger than r_x where potential curve-crossings favor mutual neutralization.

Thus the third body Z serves as an agent to degrade the internal energy of the ion-pairs at separation r where the neutralization probability is small though the Coulomb field is still strong. Neutralization is accomplished when the energy-degraded ions approach each other to within r_o where the irrevesible charge-transfer process

$$[X^+ + Y^-]^*_{r_o} \dashrightarrow X + Y \qquad (3\text{-}2)$$

stabilizes the recombination. The bracket above indicates inclusion of ion-pairs bound and excited states even transitory states, and those thermal energy free ion-pairs which eventually decay through mutual neutralization mentioned before. The sequence of events thus assures higher recombination coefficients α than those with mutual neutralization alone, even at modest gas pressure (100 torr).

A realistic description of (3-1) in terms of the recombination rate coefficient α needs two essential ingredients: (i) the basic collisional mechanisms in operation and (ii) the formulation of the subsequent course of deactiviation with time in terms of (i). Account of (i) is much simplified by noting that the relative energy of the ion-pair can be changed via an elastic collision between a given ion with the neutral as will be seen below. Since the ion-ion Coulombic

interaction is stronger and with longer range than the ion-atom interaction, the three-body collision can be viewed as two binary encounters taking place between the atom and either ion. Each binary encounter , (X^+Z) or (Y^-Z), changes the internal energy of the ion-pair. With these considerations in mind Bates and Flannery (BF2, 1968) formulated an expression for the encounter rate coefficient, for the case of the general third body,

$$K_{if}dE_f=K(E_i, E_f)dE_f \qquad (3\text{-}3)$$

describing the rate of (X^+-Z) and (Y^-Z) collisions which change the internal energy of the ion-pairs from E_i to between E_f and E_f+dE_f. The expression required the knowledge of the elastic scattering cross sections for (X^+-Z) and (Y^-Z) collisions in Langevin potential (hard core and a polarization tail).

In contrast to this, the particular case of like ions X^+ recombining in their parent gas X, (Z=X=Y in (3-1)) the energy change does not arise from direct collisions. Rather it arises from a symmetrical resonance charge-transfer collision (SRCT)

$$X^+ + X \longrightarrow X + X^+ \qquad (3\text{-}4)$$

which simply interchanges the velocity vector of the ion with the thermal velocity vector of the neutral. Bates

and Moffett (1966) were the first to realize the importance of the SRCT and derived the encounter rate coefficient (3-3) for this process assuming the charge-transfer cross section known.

In the case that Z=X (or =Y), i.e., the reaction

$$\underset{1}{X^+} + \underset{2}{Y^-} + \underset{3}{X} \longrightarrow (XY)^* + X \qquad (3\text{-}5)$$

one has to find K_{13} for (X^+X) with symmetric charge-transfer and K_{23} for (Y^-X) with direct collision. The sum of the two is the overall rate coefficient K_{if} which will be derived in CHAPTER IV and applied to the rare-gas halide system in CHAPTER V. Assuming K_{if} as known for the moment we will obtain the expression of α for the recombination rate coefficient.

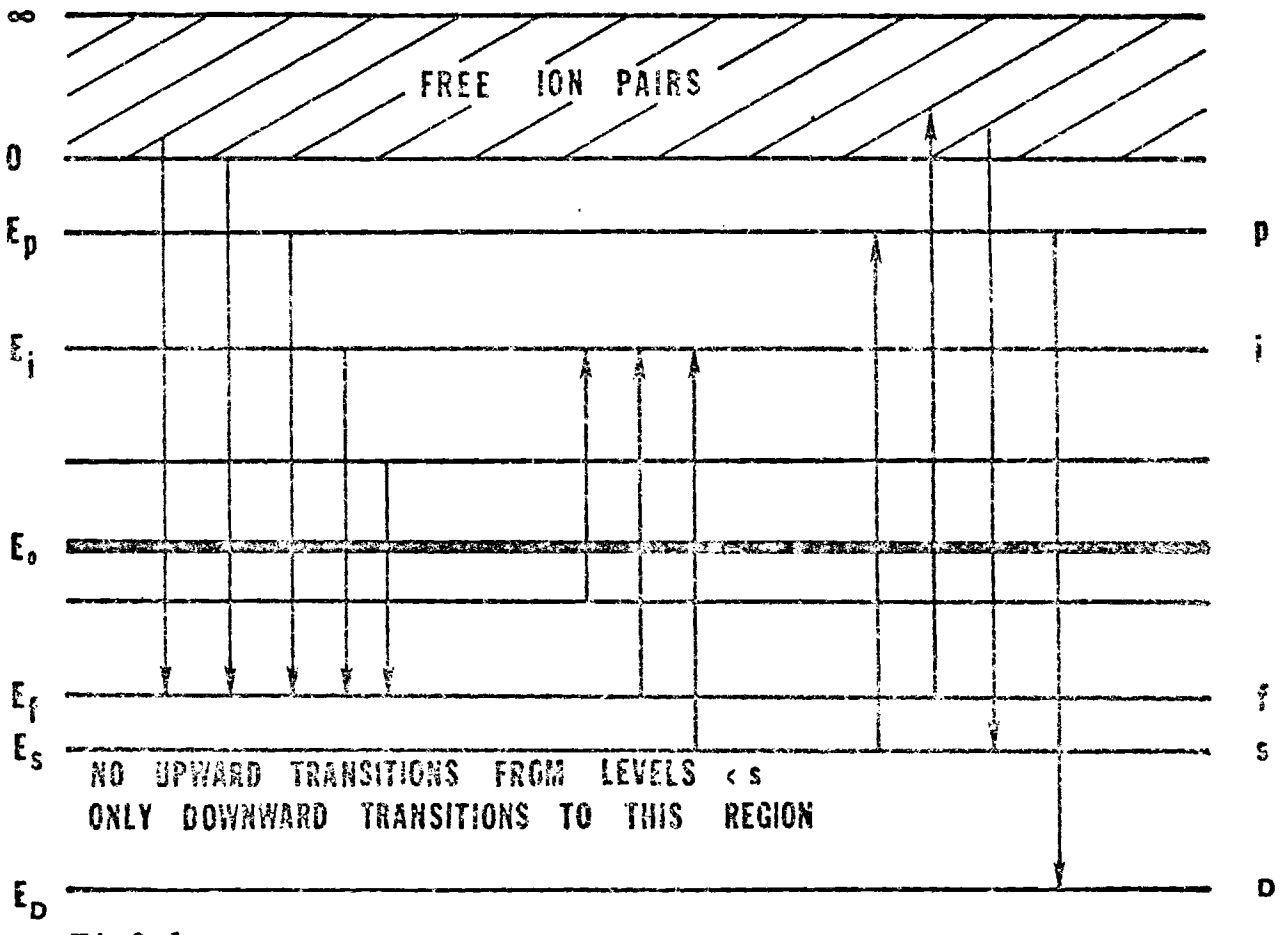

Fig3.1 Schematic energy-level diagram for ion-pairs illustrating representative transitions. $|E_D|$ is the greatest binding energy of an ion-pair, E_S is the energy lower than which charge-transfer stabilizes the recombination, and E_0 is some arbitrary negative energy level past which ion-pairs are flowing in energy-space. The remaining energy levels E are arbitrary.

3.2 Three-Body Recombination Coefficient

Let $N_1=N(X^+)$, $N_2=N(Y^-)$, $N_3=N(Z)$ be the number densities of the free positive and of negative ions, and neutral particles, respectively. The collisional rate coefficient is such that from the total number of ion-pairs $n(E_i)dE_i$ initially having energy in the interval $(E_i,\ E_i+dE_i)$, a number $n(E_i)dE_iN_3K(E_i,E_f)dE_f$ becomes formed by a single collision with the neutral gas in unit volume per second in the energy interval (E_f,E_f+dE_f). We shall normalize the number density $n(E_i)dE_i$ of ion-pairs with energy E_i when recombination is proceeding to the number densities $n_T(E_i)dE_i$ where there is a thermodynamic equilibrium between the bound and free ion-pairs by introducing the distribution function

$$\rho(E_1)=\begin{cases} n(E_i)/n_T(E_i) < 1 & E_s<E_i<0 \\ 1 & 0\leq E_i \\ 0 & E_i\leq E_s \end{cases} \qquad (3\text{-}6)$$

where E_s is the binding energy of the ion-pair at which recombination is stablized by the charge neutralization process (3-2). The probability of such ion loss by charge-transfer is an increasing function of the binding energy of the ion-pair. Its effect may be assessed by supposing that the rate of loss of the ion-pairs with B.E. greater

than E_s is so fast that collision involving them may be neglected. The presence of the sink is therefore acknowledged by assigning the value of zero to $\rho(E)$ in (3-6). For free ions, $E_i > 0$, ρ is of course unity.

The recombination rate $\alpha N_1 N_2$ is represented by the difference of the down-flow $R\downarrow$ of ion-pairs past some arbitrary bound level E_o, located between 0 and E_s, from the up-flow $R\uparrow$ past this level (see Fig 3.1)

$$N_1 N_2 = R\downarrow - R\uparrow$$

$$= N_3 \left[\int_{E_o}^{\infty} n_i dE_i \int_{E_D}^{E_o} K_{if} dE_f - \int_{E_D}^{E_o} dE_f n_f \int_{E_o}^{\infty} K_{fi} dE_i \right] \tag{3-7}$$

The greatest binding energy that an ion-pair can have (even transitory) is E_D ($\sim$5ev, normally).

In the absence of any recombination sink (3-2) the ion-pairs, via collision with the neutrals, attain thermodynamic equilibrium such that the downward and upward flows exactly balance, i.e.,

$$n_T(E_i) K(E_i, E_f) = n_T(E_f) K(E_f, E_i) \tag{3-8}$$

the principle of detailed balance between the forward and

reverse rates is satisfied. Using the normalized distribution (3-6) and interchanging the order of integration, (3-7) becomes

$$\alpha N_1 N_2 = N_3 \left[\int_{E_o}^{\infty} dE_i \int_{E_D}^{E_o} dE_f \; n_T(E_f)(\rho_i - \rho_f) K_{if} \right] \tag{3-9a}$$

or

$$\alpha = N_3 \left[\int_{E_o}^{\infty} dE_f \int_{E_D}^{E_o} dE_i \; \frac{n_T(E_i)}{N_1 N_2} (\rho_f - \rho_i) K_{if} \right] \tag{3-9b}$$

where the dummy indices i,f have been interchanged.

The number densities of ion-pairs with reduced masses m_{12} in thermodynamic equilibrium at temperature θ is given by the Maxwell-Boltzmann distribution. It is also expressed in terms of densities of free ions $N(X^+)$, $N(Y^-)$ determined by the Saha-Boltzmann equation (Fowler, 1936; Cooper, 1966) in the form

$$\frac{n_T(E_i)dE_i}{N_1 N_2} = \frac{g(E_i)dE_i}{(2\pi m_{12} k\theta)^{3/2}} \cdot e^{-E_i/k\theta} \tag{3-10}$$

where $g(E_i)dE_i$ is the statistical weight $n^2 dn$ of the discrete hydrogenic levels n with energy

$$E = -e^2/2a_o n^2 \tag{3-11a}$$

where

$$a_o = \hbar^2/e^2 m_{12} \tag{3-11b}$$

with $\hbar$ being the Planck constant divided by 2π .

Thus we have

$$g(E) = 16\pi^2 (2m_{12}^3)^{\frac{1}{2}} C(E_i) \tag{3-12a}$$

$$= (2\pi^6 m_{12}^3)^{\frac{1}{2}} e^6 / |E_i|^{5/2} \tag{3-12b}$$

from the result of Appendix I, and

$$\frac{n_T(E_i)dE_i}{N_1 N_2} = \frac{8\pi^{\frac{1}{2}} C(E_i) \exp(-E_i/k\theta)}{(k\theta)^{3/2}} dE_i \tag{3-13a}$$

$$= \frac{\theta^{3/2} e^6}{2(k\theta)^{3/2}} \frac{\exp(-E_i/k\theta)}{|E_i|^{5/2}} dE_i \tag{3-13b}$$

The recombination coefficient is now

$$\alpha = N_3 \int_{E_D}^{E_0} 8 \frac{\pi^{\frac{1}{2}} C(E_i) e^{-E_i/k\theta}}{(k\theta)^{3/2}} dE_i \int_{E_0}^{\infty} dE_f (\rho_f - \rho_i) K_{if} \tag{3-14a}$$

$$= N_3 \frac{\pi^{3/2} e^6}{2(k\theta)^{3/2}} \int_{E_D}^{E_o} dE_i \frac{e^{-E_i/k\theta}}{|E_i|^{3/2}} \int_{E_o}^{\infty} dE_f (\rho_f - \rho_i) K_{if} \tag{3-14b}$$

For the convenience of calculation, we can express above with the energy in unit of thermal energy $k\theta$. Define

$$E = -\lambda k\theta, \quad E = -\mu k\theta, \quad E = -\omega k\theta,$$

$$E_o = -\nu k\theta \ . \tag{3-15}$$

α in (3-14a,b) becomes, ρ as defined in (3-6) unchanged,

$$\alpha = N_3 \frac{8\pi^{\frac{1}{2}}}{(k\theta)^{\frac{1}{2}}} \int_{\nu}^{\omega} d\lambda e^{\lambda} C(E_i) \int_{-\infty}^{\nu} d\mu (\rho_\mu - \rho_\lambda) \kappa_{\lambda\mu} \qquad (3\text{-}16a)$$

$$= N_3 \frac{\pi^{3/2} e^6}{2(k\theta)^3} \int_{\nu}^{\omega} d\lambda \frac{e^{\lambda}}{\lambda^{5/2}} \int_{-\infty}^{\nu} d\mu (\rho_\mu - \rho_\lambda) \kappa_{\lambda\mu} \qquad (3\text{-}16b)$$

where

$$\kappa(\lambda, \mu) d\mu = K_{if} dE_f \qquad (3\text{-}17)$$

Thus for a determination of α, information on both the encounter rate $\kappa_{\lambda\mu}$ (or, K_{if}) and the distribution function ρ is required.

3.3 Quasi-Equilibrium Distribution ρ

When recombination is proceeding one does not have thermodynamic equilibrium because of the charge-transfer sink. The net number density of the ion-pairs with E_i is governed by the rate equation

$$\frac{\partial}{\partial t} n_i = N_3 \left(\int_{E_s}^{\infty} n_f K_{fi} dE_f - n_i \int_{E_D}^{\infty} K_{if} dE_f \right) \qquad (3\text{-}18)$$

i.e., the net rate of collisional formation and

destruction of ion-pairs with energy E_i. Explicit account has been taken of both the inability of those ion-pairs with $E < E_s$ to regain any energy $E > E_s$ i.e., those undergoing the irreversible process (3-2), and the possibility of that ion-pairs be degraded through direct collision. Again by the principle of detailed balance (3-7), the rate equation becomes

$$\frac{\partial}{\partial t}\rho_i = N_3 \int_{E_0}^{\infty} (\rho_f - \rho_i) K_{if} dE_f \qquad (3\text{-}19)$$

where ρ's are defined in (3-6) with boundary conditions,

$$\rho_i = \frac{n_i}{(n_i)_T} = \rho(\lambda) = \begin{cases} 1 & 0 \lesssim E_i \quad (\lambda < 0) \\ <1 & E_s < E_i < 0 \\ & (0 < \lambda < s) \\ 0 & E_i \lesssim E_s \quad (s < \lambda) \end{cases} \qquad (3\text{-}20)$$

Various physical approximatons can be made to simplify the solution of (3-19) depending on the situations encountered. In the quasi-equlibrium treatment one sets $\partial\rho/\partial t = 0$ in (3-19) such that the quasi-equilibrium distribution $\rho(E)$ satisfies the integral equation

$$\rho_i \int_{E_D}^{\infty} k_{if} dE_f = \int_{E_s}^{\infty} \rho_f K_{if} dE_f \qquad (3\text{-}21)$$

subject to boundary condition (3-20).

Note that in the absence of a charge-transfer sink, i.e., when $E_S = E_D$, $\rho = 1$ is an obvious solution corresponding to thermodynamic equilibrium. The rate of collisional excitation or de-excitation from level n to level f increases rapidly for increasing n and decreasing (n-f) as can be seen in typical figures of K_{if} (see, e.g., figures in CHAPTER 5). The relaxation time for a disturbance to ions at level n to decay is

$$\tau_n = \left[N_3 \int_{E_D}^{\infty} K_{nf} dE_f \right]^{-1}$$

which is extremely short for high n compared with that for lower levels. The highly excited state populations therefore adjust to any disturbance, e.g., that caused by charge-transfer, relatively rapidly compared with some characteristic time taken, say for recombination. Hence the rate of change of the total number density of ion-pairs with small binding important to recombination (say for $\lambda=(0,20)$) is small compared to the change of ion densities and densities of ion-pairs at low lying states. As the recombination proceeds, a quasi-equilibrium of excited states is established almost immedialely. While the rates of formation and depletion of these states are indeed very rapid, the residual population changes only slowly compared to the rate at which ions are recombining. Thus one is justified in setting $\partial\rho/\partial t = 0$ in (3-19) to obtain (3-21) for ρ. The integral equation (3-21) was

solved numerically for the case of ion-recombination in parent gas by Bates and Moffett (1966), and for the general case of ion-recombination by Bates and Flannery (1968). The procedure is to reduce the equation by quadrature (specifically, Simpson's Quadrature) to a set of linear equations and solve $\rho(E)$ by matrix inversion subject to B.C. (3-20). We will adopt this method in the following calculation by using the total encounter rate coefficient, i.e., the sum of the symmetric resonance charge-exchange rate coefficient and the direct elastic collisional rate coefficient in equation (3-21).

CHAPTER IV

THE CHANGE-IN-ENERGY RATE COEFFICIENT K_{if}

As mentioned earlier we are concerned about the 3-body reactions

$$X_1^+ + Y_2^- + X_3 \dashrightarrow (XY)^* + X_3 \quad . \qquad (3\text{-}5)$$

The total rate coefficient K_{if} is the sum of $K_{13}(E_i, E_f)$ for the symmetric charge-exchange and $K_{23}(E_i, E_f)$ for the direct collision

$$K_{if} = K(E_i, E_f) = K_{13}(E_i, E_f) + K_{23}(E_i, E_f) \quad . \qquad (4\text{-}1)$$

In the following we will use K_{13}, K_{23} with their implicit dependence on E_i, E_f (or λ, μ) assumed. The sum comes from the assumption of two binary encounters in the reaction, valid since the strong Coulomb interaction between the

ions is long-range compared to that between each ion and the neutral atom.

While K_{13} is simpler than K_{23} to obtain, it nevertheless can be deduced from K_{23} with some proper considerations so we will consider K_{23} first.

4.1 K_{23}: Case of a General Third Body

We will follow Bates and Flannery (1968) to develop the energy-change coefficients of collision between the ion-pairs and a neutral particle in a general fashion.

Consider

$$\underset{1}{X^+}+\underset{2}{Y^-}+\underset{3}{Z} \longrightarrow (XY)^*+Z \qquad (3\text{-}1)$$

(Z will be put equal to X later). We shall label the positive and the negative ions 1 and 2 respectively and the neutral atom 3, and affix these number as subscripts to the symbols of various physical quantities. For impacts at thermal energies one can first assume that the negative ion of mass m_2 and velocity $\vec{v}_2$ in an orbit about the positive ion of mass m_1 and velocity $\vec{v}_1$, collides elastically with the neutral of mass m_3 and velocity $\vec{v}_3$

such that the effect is to cause an increase (excitation or disruption), a decrease (deactivation to an orbit more tightly bound) or no change at all (elastic process) in the internal energy of the (1,2) ion-pairs.

The second assumption is the Impulse Approximaton, i.e., for each binary encounter of the ion (positive ion in the case of K_{13}) with the neutral is so brief that it does not change the ion-ion separation (hence the Coulombic potential) or the velocity vector of the other ion in the pair. As shown by Flannery (FM1, section 5) this is certainly true since the collisional time is much less than the typical orbital time for the general Langevin potential to be used:

$$V_{i3} = \begin{cases} -pe^2/2r^4 & r > S_{i3} \\ \infty & S_{i3} \geq r \end{cases} \qquad i=1,2 \qquad (4\text{-}2)$$

where r is the distance between the ion and the neutral, p the polarizability of the neutral atom and S is the hard core parameter.

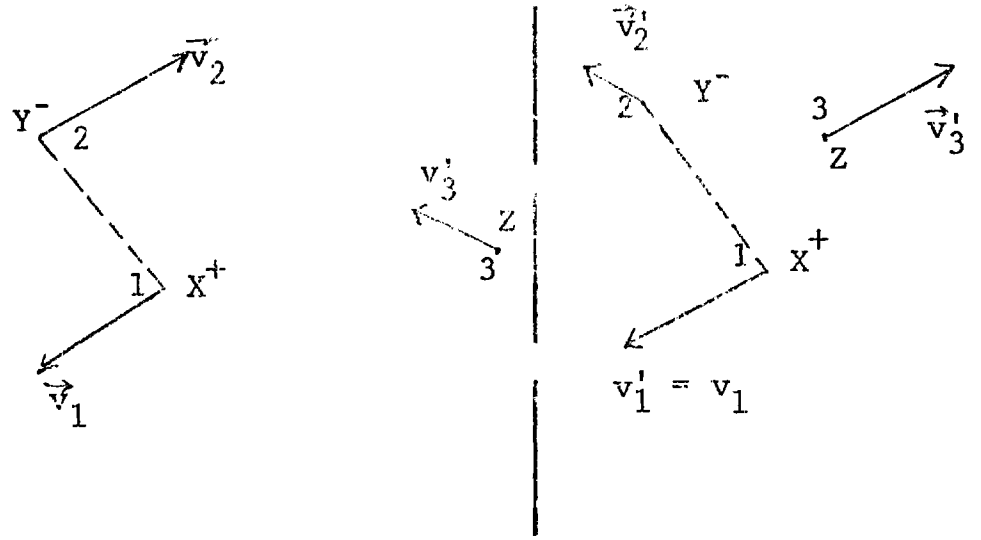

before (2,3) collision after collision

(a) direct collision $\sim K_{23}$

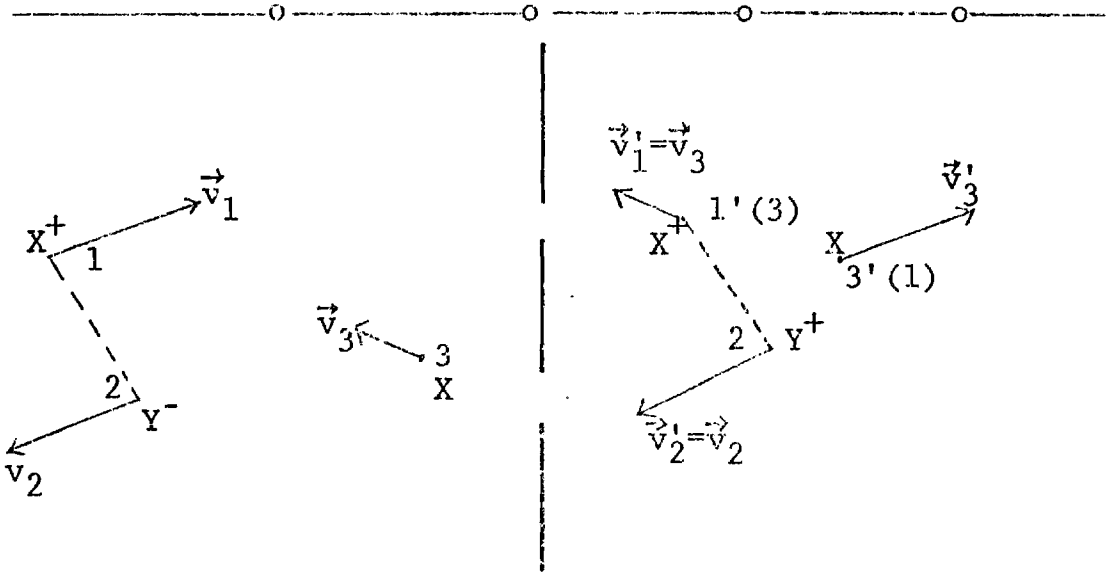

before (1,3) encounter after collision

(b) charge exchange collision $\sim K_{13}$

Fig. 4.1 Recombination

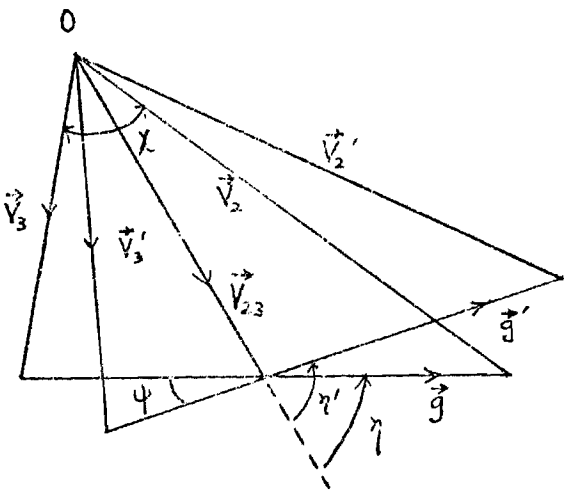
0
χ
$\vec{V}_2'$
$\vec{V}_3$
$\vec{V}_2$
$\vec{V}_3'$
$\vec{V}_{23}$
$\vec{g}'$
ψ
η'
$\vec{g}$
η

(a)

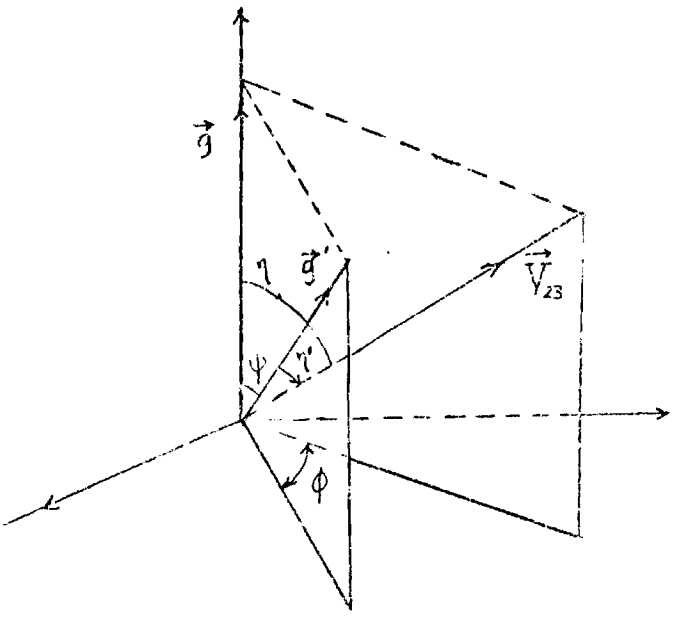
$\vec{g}$
η
$\vec{g}'$
$\vec{V}_{23}$
ψ
η'
φ

(b)

Fig 4.2

a) Kinematics

Let the velocities of the 3 bodies after collision be $\vec{v}_1'$, $\vec{v}_2'$, $\vec{v}_3'$ and the reduced mass and center-of-mass velocity of (i,j) system be m_{ij}, $\vec{V}_{ij}$ respectively (see Fig 4.1a, 4.2). Denote $\vec{g}$, $\vec{g}'$ the initial and final relative velocities of the (2,3) collisional partner, i.e.,

$$\vec{g}=\vec{v}_2-\vec{v}_3, \qquad \vec{g}=\vec{v}_2'-\vec{v}_3' \ . \tag{4-3}$$

An immediate consquence of the Impulse Approximation is that the velocity of the spectator ion after the (2,3) collision is unchanged, i.e.,

$$\vec{v}_1'=\vec{v}_1 \ . \tag{4-4}$$

A second result of this is that the change of internal energy of the positive-negative ion-pair from E_i to E_f is equal to the change of their relative kinetic energy T_f-T_i, or

$$\Delta=E_f-E_i=T_f+V_f-(T_i+V_i)=T_f-T_i \tag{4-5}$$

since the ion-ion separation (hence the potential energy) stays unchanged.

To calculate $T_f - T_i$ we choose the center-of-mass frame of the initial (1,2) system, i.e.,

$$m_1 \vec{v}_1 + m_2 \vec{v}_2 = 0 \tag{4-6}$$

such that

$$\vec{v}_1 = -(m_2/m_1)\vec{v}_2 \ . \tag{4-7}$$

One can express $\vec{v}_2$ in terms of $\vec{V}_{23}$ and $\vec{g}$ (similarly for $\vec{v}_2'$), by

$$\vec{v}_2 = \vec{V}_{23} + m_{23}\vec{g}/m_2 \ . \tag{4-8}$$

The initial relative kinetic energy is therefore

$$T_i = m_{12}(\vec{v}_1 - \vec{v}_2)^2/2 = m_2^2 \vec{v}_2^2 / 2m_{12} \tag{4-9}$$

by (4-7). Since the collision is elastic the C.M. velocity of (2,3) system $\vec{V}_{23}$ remains unchanged, their relative velocity $\vec{g}$ simply rotates by an angle ψ into $\vec{g}'$ with the magnitude unchanged (see Fig 4.2a). We have therefore

$$T_f - T_i = M_{12}\left[(\vec{v}_2' - \vec{v}_1)^2 - (\vec{v}_2 - \vec{v}_1)^2\right]/2 \tag{4-10}$$

$$= m_{23} V_{23}(\vec{g}' - \vec{g}) - \frac{m_{23}^2 g^2}{m_1 + m_2}(1 - \cos\psi)$$

where $\cos\psi = \hat{g}.\hat{g}'$.

Thus,

$$E_f - E_i = m_{23} V_{23} g(\cos\eta' - \cos\eta) - \frac{m_{23}^2 g^2}{m_1+m_2}(1-\cos\psi)$$

$$= m_{23} V_{23} g \sin\eta \sin\psi \cos\phi - (1-\cos\psi) \times \left(\frac{m_{23}^2 g^2}{m_1+m_2} g^2 + m_{23} V_{23} g \cos\eta\right) \qquad (4\text{-}11)$$

where $\cos\eta^{(')} = \hat{V}_{23} \cdot \hat{g}^{(')}$, $\cos\eta' = \cos\eta \cos\psi + \sin\eta \sin\psi \cos\phi$, with ϕ being the angle between two planes defined by $(\vec{V}_{23}, \vec{g})$ and $(\vec{g}, \vec{g}')$ respectively (see Fig 4.2b).

When ϕ varies between 0 and 2π with ψ, η, $\vec{g}$, $\vec{V}_{23}$ and E_i held constant, each value of E_f in the range defined by

$$E_i + m_{23} V_{23} g(\cos(\psi+\eta) - \cos\eta) - \frac{m_{23}^2 g^2}{m_1+m_2}(1-\cos\psi) \leq E_f$$

$$\leq E_i + m_{23} V_{23} g(\cos(\psi-\eta) - \cos\eta) - \frac{m_{23}^2 g^2}{m_1+m_2}(1-\cos\psi) \qquad (4\text{-}12)$$

is passed through twice. Alternately for a given E_f, (4-14) can be used to determine the range of ψ satisfying

$$E_f - E_i - m_{23} V_{23} g(\cos(\psi_\pm + \eta) - \cos\eta) + \frac{m_{23}^2 g^2}{m_1+m_2}(1-\cos\psi_\pm) = 0 \qquad (4\text{-}13)$$

with solution

$$\omega_{\pm}=\cos\psi_{\pm}=\gamma^{-2}\left(\alpha(\alpha+\Delta) \pm\beta\left[\gamma^2-(\alpha+\Delta)^2\right]^{\frac{1}{2}}\right) \tag{4-14a}$$

where

$$\alpha=\tfrac{1}{2}\, m_{23}(V_2^2 - V_3^2 - \frac{1-b}{1+b}\, g^2) \tag{4-14b}$$

$$\beta=\tfrac{1}{2}\, m_{23}\left(g^2(2V_2^2 + 2V_3^2 - g^2)-(V^2- V_3^2)^2\right)^{\frac{1}{2}} \tag{4-14c}$$

and

$$\gamma^2=\alpha^2 + \beta^2=\left(\frac{m_{23}g}{1+b}\right)^2 \left[(1+b)(v_2^2 + bv_3^2)-bg^2\right] \tag{4-14d}$$

with the mass ratio parameter b defined by

$$b=m_1 m_3 /m_2 (m_1+m_2+m_3) \quad . \tag{4-15}$$

With parameters α,β defined, (4-11) can be expressed as

$$E_f =E_i +\beta \sin\psi\cos\phi - \alpha(1-\cos\psi) \quad . \tag{4-16}$$

The ranges of the variables ψ and ϕ are mutually dependent in that as ϕ varies from 0 to 2π, the scattering angle is confined to within $\psi_{\pm}$ for a given change of internal energy Δ of (1,2) system. Obviously g lies within the range:

$$g_1=|v_2-v_3|\leq g \leq(v_2+v_3)=g_2 \tag{4-17}$$

and is further restricted by the reality condition of $\omega_{\pm}$. The latter conditon demands that g lies between $G_{\pm}$ that

$$(G \pm)^2 = (F \mp H)^2 \tag{4-18a}$$

with

$$F = \left[v_2^2 + \frac{2(E_f - E_i)}{m_{23}} \frac{b}{1+b} \right]^{\frac{1}{2}} \tag{4-18b}$$

and

$$H = \left[v_3^2 - \frac{2(E_f - E_i)}{m_{23}} \frac{1}{1+b} \right]^{\frac{1}{2}} \tag{4-18c}$$

And the reality condition of both F and H leads to

$$X = m^2 v_2^2 / 2m_{12} + (E_f - E_i) \geq 0 \tag{4-19a}$$

and

$$Y = m_2 v_3^2 / 2m_{12} - (E_f - E_i) \geq 0 \tag{4-19b}$$

respectively. The condition (4-19b) is equivalent to

$$\mu v_3^2 / 2 \geq E_f - E_i \tag{4-19c}$$

with the reduced mass of the neutral and the ion-pair system given by

$$\mu = \frac{m_3(m_1+m_2)}{m_1+m_2+m_3} = \frac{b m_2^2}{m_{12}} \tag{4-19d}$$

Of course the limit of g is subject to both conditions (4-17) and (4-18) with (4-19). Conditions (4-19) also set the limits to v_2, v_3 for a given excitation or de-excitation, i.e.,

$$(V_2^2)_{min} = \begin{cases} 0 & \text{for } E_i < E_f, \text{excitation} \quad (4\text{-}20a) \\ -\frac{2m_{12}}{m_2^2}(E_f - E_i) & \text{for } E_f < E_i, \text{de-excitation} \quad (4\text{-}20b) \end{cases}$$

and

$$(V_2^2)_{min} = \begin{cases} \frac{2m_{12}b(E_f - E_i)}{m_2^2} & \text{for excitation} \quad (4\text{-}21a) \\ 0 & \text{for de-excitation} \quad (4\text{-}21b) \end{cases}$$

i.e., the third body must have sufficient kinetic energy to excite the ion-pair while the ion-pair must have enough energy to have de-excitation. For a known change in the internal energy of the ion-pair, the available ranges of the set of the variables $(v_2, v_3, \vec{g}, \psi)$ are restricted by the conditions: (4-14), (4-17) (4-18), (4-20) and (4-21).

b) Expression of K_{23}

Let $\sigma(\psi, g)$ be the elastic differential scattering cross section for the ion,neutral(i.e.,(2-3)) collisions with the scattering angle ψ and the relative velocity $\vec{g}$ given by

$$g^2 = v_2^2 + v_3^2 - 2sv_2v_3, \quad s = \cos\chi \tag{4-22}$$

where χ is the angle between v_2 and v_3. Then for a given v_2 and v_3, the rate coefficient dK_{23} for collisions in $(s+ds, s)$ and the scattering into unit solid angle $d\Omega = \sin\psi\, d\psi\, d\phi$ about the direction (ψ, ϕ) is

$$dK_{23} = g(\sigma(\psi, g)\sin\psi\, d\psi\, d\phi)ds/2 . \tag{4-23}$$

Differentiation of (4-16) subject to the initial condition with ψ given, yields

$$dE_f = -\beta \sin\psi \sin\phi\, d\phi . \tag{4-24a}$$

Again from (4-16) one has,

$$\cos\phi = (\Delta + \alpha(1-\cos\psi))/\beta\sin\psi \tag{4-24b}$$

such that

$$d\phi = -dE_f/R \tag{4-24c}$$

where

$$R = \{\beta^2 - (\alpha+\Delta)^2 + 2\alpha(\alpha+\Delta)\cos\psi - (\alpha^2+\beta^2)\cos^2\psi\}^{\frac{1}{2}} \tag{4-24d}$$

$$= \gamma\{(\cos\psi_+ - \cos\psi)(\cos\psi - \cos\psi_-)\}^{\frac{1}{2}}$$

with $\cos\psi_\pm$ defined in (4-14a). Also with (4-22) one has

$$ds = -gdg/v_2v_3 . \tag{4-24e}$$

We now integrate over all permissible ψ and g of (4-23) with the help of (4-24c, d, e) and the fact that each

element $d\phi$ contains two elements dE_f. One finds the rate coefficient for (2,3) collision that leaves (1,2) internal energy in the interval (E_f+dE_f, E_f) for a given v_2, v_3 equal to $\Gamma\, dE_f$ where

$$\Gamma=\frac{1}{V_2V_3}\int_{g_-}^{g_+} dg\frac{g^2}{(\alpha^2+\beta^2)^{\frac{1}{2}}}\int_{\psi_-}^{\psi_+} d(\cos\psi)\frac{\sigma_{23}(g,\psi)}{((\cos\psi_+-\cos\psi)(\cos\psi-\cos\psi_-))^{\frac{1}{2}}} \tag{4-25}$$

in which g_+ is the smaller of g_2 and G_+, while g_- is the larger of g_1 and G_- defined in (4-17) and (4-18) such that $g_- < g_+$ for non-zero Γ.

To obtain the total rate coefficient for a given transition of the ion-pair from E_i to E_f, one must integrate over all possible values of v_2, v_3. First assume that the center-of-mass of the ion-pair has thermal motion corresponding to the temperature θ of the neutral gas. One has the distribution function for the incident velocity v_3

$$\mathcal{J}(v_3)dv_3=4\pi v_3^2(\mu/2\pi k\theta)^{3/2}\, e^{-\mu v_3^2/2k\theta}dv_3 \tag{4-26}$$

with the reduced mass of the third body with the ion-pair defined in (4-19d). For the ion-ion relative motion, one can assume the microcanonical distribution, i.e., assume that all elements of the phase space $(\vec{p}, \vec{r})$ associated

with a given internal energy E_i are equally populated. Then

$$f(\vec{p}\,,\,\vec{r}\,)=A\,\delta(E_i-\vec{p}^{\,2}/2m_{12}+e^2/r) \qquad (4\text{-}27a)$$

is the distribution function of the ion-pair with the reduced mass m_{12}, the internal energy E_i (separated by r). The constant A is determined from the normalization condition for a single ion-pair

$$\int f(\vec{p}\,,\vec{r}\,)\,d\vec{p}\;d\vec{r} = 1 \quad . \qquad (4\text{-}27b)$$

For the Coulombic potential we have, from the result of Appendix A, the normalized number of ion-pairs with speeds between v_2 and v_2+dv_2

$$\mathcal{J}(v_2)\,dv_2 = \frac{dr\;r^2}{C(E_i)}\,(E_i-V)^{\frac{1}{2}} \qquad (4\text{-}28a)$$

in terms of r integration, where

$$C(E_i)=\int dr\;r^2(E_i-V)^{\frac{1}{2}}$$

$$\left.\begin{aligned} &= \frac{e^6}{16|E_i|^{5/2}} \\ &= e^6/H_R(k\theta)^{5/2} \end{aligned}\right\} \text{ for Coulombic potential } -e^2/r \qquad (4\text{-}28b)$$

in which we use the definition of H_R,

$$H_R=16\,\lambda^{5/2}/\,\pi\,. \qquad (4\text{-}28c)$$

Hence

$$\mathcal{F}(v_2)\,dv_2/v_2 = \frac{m_2 r^2 dr}{C(E_i)(2m_{12})^{\frac{1}{2}}} \qquad (4\text{-}28d)$$

The rate coefficient K_{23} is obtained by integrating over distributions $\mathcal{F}(v_2)$ and $\mathcal{G}(v_3)$ such that

$$K_{23}(E_i,E_f)\,dE_f = dE_f \int\int dv_2 dv_3 \frac{\mathcal{F}(v_2)}{v_2} \frac{\mathcal{G}(v_3)}{v_3} \Gamma(v_2 v_3 E_i E_f)$$

$$= dE_f \int \frac{dr\, r^2 m_2}{C(E_i)(2m_{12})^{\frac{1}{2}}} \int dv_3\, 4\pi v_3 \left(\frac{\mathcal{M}}{2\pi k\theta}\right)^{3/2} e^{-\frac{\mathcal{M}v_3^2}{2k\theta}}$$

$$\times \int_{g_-}^{g_+} dg \frac{g^2}{(\alpha^2+\beta^2)^{\frac{1}{2}}} \int_{\psi_-}^{\psi_+} \frac{\sigma(g,\psi)\, d(\cos\psi)}{\left[(\cos\psi-\cos\psi)(\cos\psi-\cos\psi_-)\right]^{\frac{1}{2}}} \qquad (4\text{-}29)$$

with the aid of (4-25). To facilitate the calculation we define the following variables (S,y,z) instead of (v_2, v_3, g)

$$1/s = e^2/k\theta r, \qquad x = -\lambda + 1/s$$

$$y = \frac{1}{k\theta} \frac{m_2^2 v_3^2}{2m_{12}} = \frac{\mathcal{M}v_3^2}{b2k\theta} \qquad Y = by \qquad (4\text{-}30)$$

$$z = m_2^2 g^2/2m_{12}k\theta$$

so that

$$\gamma^2 = \left(\frac{m_{23}}{1+b}\right)^2 \left(\frac{2m_{12}k\theta}{m_2^2}\right)^2 z\left((1+b)(-\lambda + \frac{1}{s} + by) - bz\right) \qquad (4\text{-}30)$$

where $E_i = -k\theta\lambda$ is used. Note also $K_{23}\, d\mu = K_{23}\, dE_f$

$= K_{23} k\,\theta\, d\mu$ that we have

$$\kappa_{23} = B'\, I'_{23} k\,\theta \tag{4-31a}$$

where the constant B' is given as

$$B' = \frac{e^6(1+b)}{C(E_i)k^3\theta^3(2\pi m_{23})^{\frac{1}{2}}} \tag{4-31b}$$

with $C(E_i)$ given by (4-28b), b by(4-15). The other factor I'_{23} is

$$I'_{23} = \int_{s_-}^{s_+} ds\; s^2 \int_{Y_-}^{Y_+} dY e^{-Y} \int_{Z_-}^{Z_+} dz \frac{1}{(Y+\frac{1}{s}-\lambda-\frac{bz}{1+b})^{\frac{1}{2}}} \int_{\omega_-}^{\omega_+} d\omega \frac{\sigma(\omega,z)}{((\omega_+-\omega)(\omega-\omega_-))^{\frac{1}{2}}} . \tag{4-31c}$$

The limits of integration in I'_{23} are:

(i) S_+=minimum of $(1/\lambda, 1/\mu)$

$S_-=0.$ for $-e^2/r$, (4-32a)

(ii) $Y_+ = \infty$

$$Y_- = \begin{cases} \lambda - \mu & \text{for excitation } \lambda > \mu \\ 0. & \text{for de-excitation,} \end{cases} \tag{4-32b}$$

(iii) Z_+ = minimum of (z_2, Z_2), where

$$z_2 = (x^{\frac{1}{2}} + y^{\frac{1}{2}})^2 \tag{4-32c}$$

$$Z_2 = ((x+\lambda-\mu)^{\frac{1}{2}} + (y-(\lambda-\mu)/b)^{\frac{1}{2}})^2,$$

Z_-=max. of (z_1, Z_1) where

$$z_1=(x^{\frac{1}{2}} - y^{\frac{1}{2}})^2 \tag{4-32d}$$

$$Z_1=((x+\lambda-\mu)^{\frac{1}{2}} - (y-(\lambda-\mu)/b)^{\frac{1}{2}})^2$$

and finally

$$\omega_{\pm}=A_1(A_1+A_o)\pm A_2(1-(A_1+A_o)^2)^{\frac{1}{2}} \tag{4-33a}$$

with

$$A_o=\frac{k\theta(\lambda-\mu)}{\gamma} = \frac{(1+b)^{3/2}(\lambda-\mu)}{2bz^{\frac{1}{2}}(x+Y-bz/(1+b))^{\frac{1}{2}}} \tag{4-33b}$$

$$A_1=\frac{\alpha}{\gamma} = \frac{(1+b)^{\frac{1}{2}}}{2} \frac{x-Y/b+(1-b)z/(1+b)}{(x+Y-bz/(1+b))^{\frac{1}{2}}z^{\frac{1}{2}}} \tag{4-33c}$$

$$A_2=\frac{\beta}{\gamma} =\frac{(1+b)^{\frac{1}{2}}}{2} \frac{\left[(z(2x+2Y/b-z)-(x-Y/b)^2)\right]^{\frac{1}{2}}}{z^{\frac{1}{2}}(x+Y-bz/(1+b))^{\frac{1}{2}}} \tag{4-33d}$$

.

The parameters α, β, γ are defined in (4-16b, c, d) and can be put into the new forms

$$\alpha = k\theta\frac{m_{12}m_{23}}{m_1^2}(x-y-\frac{1-b}{1+b}z)^{\frac{1}{2}} \tag{4-34a}$$

$$\beta = k\theta\frac{m_{12}m_{23}}{m_1^2}\left[z(2x+2y-z)-(x-y)^2\right]^{\frac{1}{2}} \tag{4-34b}$$

$$\gamma = k\theta\frac{2m_{12}m_{23}}{m_2^2(1+b)^{\frac{1}{2}}}\left[z(x+by)-\frac{bz^2}{1+b}\right]^{\frac{1}{2}} \tag{4-34c}$$

.

Thus, eqs. (4-31) to (4-34) completely define the

change-of-energy rate rate coefficient due to the elastic collision of (2,3).

Knowledge of $\sigma(\psi, g)$ is needed to proceed further. We reserve the simpler case of isotropic scattering of the charge-transfer (SRCT), i.e., K_{13}, in section 4.2 and consider now the Langevin potential case.

c) σ_{23}:scattering cross section from Langevin potential

N.B. The letters b,x,Y,Z defined below are used in this subsection only.

From classical mechanics the scattering cross section can be expressed in terms of the relation between the scattering angle ψ and the impact parameter q (Goldstein, 1950 ; Landau, 1960) as

$$\sigma(\psi, g) = \sum_{\psi} \left| \frac{q dq}{d(\cos\psi)} \right| \qquad (4\text{-}35a)$$

where the sum over ψ is due to the fact that q is not a single valued function of ψ . In practice one sums over $\pm\psi$, $-2\pi\pm\psi$, $-4\pi\pm\psi$, ---, where $0 \leq \psi \leq \pi$. The scattering angle in terms of q and the potential is given by

$$\psi = \pi - 2q \int_{r_c}^{\infty} dr\, r^{-2}\left[(1-V(r)/E-q^2/r^2)\right]^{-\frac{1}{2}} \qquad (4\text{-}35b)$$

For our case V(r) is the potential given in (4-2) and r_c is the distance of closest approach. This can be converted into a more convenient form by changing the integration variable

$$x = r_c/r \qquad (4\text{-}35c)$$

so that

$$\psi = \pi - 2\,\frac{q}{r_c}\int_0^1 dx \frac{(1-x^2)^{\frac{1}{2}}(1-V(r_c/x)/E-q^2x^2/r_c^2)^{-\frac{1}{2}}}{(1-x^2)^{\frac{1}{2}}} \qquad (4\text{-}35d)$$

This integral is in a standard form so one can use the Gauss-Mehler qudrature formul

$$\int_{-1}^{1} dx \frac{f(x)}{(1-x^2)^{\frac{1}{2}}} = \frac{\pi}{n}\sum_{j=1}^{n} f(\cos\frac{2j-1}{2n}\pi) \qquad (4\text{-}35e)$$

with n being an even integer to yield

$$\psi = \pi - \frac{2q}{r_c}\frac{\pi}{n}\sum_{j=1}^{n/2} a_k g(a_j) \quad , \qquad (4\text{-}36a)$$

where

$$a_j=\cos(2j-1)\pi/2n$$
$$k=n/2+1-j \qquad (4\text{-}36b)$$

and

$$g(x)=\left[1-\frac{V(r_c/x)}{E}-\frac{q^2x^2}{r_c^2}\right]^{-\frac{1}{2}} \qquad (4\text{-}36c)$$

which is an even function of x (if g(x) is not an even function the sum in (4-36a) will be in a slightly different form). Though one can proceed to calculate and σ_{23}, a more accurate numerical procedure, as pointed out by Flannery (FM1), is first to calculate $d\psi/dq$ from

$$\frac{d\psi}{dq}=\frac{\partial\psi}{\partial q}+\frac{\partial\psi}{\partial r_c}\frac{dr_c}{dq} \qquad (4\text{-}37a)$$

Hence, with the aid of (4-36a, b, c)

$$\frac{d\psi}{dq}=\frac{dr_c}{dq}\frac{\pi}{nE}\left\{\frac{q}{r_c}\sum_{j=1}^{n/2}a_k g^3(a_j)(a_j^2V'(r_c)-V'(r_c/a_j))+\frac{r_c}{q}\sum_{j=1}^{n/2}a_k g(a_j)V'(r_c)\right\} \qquad (4\text{-}37b)$$

where

$$V'(r_c/a_j)=\left[\frac{d}{dr}V(r/a_j)\right]_{r=r_c} \qquad (4\text{-}37c)$$
$$\frac{dr_c}{dq}=(q/r_c-r_c^2V'/2qE)^{-1} \qquad (4\text{-}37d)$$

and k defined as before.

We have two cases to consider:

(i) when $r_c > S$ (the hard core radius), then only the polarization part of the interaction is effective. The scattering angle is denoted by ψ_p .

(ii) when $r_c < S$, the interaction range is replaced by (S, ∞) so that the full Langevin potential is operative. Denote the scattering angle by ψ_f.

Let

$$Y = q^2(2E/pe^2)^{\frac{1}{2}} \tag{4-38a}$$

and

$$Z = YS^2/q^2 \tag{4-38b}$$

where p is the polarizability of the neutral atom, E is the energy of the (2,3) system, and S the hard core radius.

case (i): $S < r_c$

One has

$$\psi_p = \pi - \rho_o \int_{-1}^{1} dx \frac{(1-x2)^{\frac{1}{2}} g(x)}{(1-x^2)^{\frac{1}{2}}} \qquad Y \geq 2 \tag{4-39a}$$

where

$$\rho = q/r, \quad \rho_o = q/r_c, \quad x = \rho/\rho_o \tag{4-39b}$$

and

$$g(x) = (1-\rho_o^2 x^2-\rho_o^4 x^4/Y^2)^{-\frac{1}{2}} \qquad (4\text{-}39c)$$

so that

$$\psi_p = \pi - \rho_o \frac{2\pi}{n} \sum_{j=1}^{n/2} a_k g(a_j) \qquad (4\text{-}40a)$$

with a_j and k defined as before. In (4-40a) we have

$$g(a_j)=(1-a_j^4+\rho_o^2 a_j^2(a_j^2-1))^{-\frac{1}{2}} \qquad (4\text{-}40b)$$

since ρ_o^2 is determined from the condition of being the root of the equation

$$1-\rho_o^2+\rho_o^4/Y^2=0 \qquad (4\text{-}40c)$$

so that we have

$$\rho_o^2=Y(Y-(Y^2-4)^{\frac{1}{2}})/2 \qquad (4\text{-}40d)$$

and of course $Y \geq 2$. (4-40e)

The derivative of ψ_p w.r.t. q is put into a more convenient form

$$\frac{d\psi_p}{dY} = \frac{2\pi}{n} \frac{d\rho_o}{dY} \sum_{j=1}^{n/2} a_k g(a_j) \left[\rho_o^2(a_j^4-a_j^2)g^2(a_j)-1\right] \qquad (4\text{-}41a)$$

with

$$\frac{d\rho_o}{dY} = \frac{\rho_o^3}{Y^2(Y^2-4)^{\frac{1}{2}}} \quad .$$

case(ii): $r_c < S$

The lower limit r_c is now replaced by S (r_c is the larger root of $1-V/E-q^2/r_c^2=0$).

Let

$$\rho = S/r. \tag{4-42a}$$

We have now the scattering angle

$$\psi_f = \pi - \left(\frac{Y}{Z}\right)^{\frac{1}{2}} \int_{-1}^{1} d\rho \frac{(1-\rho^2)^{\frac{1}{2}}}{(1-\rho^2)^{\frac{1}{2}}} g_1 \qquad Y \leq Z+1/Z \tag{4-42b}$$

following the same procedure as (i), where

$$g_1(\rho) = \left(1+\frac{\rho^4}{Z^2} - \frac{Y}{Z}\rho^2\right)^{-\frac{1}{2}} , \tag{4-42c}$$

the factor in front of the integral sign is from the relation

$$q/S = (Y/Z)^{\frac{1}{2}} . \tag{4-42d}$$

In terms of the Gauss-Mehler formula one has

$$\psi_f = \pi - (Y/Z)^{\frac{1}{2}} \frac{2\pi}{n} \sum_{j=1}^{n/2} a_k g(a_j) \tag{4-43a}$$

subject to the condition of reality of ρ ($\rho < 1$)

$$Z+1/Z > Y. \qquad (4\text{-}43b)$$

Hence,

$$\frac{d\psi_f}{dY} = -\frac{\pi}{n}(Y/Z)^{\frac{1}{2}} \sum_{j=1}^{n/2} a_k g(a_j)(1/Y+\frac{1}{Z}a_j^2 g(a_j)) \qquad (4\text{-}43c)$$

Here we note that for the two cases there are two different conditions (4-40e) and (4-43b) depending on $S < r_c$ or $S > r_c$ respectively. The two conditions coincide at $Y=2$ (when $Z=1$ for the latter case). This is the "orbiting" condition. With ψ_p, $d\psi_p/dY$, ψ_f, $d\psi_f/dY$ explicitly given, one can now calculate σ_{23} by noting its relation with $\Delta(\psi, Z)$ defined in the following way. From (4-35a) and (4-38a) with $E=m_{23}g^2/2$, the initial energy of (2,3) system, one has

$$Y = \left[\frac{m_{23}g^2}{pe^2}\right]^{\frac{1}{2}} q^2 = \left[\frac{2k_\theta bz}{pe^2(1+b)}\right]^{\frac{1}{2}} q^2$$

where the second equality followed from definition of z and b (see (4-15) and (4-30)).

Thus one has

$$\sigma = \frac{1}{2} (pe^2/k\theta)^{\frac{1}{2}}(1+b/bz)^{\frac{1}{2}} \Delta(\psi,Z) \qquad (4\text{-}44a)$$

where

$$\Delta(\psi,Z)= \sum_{\psi} \left| \frac{1}{\sin\psi} \frac{1}{d\psi/dY} \right| \qquad (4\text{-}44b)$$

which can be tabulated according to the case from the expressions of ψ and $d\psi/dY$ given in (4-40) and (4-41) or (4-43).

The interaction parameter A is given by

$$A=(2k\theta/pe^2)^{\frac{1}{2}} S \qquad (4\text{-}45a)$$

which relates Z and z by

$$Z=A(bz/(1+b))^{\frac{1}{2}} . \qquad (4\text{-}45b)$$

The parameter A varies from system to system due to the change of the atomic polarizability p and the hard core radius S. So we can make a "general" table of $\Delta(\psi,Z)$ covering a reasonably wide range of Z with respect to the angle ψ for the systems to be studied (see CHAP 5).

With the table $\Delta(\psi, Z)$ given, the integral over $\omega = \cos\psi$ can be cast into the standard Gauss-Mehler form

$$\Omega = \int_{\omega_-}^{\omega_+} \frac{\Delta(\omega, Z)\, d\omega}{((\omega_+ - \omega)(\omega - \omega_-))^{\frac{1}{2}}} = \int_{-1}^{1} dx \frac{\Delta(x, A(bz/(1+z))^{\frac{1}{2}})}{(1-x^2)^{\frac{1}{2}}} \tag{4-46a}$$

with

$$x = 2\frac{\omega - (\omega_+ + \omega_-)/2}{\omega_+ - \omega_-} \tag{4-46b}$$

such that

$$\Omega = \frac{\pi}{n} \sum_{j=1}^{n} \Delta(\omega_j, A(bz/(1+z)) \tag{4-47a}$$

with the definition

$$\omega_j = \frac{1}{2}(\omega_+ + \omega_-) + \frac{1}{2}(\omega_+ - \omega_-)\cos((2j-1)\pi/2n) \tag{4-47b}$$

and where $\omega_\pm$ are defined in (4-14a).

We define B_2, I_{23} as following:

$$B_2 = \frac{e^6 (1+b)^{3/2}}{C(E_i)(k\theta)^{5/2} b^{\frac{1}{2}}\, 4} \left[\frac{pe^2}{\pi m_{23}}\right]^{\frac{1}{2}}$$

$$= H_R \frac{(1+b)^{3/2}}{4b^{\frac{1}{2}}} \frac{p^{\frac{1}{2}} e}{(\pi m_{23})^{\frac{1}{2}}} \tag{4-48a}$$

with the aid of (4-28b), and

$$I_{23}=\int_{s_-}^{s_+} ds\ s^2 \int_{Y_-}^{\infty} dY e^{-Y} \int_{Z_-}^{Z_+} dz\left[z(Y-1/s-\lambda-bz/(1+b))\right]^{-\frac{1}{2}}\ \Omega \qquad (4\text{-}48b)$$

where Ω is given in (4-47). We therefore find the reduced rate coefficient from the direct collision (c.f. eq.(4-31))

$$\kappa_{23}=B_2 I_{23} \qquad (4\text{-}48c)$$

4.2 K_{13}: Case of the symmetric resonance charge-exchange

For the (1,3) encounter the basic physics involved is the symmetric resonance charge-transfer. The interaction between the ion $X^+(1)$ and the parent gas X(3) is acknowledged by the use of the total charge-transfer cross section q^+. The rate coefficient of encounter is given by (c.f., K_{23}),

$$dK_{13}=q^+|\vec{v}_1-\vec{v}_3|ds/2 \qquad (4\text{-}49)$$

where $s=\cos(\hat{v}_1\hat{v}_3)$.

Following section 4.1, a general expression for K_{13} can be derived. The expression can then be simplified by (i) setting $m_3=m_1$, (ii) treating q^+ constant in the angular integration of (4-46a) since it is isotropic and (iii) taking q^+ oustide the velocity integration since it is a slowly varing function of v . It is however simpler to use these facts at the beginning of the derivation of K_{13} for the process,

$$X^+ + Y^- + X \longrightarrow XY^* + X \ .$$
$$1 \quad 2 \quad 3$$

A useful parameter is a, defined by

$$a=m_1/m_2=m_x/m_y \tag{4-50a}$$

so that

$$m_{12}=m_1/(1+a) \ . \tag{4-50b}$$

Again we consider the system in the C.M. frame of (1,2) so that (see Fig 4.1b)

$$\vec{v}_2=-a\vec{v}_1 .$$

The encounter of (1,3) results in an interchange of the velocities of the two particles, i.e.,

$$\vec{v}_1'=\vec{v}_3, \qquad \vec{v}_3'=\vec{v}_1 \tag{4-51a}$$

while the velocity of the spectator 2 is left unchanged, i.e.,

$$\vec{v}_2'=\vec{v}_2 \ . \tag{4-51b}$$

The energy-change is

$$\Delta = E_f - E_i = T_f - T_i \tag{4-51c}$$

where

$$T_i = m_{12}(\vec{v}_1-\vec{v}_2)^2/2=(1+a)m_1\vec{v}_1^{\,2}/2 \tag{4-51d}$$

$$T_f = m_{12}(\vec{v}_1'-\vec{v}_2')^2/2=m_{12}\vec{g}_f^{\,2}/2 \tag{4-51e}$$

with

$$\vec{g}_f = \vec{v}_1'-\vec{v}_2'=\vec{v}_3-\vec{v}_2=\vec{v}_3+a\vec{v}_1. \tag{4-51f}$$

The obvious limits of g are

$$|v_3-av_1| \leq g_f \leq v_3+av_1. \tag{4-52a}$$

Eq. (4-51c) can be put as

$$g_f^{\,2}=2\Delta/m_{12}+(1+a)^2\vec{v}_1^{\,2} \tag{4-52b}$$

which, when combined with (4-51f), gives

$$(v_3\pm av_1)^2 = 2\Delta/m_{12}+(1+a)^2v_1^{\,2} \tag{4-52c}$$

which has solutions

$$(v_3)_{\pm} = \pm a v_1 + ((1+a)^2 v_1^2 + 2\Delta/m_{12})^{\frac{1}{2}} \qquad (4\text{-}52d)$$

The reality condition of the above implies

$$(v_1^2)_{min} = -\frac{2\Delta}{m_{12}(1+a)^2}, \quad (v_3^2)_{min} = (\frac{a}{1+a})^2(\frac{-2\Delta}{m_{12}}) \qquad (4\text{-}53a)$$

for de-excitation, $\Delta < 0$, or

$$(v_1^2)_{min} = 0 \quad \text{and} \quad (v_3^2)_{min} = \frac{2\Delta}{m_{12}} \qquad (4\text{-}53b)$$

for excitation, $\Delta > 0$. The values of v_3^2 will be further limited by the condition (4-55b) as we will see below.

Since

$$\Delta = E_f - E_i = \tfrac{1}{2} m_{12}(v_3^2 + 2a v_1 v_3 s - (1+2a) v_1^2) \qquad (4\text{-}54a)$$

one has

$$ds = dE_f / a m_{12} v_1 v_3 \qquad (4\text{-}54b)$$

with v_1, v_3 held fixed. Thus dK_{23} in (4-49a) becomes

$$dK_{13} = \frac{dE_f q^+}{2 m_{12} a v_1 v_3}(\frac{1+a}{a})^{\frac{1}{2}}(v_3^2 - v_1^2 - \frac{2\Delta}{m_{12}(1+a)})^{\frac{1}{2}} \qquad (4\text{-}55a)$$

and since dK_{13} must be real one has,

$$v_3^2 \geq v_1^2 + 2\Delta/m_{12}(1+a) \quad . \tag{4-55b}$$

Hence (4-53a), (4-53b) together with (4-55b) will constrain the physical regions of v_1 and v_3 .

Assume that the C.M. of the ion-pairs (1,2) has thermal motion with the neutral gas 3, such that the distribution function for v_3 is

$$\mathcal{G}(v_3)dv_3 = 4\pi v_3^2 (\mathcal{M}/2\pi k\theta)^{3/2} e^{\left(-\frac{\mathcal{M}v_3^2}{2k\theta}\right)} dv_3 \tag{4-56a}$$

where

$$\mathcal{M} = m_1(1+a)/(1+2a) \tag{4-56b}$$

by using (4-50a, b). The relative motion of the ion-pairs has distribution $\mathcal{F}(v_1)dv_1$ defined in (4-28a, b).

Therefore from (4-55a) the SRCT rate coefficient is

$$K_{13}dE_f = dE_f(q^+/2m_{12}a)((1+a)/a)^{\frac{1}{2}} \int dv_1 (\mathcal{F}(v_1)/v_1) \times \int dv_3 (\mathcal{G}(v_3)/v_3)(v_3^2 - v_1^2 - 2\Delta/m_{12}(1+a))^{\frac{1}{2}} \quad . \tag{4-57}$$

Define x, y, s, λ, μ as following

$$x=\frac{T_i}{k\theta}=-\lambda+1/s \quad \text{and} \quad x=\frac{m_1(1+a)v_1^2}{2k\theta} \tag{4-58a}$$

$$s=k\theta\, r/e^2 \tag{4-58b}$$

$$y=\mu v_3^2/2k\theta \tag{4-58c}$$

$$\lambda=-E_i/k\theta, \qquad \mu=-E_f/k\theta \tag{4-58d}$$

Using (4-58a, b) the v_1-integration becomes integration over s (via (4-58b)), while the v_3-integration becomes integration of y. Hence (4-57) becomes, with the definitions (4-58),

$$K_{13}dE_f=dE_f\frac{q^+e^6(1+a)^2}{C(E_i)(2\pi m_1)^{\frac{1}{2}}a^{3/2}k^3\theta^3}$$

$$\times\int_{S_-}^{S_+}ds\ s^2\int_{y_-}^{y_+}dy\ e^{-y}\left(y-\frac{x}{1+2a}-\frac{1+a}{1+2a}(\lambda-\mu)\right)^{\frac{1}{2}} \tag{4-59a}$$

The limits of the above expression are

$$S_+=\text{min. of } (1/\lambda\ ,1/\mu\ )$$

$$S_-=0 \tag{4-59b}$$

from the definition of s(r) and the phase space available for a transition from λ to μ ; and

$$y_{\pm} = \frac{(1+2a+2a^2)x+(1+a)^2(\lambda-\mu)\pm 2a(1+a)x^{\frac{1}{2}}(x+\lambda-\mu)^{\frac{1}{2}}}{(1+2a)} \tag{4-59c}$$

from (4-52c) with conditions (4-53) and (4-55b).

The integration of y can be easily carried out by the transformation

$$Y=y-x/(1+2a)-(1+a)(\lambda-\mu)/(1+2a) \tag{4-60a}$$

By the use of the error function

$$\mathrm{erf}(t)= \frac{2}{(\pi)^{\frac{1}{2}}}\int_0^t e^{-u^2}du \tag{4-60b}$$

we can write

$$K_{13}=B_1 \int_{S_-}^{S_+} ds\ s^2\ \vartheta_{13} \tag{4-61a}$$

where

$$\vartheta_{13}=\exp[-(x+(1+a)(\lambda-\mu))/(1+2a)]\ x$$

$$[(\mathrm{erf}(\sqrt{Y_+})-\mathrm{erf}(\sqrt{Y_-})-[2/\sqrt{\pi}](\sqrt{Y_+}e^{-Y_+}-\sqrt{Y_-}e^{-Y_-})] \tag{4-61b}$$

with

$$Y_{\pm}=(a(1+a)/(1+2a))[x^{\frac{1}{2}}\pm(x+\lambda-\mu)^{\frac{1}{2}}]^2 \qquad (4\text{-}61c)$$

and where the constant B_1,

$$B_1=\frac{q^+(1+a)^2e^6}{(2a)^{3/2}m_1^{\frac{1}{2}}k^3\theta^3C(E_i)}$$

$$=H_R\frac{(1+a)^2}{a^{3/2}}\frac{q^+}{(8m_1k\theta)^{\frac{1}{2}}} \qquad (4\text{-}61d)$$

with $C(E_i)$ given in (3-38b). Of course the reduced coefficient κ_{13} is given by

$$\kappa_{13}=k_\theta K_{13}.$$

CHAPTER V

APPLICATION TO RARE GAS SYSTEMS

Armed with the expressions for the rate coefficients κ_{13} of the symmetric resonance charge-transfer and κ_{23} of the direct elastic collision we are ready to calculate the distribution $\rho(x)$, and have the recombination rate coefficient α_R for the specific system provided that suitable information is at hand.

To see more clearly what will be involved and what are the parameters needed in the calculation of the reaction,

$$\underset{1}{Rg^+} + \underset{2}{F^-} + \underset{3}{Rg} \longrightarrow (RgF)^* + Rg \qquad (5\text{-}1)$$

where Rg=rare gas, i.e., He, Ne, Ar, Kr and Xe, we once more list the main equations.

(I) First we have the expression of the recombination rate coefficient from (3-16b),

$$\alpha_R=\frac{N_3\pi^{3/2}e^6}{2(k\theta)^3}\int_\nu^\omega d\lambda\frac{e^\lambda}{\lambda^{3/2}}\int_{-\infty}^{\nu}du(\rho(\mu)-\rho(\lambda))\kappa_{\lambda\mu} \qquad (5\text{-}2)$$

with $\kappa_{\lambda\mu}=\kappa_{13}+\kappa_{23}$, and the subscript R standing for recombination. We see that κ_{13} and κ_{23} are needed not only in solving $\rho(x)$ but also in calculating α_R.

(II) The rate of the (1,3) collision in (5-2b) is (c.f. Eqs. (4-61))

$$\kappa_{13}=(k\theta)^{\frac{1}{2}}H_R\frac{(1+a)^2}{a^{3/2}}\frac{q^+}{(8m_1)^{\frac{1}{2}}}I_{13} \qquad (5\text{-}3a)$$

where a is the ratio of the mass of the rare gas m_1 to the mass of fluorine m_2,

$$a=m_1/m_2 \qquad (5\text{-}3b)$$

$$H_R=16\lambda^{5/2}/\pi \qquad (5\text{-}3c)$$

$$I_{13}=\int_{S_-}^{S_+}ds\ s^2\vartheta_{13} \qquad (5\text{-}3d)$$

with

$$\vartheta_{13} = \exp\left[-\frac{x+(1+a)(\lambda-\mu)}{1+2a}\right] \left[\operatorname{erf}(\sqrt{Y_+}) - \operatorname{erf}(\sqrt{Y_-}) - \frac{2}{\sqrt{\pi}}(\sqrt{Y_+}\, e^{-Y_+} - \sqrt{Y_-}\, e^{-Y_-}) \right] \tag{5-3e}$$

$$x=-\lambda+1/s \tag{5-3f}$$

and

$$Y_{\pm}=\frac{a(1+a)}{1+2a}\left[(x^{\frac{1}{2}}\pm(x+\lambda-\mu)^{\frac{1}{2}}\right]^2 . \tag{5-3g}$$

(III) The rate of (2,3) collision in (5-2b) is (c.f. Eqs. (4-47))

$$\kappa_{23}=H_R\frac{(1+b)^{3/2}}{4b^{\frac{1}{2}}}\frac{p^{\frac{1}{2}}e}{(\pi m_1)^{\frac{1}{2}}}(1+a)^{\frac{1}{2}}\, I_{23} \tag{5-4a}$$

where the fact $m_3=m_1$ has been used and where

$$b=a^2/(1+2a) \tag{5-4b}$$

$$I_{23}=\int_{S_-}^{S_+} ds\, s^2 \int_{Y_-}^{\infty} dy\, e^{-y} \int_{Z_-}^{Z_+} dz\left[(z(y+1/s-\lambda-\frac{b}{1+b}\, z)\right]^{-\frac{1}{2}}\, \Omega \tag{5-4c}$$

with

$$\Omega=(\pi/n)\sum_{j=1}^{n}{}'\Delta(\omega_j,Z) \qquad (5\text{-}4d)$$

in which n is an integer. The convergence of the sum will be independent of n if it is sufficiently large. The parameter Z is proportional to the interaction parameter A defined before

$$Z=A(bz/(1+b))^{\frac{1}{2}} \qquad (5\text{-}4e)$$

$$A=S(2k\theta/pe^2)^{\frac{1}{2}} \qquad (5\text{-}4f)$$

with S being the hard core radius. Finally ω_j is defined in (4-35).

5.1 Parameters for κ_{13} and κ_{23}

(a) The parameters involved in κ_{13} are m_1 (mass of the rare gas), m_2 (fluorine) and q^+ (charge-transfer cross section) which can be expressed in terms of the reduced mobility k_m via the definition of the mean free path ℓ and its relation with the diffusion coefficient D (hence the diffusion momentum transfer cross section Q_D where

$Q_D=2q^+$ (Dalgarno, 1958)). Thus (see e.g., McDaniel, 1964, pp 24, 50, 435)

$$\ell=1/N_3Q_D \tag{5-5a}$$

$$D=3(2\pi k\theta/m_r)^{\frac{1}{2}}\ell/16 \tag{5-5b}$$

and

$$\bar{K}=eD/k\theta \tag{5-5c}$$

where $\bar{K}$ is the mobility, m_r is the reduced mass of (1,3) here. The mean free path ℓ is then

$$\ell=(16k\theta/3e)(m_r/2\pi k\theta)^{\frac{1}{2}}\bar{K}\ . \tag{5-5d}$$

With the aid of these relations, we have

$$q^+=Q_D/2 = (e/1600N_Lk_m)(\pi/m_1k\theta)^{\frac{1}{2}} \tag{5-5e}$$

where the reduced mass $m_r=m_{13}=m_1/2$; the definitions

$$k_m=k_o/300\ (cm^2/s.volt\text{-}sec.) \tag{5-5f}$$

$$k_o=KN_3/N_L \tag{5-5g}$$

and $N_L=2.6885\times10^{19}/cm^3$, the Loschmidt's number have been used. By substituting this expression of q^+, κ_{13} of (5-3a) is now

$$\kappa_{13}=H_R\frac{(1+a)^2}{4a^{3/2}}\frac{e}{1600\sqrt{m}_1}\left(\frac{2\pi}{m_1}\right)^{\frac{1}{2}}\frac{I_{13}}{N_L k_m} \qquad (5\text{-}6a)$$

$$=H_R\frac{(1+a)^2}{4a^{3/2}}\frac{10^{-10}}{\sqrt{m_1}^*}\left(\frac{1.68607\times10^2}{k_m\sqrt{m_1}^*}\,I_{13}\right) \qquad (5\text{-}6b)$$

where the numerical factor follows from using (i) the reduced mass unit

$$m_1=m_1^*\,(1.66047\times10^{-24})\ \text{g} \qquad (5\text{-}6c)$$

so that the mass of atomic O^{16} is 16 in the chemical system, (ii) the value of N_L just given, (iii) the charge of electron, 4.80325×10^{-10} e.s.u.

So in κ_{13} we need (i) the mass m* of rare gas (ii) a, mass ratio of rare gas to fluorine, (iii) the reduced mobility k_m of ion in its parent gas.

(b) For κ_{23} we first express b in terms of a and use the reduced mass m_1^* and the reduced polarizability p* which is defined as

$$p=p^*\times10^{-24}\ \text{cm} \qquad (5\text{-}7a)$$

so that

$$\kappa_{23}=H_R\frac{(1+a)^{7/2}}{4a^{3/2}(1+2a)}\left(\frac{p^*a}{\pi m_1^*}\right)^{\frac{1}{2}}\times3.72792\times10^{-10}I_{23}. \qquad (5\text{-}7b)$$

Also note that in I_{23}, we need the interaction parameter A

which can be easily calculated from (5-4f) with the knowledge of the polarizability p and the hard core radius S. A in turn dictates variation of Z, which then determines Ω over z. The parameters needed here are : (i) m* , (ii)a, (iii)p*, the reduced polarizability of the neutral and (iv) A, the interacton parameter. We list all the parameters involved in κ_{13} and κ_{23} in Table 5.1 and Table 5.2 respectively. The total encounter rate coefficient $\kappa_{\lambda\mu}$ is, following (5-2b), (5-6b) and (5-7b),

$$\kappa_{\lambda\mu}=H_R \frac{(1+a)^2}{4a^{3/2}} \frac{10^{-10}}{\sqrt{m_1^*}} I(\lambda,\mu) \qquad (5\text{-}8a)$$

where

$$I(\lambda,\mu)=I_{\lambda\mu}=C_{13}I_{13}+C_{23}I_{23} \qquad (5\text{-}8b)$$

$$C_{13}=1.68607\times10^2/k_m(m^*)^{\frac{1}{2}} \qquad (5\text{-}8c)$$

$$C_{23}=3.72792\times(p^*a/\pi)^{\frac{1}{2}}\times(1+a)^{3/2}/(1+2a) \qquad (5\text{-}8d)$$

This $\kappa_{\lambda\mu}$ together with I_{13}, I_{23} defined in (5-3d to 5-3g) and (5-4b to 5-4f) respectively will be used in the following calculation. Note that this $\kappa_{\lambda\mu}$ of (5-8a) and (5-2a) will finally lead to the expression of α_R

$$\alpha_R=C_\alpha \int_\nu^\omega d\lambda e^\lambda \int_{-\infty}^{\nu} d\mu (\rho(\mu)-\rho(\lambda))(C_{13}I_{13}+C_{23}I_{23}) \qquad (5\text{-}8e)$$

where

$$C_\alpha = N_3^* N_L (\pi/m_1^*)^{\frac{1}{2}} \frac{2e^6}{(kx10^2\theta^*)^3} \frac{(1+a)^2}{a^{3/2}} x10^{-10}$$

$$= N_3^* (\pi/m_1^*)^{\frac{1}{2}} \frac{(1+a)^2}{a^{3/2}} \frac{4.4478x10^{-5}}{(\theta^*)^3} \qquad (5\text{-}8f)$$

in which H_R, the Loschimidt number N_L, electron charge e and Boltzmann constant k have been inserted. Note that ν is a positive number $\nu \leq s$ and C_α is linearly proportional to the neutral gas density N_3^* (in unit of N_L).

Table 5.1 parameters of κ_{13}

$m_F^*=18.9984$

Rg	m_1^*	a	$k_m^{(a)}$	C_{13}
He	4.003	0.2107	10.3	8.181738
Ne	20.183	1.0623	4.08	9.198618
Ar	39.944	2.1023	1.52	17.551177
Kr	83.80	4.4105	0.823	22.379674
Xe	131.30	6.9105	0.57	25.814177

(a) Ellis et al, Atomic Data & Nucl. Data Tables, 17,177,1976

Table 5.2: parameters of κ_{23}

(m_1^* and a are the same as in Table 5.1)

Rg	$b=a^2/(1+2a)$	$p^{*(b)}$	$A^{(c)}$	C_{23}
He	0.03213	0.205	0.6357	0.406975
Ne	0.3612	0.395	0.5080	1.291360
Ar	0.8492	1.640	0.3219	4.100145
Kr	1.9807	2.480	0.2813	8.913778
Xe	3.2221	4.040	0.2579	16.682666

(b) McDaniel and Mason , 1973

(c) from (5-4f)

5.2 General Calculational Procedure

We may separately calculate κ_{13}, κ_{23} using (5-3a) and (5-4a) to get $\kappa_{\lambda\mu}$ for solving the distribution function $\rho(\lambda)$. For practical purpose only tables of I_{13}, I_{23} are needed as can be seen from equations (5-8).

Since the parameters involved vary from one rare gas to another I_{13} and I_{23} are not the same for different systems. They should therefore be generated for each system. The binding energy for the system (RgF)* is $E_D \simeq$ 5ev corresponding to $\omega \simeq 200$ (in $k\theta$ unit of room temperature $\theta = 300^{\circ}k$) and $E_s \simeq$ 0.5ev corresponding to $s \simeq 20$. Since $\kappa_{13}(\lambda, \mu)$, $\kappa_{23}(\lambda, \mu)$ decay quickly for increasing $(\lambda - \mu)$, (i.e., the energy difference), for decreasing μ (to $-\infty$) or for increasing λ for a fixed μ (and vice versa), the choice of s=10, and ω =12.5 are practical values for calculation. See figures of $F_R^{(1)}(\sim \kappa_{13})$, $F_R^{(2)}(\sim \kappa_{23})$, and $F_R(\sim \kappa_{\lambda\mu})$ for each particular case, where $F_R^{(i)}$ and F_R are, apart from a constant factor, the rate coefficients of the (i,3) encounter and the sum of (1,3) and (2,3) encounters respectively

$$F_R^{(i)} \simeq C_{i3} \lambda^{5/2} I_{i3}, \quad i=1,2$$

$$F_R = F_R^{(1)} + F_R^{(2)} \tag{5-9}$$

(typical behaviour of F_{13}^R and F_R can be seen in Fig 5.1

to 5.8 for Ar and Fig 5.10 to 5.17 for Kr).

Note that negative λ and μ correspond to free states while positive λ and μ represent bound states. Opposite sign of λ and μ represents either a bound-free or a free-bound transition. In both equations of α_R ((5-2a) or (5-8e)) and the integral equation of $\rho(\lambda)$ no negative values of λ are involved.

(a) $I_{13}(\nu\kappa_{13})$

I_{13} involves only a one-dimensional integration as can be seen in (5-3d,e) hence can be generated very quickly. There is a finite peak for each range close to $\lambda=\mu$ as physically expected. Tables of I_{13} are generated at the mesh size equal to 0.25. When finer mesh (say 1/16) is needed, interpolation from the tables will suffice. Tables of I_{13} for each gas are presented in Tables 5.3, 5.4, 5.5, 5.6 and 5.7.

Table 5.3 I_{13} for He

μ/λ	0.25	0.5	1.	2.	3.	4.	5.	6.
-8.	3.0144E-03	3.6992E-04	3.3101E-05	1.6624E-06	1.8391E-07	2.8440E-08	5.3044E-09	1.1163E-09
-6.	1.7982E-02	2.2265E-03	2.0215E-04	1.0377E-05	1.1671E-06	1.8287E-07	3.4481E-08	7.3229E-09
-4.	9.7043E-02	1.2268E-02	1.1487E-03	6.1463E-05	7.1112E-06	1.1380E-06	2.1815E-07	4.6955E-08
-2.	4.1945E-01	5.6200E-02	5.6893E-03	3.3292E-04	4.0624E-05	6.7413E-06	1.3274E-06	2.9154E-07
0.	6.3140E-01	1.3276E-01	1.9389E-02	1.4951E-03	2.0633E-04	3.6788E-05	7.5978E-06	1.7274E-06
.25	---	1.2273E-01	2.1074E-02	1.7585E-03	2.4933E-04	4.5080E-05	9.3910E-06	2.1477E-06
.5	1.5759E-01	---	2.2097E-02	2.0490E-03	2.9995E-04	5.5097E-05	1.1587E-05	2.6669E-06
1.	4.4614E-02	3.6432E-02	---	2.6791E-03	4.2718E-04	8.1553E-05	1.7536E-05	4.0953E-06
2.	1.0120E-02	9.1828E-03	7.2825E-03	---	7.8640E-04	1.7015E-04	3.8970E-05	9.4624E-06
3.	3.9001E-03	3.6542E-03	3.1565E-03	2.1377E-03	---	3.1855E-04	8.1758E-05	2.1081E-05
4.	1.9169E-03	1.8246E-03	1.6380E-03	1.2573E-03	8.6591E-04	---	1.5492E-04	4.4404E-05
5.	1.0854E-03	1.0430E-03	9.5742E-04	7.8274E-04	6.0411E-04	4.2111E-04	---	8.4863E-05
6.	6.7479E-04	6.5257E-04	6.0780E-04	5.1663E-04	4.2342E-04	3.2811E-04	2.3058E-04	---
8.	3.1327E-04	3.0540E-04	2.8954E-04	2.5737E-04	2.2459E-04	1.9120E-04	1.5718E-04	1.2253E-04
10.	1.7055E-04	1.6707E-04	1.6009E-04	1.4593E-04	1.3156E-04	1.1695E-04	1.0210E-04	8.7009E-05

Table 5.4 I_{13} for Ne

μ / λ	0.25	0.5	1.	2.	3.	4.	5.	6.
-8.	2.0070E-03	2.7554E-04	2.8479E-05	1.6786E-06	2.0384E-07	3.3563E-08	6.5562E-09	1.4293E-09
-6.	2.0825E-02	2.7042E-03	2.6108E-04	1.4345E-05	1.6789E-06	2.7012E-07	5.1932E-08	1.1193E-08
-4.	1.9620E-01	2.4423E-02	2.2434E-03	1.1720E-04	1.3363E-05	2.1159E-06	4.0236E-07	8.6069E-08
-2.	1.4809E+00	1.8407E-01	1.6875E-02	8.8040E-04	1.0029E-04	1.5864E-05	3.0141E-06	6.4411E-07
0.	3.7621E+00	6.9642E-01	8.6117E-02	5.4727E-03	6.7028E-04	1.0990E-04	2.1310E-05	4.6124E-06
.25	---	6.6952E-01	9.7855E-02	6.6936E-03	8.3794E-04	1.3875E-04	2.7049E-05	5.8733E-06
.5	8.5968E-01	---	1.0675E-01	8.1040E-03	1.0427E-03	1.7470E-04	3.4273E-05	7.4647E-06
1.	2.0716E-01	1.7600E-01	---	1.1397E-02	1.5868E-03	2.7435E-04	5.4693E-05	1.2032E-05
2.	3.8519E-02	3.6320E-02	3.0979E-02	---	3.3059E-03	6.4260E-04	1.3509E-04	3.0595E-05
3.	1.3108E-02	1.2702E-02	1.1725E-02	8.9864E-03	---	1.3373E-03	3.1390E-04	7.4944E-05
4.	5.8997E-03	5.7851E-03	5.5104E-03	4.7482E-03	3.6352E-03	---	6.5255E-04	1.7306E-04
5.	3.1265E-03	3.0851E-03	2.9861E-03	2.7133E-03	2.3195E-03	1.7738E-03	---	3.5936E-04
6.	1.8453E-03	1.8278E-03	1.7858E-03	1.6705E-03	1.5053E-03	1.2787E-03	9.7684E-04	---
8.	7.9325E-04	7.8891E-04	7.7850E-04	7.4999E-04	7.0952E-04	6.5484E-04	5.8292E-04	4.9057E-04
10.	4.0875E-04	4.0735E-04	4.0395E-04	3.9469E-04	3.8151E-04	3.6375E-04	3.4065E-04	3.1132E-04

Table 5.5 I_{13} for Ar

μ/λ	0.25	0.5	1.	2.	3.	4.	5.	6.
-8.	1.8931E-04	3.6314E-05	5.3487E-06	4.3628E-07	6.2354E-08	1.1356E-08	2.3773E-09	5.4549E-10
-6.	3.9414E-03	6.2387E-04	7.4899E-05	5.0448E-06	6.5416E-07	1.1207E-07	2.2491E-08	5.0017E-09
-4.	7.7335E-02	1.0365E-02	1.0306E-03	5.7834E-05	6.8200E-06	1.1008E-06	2.1193E-07	4.5708E-08
-2.	1.2485E+00	1.4887E-01	1.2911E-02	6.3040E-04	6.8885E-05	1.0580E-05	1.9656E-06	4.1276E-07
0.	6.6649E+00	1.0741E+00	1.1174E-01	5.8300E-03	6.3456E-04	9.5968E-05	1.7531E-05	3.6244E-06
.25	---	1.0997E+00	1.3504E-01	7.4965E-03	8.2669E-04	1.2547E-04	2.2934E-05	4.7394E-06
.5	1.4120E+00	---	1.5590E-01	9.5374E-03	1.0721E-03	1.6363E-04	2.9955E-05	6.1911E-06
1.	2.8589E-01	2.5703E-01	---	1.4764E-02	1.7727E-03	2.7583E-04	5.0854E-05	1.0528E-05
2.	4.3139E-02	4.2744E-02	4.0134E-02	---	4.3301E-03	7.4509E-04	1.4235E-04	2.9916E-05
3.	1.2932E-02	1.3061E-02	1.3099E-02	1.1770E-02	---	1.7761E-03	3.7523E-04	8.2077E-05
4.	5.3350E-03	5.4187E-03	5.5402E-03	5.5055E-03	4.8279E-03	---	8.7802E-04	2.1230E-04
5.	2.6508E-03	2.6965E-03	2.7766E-03	2.8593E-03	2.7726E-03	2.3889E-03	---	4.9019E-04
6.	1.4891E-03	1.5149E-03	1.5625E-03	1.6333E-03	1.6486E-03	1.5687E-03	1.3325E-03	---
8.	5.9566E-04	6.0525E-04	6.2377E-04	6.5646E-04	6.8186E-04	6.9142E-04	6.7748E-04	6.2717E-04
10.	2.9213E-04	2.9644E-04	3.0479E-04	3.2067E-04	3.3454E-04	3.4527E-04	3.4890E-04	3.4807E-04

Table 5.6 I_{13} for Kr

μ/λ	0.25	0.5	1.	2.	3.	4.	5.	6.
-8.	2.6276E-06	1.1622E-06	3.3656E-07	4.6440E-08	8.4603E-09	1.7810E-09	4.1102E-10	1.0117E-10
-6.	1.0557E-04	3.2582E-05	6.8794E-06	7.1660E-07	1.1280E-07	2.1621E-08	4.6691E-09	1.0934E-09
-4.	6.2207E-03	1.2096E-03	1.6832E-04	1.2244E-05	1.6109E-06	2.7600E-07	5.5131E-08	1.2186E-08
-2.	4.1365E-01	5.1831E-02	4.6359E-03	2.2643E-04	2.4376E-05	3.6842E-06	6.7459E-07	1.3982E-07
0.	1.0431E+01	1.3344E+00	1.0509E-01	4.0519E-03	3.7056E-04	5.0030E-05	8.4221E-06	1.6363E-06
.25	---	1.5725E+00	1.4368E-01	5.7028E-03	5.1714E-04	6.9188E-05	1.1542E-05	2.2261E-06
.5	2.0192E+00	---	1.8665E-01	7.9456E-03	7.1480E-04	9.5534E-05	1.5811E-05	3.0280E-06
1.	3.0418E-01	3.0773E-01	---	1.4751E-02	1.3789E-03	1.8112E-04	2.9596E-05	5.5971E-06
2.	3.2818E-02	3.5610E-02	4.0099E-02	---	4.5213E-03	6.2659E-04	1.0189E-04	1.8979E-05
3.	8.0894E-03	8.7080E-03	1.0189E-02	1.2290E-02	---	1.9206E-03	3.3486E-04	6.2914E-05
4.	2.9420E-03	3.1637E-03	3.6379E-03	4.6299E-03	5.2208E-03	---	9.7822E-04	1.9868E-04
5.	1.3341E-03	1.4232E-03	1.6159E-03	2.0465E-03	2.4743E-03	2.6591E-03	---	5.5960E-04
6.	6.9942E-04	7.4092E-04	8.3068E-04	1.0360E-03	1.2637E-03	1.4680E-03	1.5212E-03	---
8.	2.5399E-04	2.6615E-04	2.9227E-04	3.5205E-04	4.2183E-04	4.9924E-04	5.7582E-04	6.3189E-04
10.	1.1674E-04	1.2139E-04	1.3130E-04	1.5369E-04	1.7977E-04	2.0956E-04	2.4241E-04	2.7631E-04

Table 5.7 I_{13} for Xe

μ/λ	0.25	0.5	1.	2.	3.	4.	5.	6.
-8.	2.8006E-07	1.6255E-07	6.0624E-08	1.0507E-08	2.1458E-09	4.9149E-10	1.1558E-10	2.9465E-11
-6.	9.4568E-06	4.4750E-06	1.3192E-06	1.7756E-07	3.1359E-08	6.4185E-09	1.4443E-09	3.4721E-10
-4.	6.8482E-04	2.0508E-04	3.9476E-05	3.5916E-06	5.1682E-07	9.2832E-08	1.9070E-08	4.2884E-09
-2.	1.1465E-01	1.6680E-02	1.7083E-03	8.9464E-05	9.7969E-06	1.4862E-06	2.7186E-07	5.6179E-08
0.	1.2146E+01	1.2950E+00	8.2742E-02	2.5699E-03	2.0975E-04	2.6258E-05	4.1964E-06	7.6483E-07
.25	---	1.7565E+00	1.2640E-01	3.8914E-03	3.0852E-04	3.7776E-05	5.9359E-06	1.0959E-06
.5	2.2554E+00	---	1.8321E-01	5.8458E-03	4.5340E-04	5.4366E-05	8.4026E-06	1.5314E-06
1.	2.6759E-01	3.0206E-01	---	1.2679E-02	9.7119E-04	1.1253E-04	1.6863E-05	2.9966E-06
2.	2.2393E-02	2.6199E-02	3.4465E-02	---	4.0830E-03	4.7269E-04	6.7843E-05	1.1531E-05
3.	4.8260E-03	5.5235E-03	7.1762E-03	1.1099E-02	---	1.7947E-03	2.6562E-04	4.4178E-05
4.	1.6063E-03	1.8003E-03	2.2602E-03	3.4927E-03	4.8785E-03	---	9.3828E-04	1.6392E-04
5.	6.8609E-04	7.5638E-04	9.2069E-04	1.3627E-03	1.9627E-03	2.5505E-03	---	5.4823E-04
6.	3.4471E-04	3.7471E-04	4.4473E-04	6.2958E-04	8.8733E-04	1.2112E-03	1.4902E-03	---
8.	1.1774E-04	1.2581E-04	1.4392E-04	1.8974E-04	2.5169E-04	3.3407E-04	4.3815E-04	5.5314E-04
10.	5.1908E-05	5.4819E-05	6.1225E-05	7.6806E-05	9.7005E-05	1.2318E-04	1.5671E-04	1.9849E-04

(b) $I_{23}(\nu\ \kappa_{23})$

In this three-dimensional integration of I_{23}, a table for the cross section $\Delta(\cos\psi, Z)$ is required, where Z is proportional to the square root of $bz/(1+b)$ and is linearly proportional to the interacton parameter A. Since b and A vary from one system to another, a table general enough to cover all five cases is needed. We prepare a table of $\Delta(\cos\psi, Z)$ with 61 sets of Z (for Z from 0. to 5. at step mostly equal to 0.1) and in each set there are 101 points of ψ from 1.8° to 179.1° at interval mostly equal to 1.8°. Reprsentative results are displayed in Table 5.8.

Even with the availability of table $\Delta(\cos\psi, Z)$, the three dimensional integration is still very time consuming. In order to reduce computing time we did not generate full tables of I_{23} as in the case of I_{13}. Instead we generated I_{23} for λ =(0.25, to 12.5) with μ =(-10 to 0), then for the same range of μ with λ =(0.25 to 12.5) for $\lambda > \mu$. The use of detailed balance permitted the calculation of the remaining elements of I_{23}. We have compared some elements generated directly and those from using the detailed balance, with excellent agreement. After various tests we adopted the Gauss Quadrature which

for a given relative accuracy of 10^{-4} is much faster than Simpson's Quadrature. Tables for the five cases of I_{23} with the mesh size equal to 0.25 have been generated. Partial results are shown in Tables 5.9 to 5.13. Tables 5.14 to 5.18 give partial results of $I_{\lambda\mu}$ defined in (5-8).

At $\lambda=\mu$, I_{23} has a singularity, an indication of the failure of this classical approach at $\lambda=\mu$. No attempt is made to generate these I_{23} in this neighborhood. Fortunately in neither the equation of the quasi-equilibrium distribution $\rho(\lambda)$ nor the final calculation of the recombination coefficient α_R are the $\lambda=\mu$ elements needed. (although additional points are required in the neighborhood of $\lambda=\mu$ for interpolation in the precise calculation). This is obvious from Eq. (5-2a) since all values of λ are greater than values of μ except $\lambda=\mu=\nu$ where exact cancellation occurs. So the point of $\lambda=\mu$ will not contribute to α_R. For the case of $\rho(\lambda)$ we will have a separate discussion in (c).

Table 5.8 $\Delta(\psi, z)$: scattering due to Langevin's Potential

ψ /Z	0.	0.3	0.9	1.55	2.0	3.0	4.0	8.0
	---	---	---	-63.96	-35.97	-15.36	-8.55	-2.11
2	3317.39	3342.191	3342.453	3340.606	3338.842	3334.992	3331.944	3325.640
10	55.703	60.675	60.736	60.385	60.044	59.290	3.211	4.684
20	9.126	11.630	11.674	11.526	11.374	2.138	2.511	4.278
30	3.081	4.771	4.815	4.747	4.666	1.868	2.292	4.156
40	1.403	2.692	2.740	2.719	1.324	1.742	2.190	4.100
50	.754	1.809	1.861	1.875	1.233	1.671	2.134	4.070
60	.452	1.356	1.412	1.453	1.177	1.628	2.100	4.051
80	.201	.933	.991	.912	1.114	1.581	2.062	4.032
100	.110	.762	.813	.874	1.081	1.557	2.044	4.022
120	.072	.708	.733	.853	1.064	1.544	2.034	4.017
140	.056	.759	.710	.842	1.054	1.537	2.028	4.014
160	.063	1.083	.781	.835	1.049	1.534	2.025	4.013

N.B. a) ψ in degree, b) 2nd row gives ψ_c: critical angle of orbiting ($Z \geq 1$ only)

Table 5.9 I_{23} for He

μ/λ	0.25	0.5	1.	2.	3.	4.	5.	6.
-8.	7.9718E-10	2.0666E-09	1.5197E-09	2.7634E-10	4.9191E-11	9.6337E-12	1.7510E-12	3.0930E-13
-6.	1.2683E-07	1.1265E-07	4.1316E-08	6.2398E-09	1.1229E-09	2.0925E-10	4.0955E-11	7.7465E-12
-4.	1.0079E-05	4.6771E-06	1.3382E-06	1.7378E-07	2.6866E-08	4.7797E-09	8.6344E-10	1.7432E-10
-2.	1.9417E-03	6.0839E-04	1.1062E-04	7.4339E-06	8.3970E-07	1.2239E-07	2.0105E-08	3.8051E-09
0.	3.4187E+01	1.5378E+00	4.2598E-02	7.0635E-04	4.1438E-05	4.1012E-06	5.8044E-07	8.9602E-08
.25	---	6.6632E+00	1.1830E-01	1.4072E-03	7.1719E-05	6.8937E-06	8.8725E-07	1.3539E-07
.5	8.5540E+00	---	3.4418E-01	2.8192E-03	1.2632E-04	1.1009E-05	1.3201E-06	2.0887E-07
1.	2.4879E-01	5.6572E-01	---	1.2731E-02	4.1363E-04	2.9977E-05	3.4203E-06	4.7816E-07
2.	8.1862E-03	1.2426E-02	3.4308E-02	---	5.8136E-03	2.6049E-04	2.2570E-05	2.7288E-06
3.	1.1127E-03	1.5105E-03	3.0533E-03	1.5899E-02	---	3.2770E-03	1.8479E-04	1.7920E-05
4.	2.8798E-04	3.6823E-04	6.0620E-04	1.9112E-03	8.8977E-03	---	2.0319E-03	1.3681E-04
5.	1.0090E-04	1.2359E-04	1.8447E-04	4.6097E-04	1.3781E-03	5.5011E-03	---	1.3642E-03
6.	4.3558E-05	4.9940E-05	7.1767E-05	1.4940E-04	3.6019E-04	1.0182E-03	3.7118E-03	---
8.	1.0343E-05	1.1468E-05	1.5878E-05	2.7520E-05	5.2473E-05	1.0533E-04	2.3138E-04	5.9151E-04
10.	2.9490E-06	3.4473E-06	4.5681E-06	7.2541E-06	1.2790E-05	2.2426E-05	4.0431E-05	7.8743E-05

Table 5.10 I_{23} for Ne

μ/λ	0.25	0.5	1.0	1.	2.	3.	4.	5
-8.	1.1298E-03	1.6895E-04	1.9580E-05	1.3025E-06	1.7000E-07	2.9193E-08	5.8576E-09	1.3006E-09
-6.	1.4471E-02	2.0588E-03	2.2207E-04	1.3520E-05	1.6586E-06	2.7392E-07	5.3353E-08	1.1581E-08
-4.	2.1054E-01	2.7645E-02	2.6998E-03	1.4872E-04	1.7041E-05	2.6663E-06	4.9950E-07	1.0555E-07
-2.	3.4222E+00	4.1796E-01	3.6518E-02	1.7385E-03	1.8377E-04	2.7034E-05	4.8659E-06	9.8791E-07
0.	1.3900E+02	1.0777E+01	6.5587E-01	2.3591E-02	2.1540E-03	2.9493E-04	5.0066E-05	9.7276E-06
.25	---	2.4266E+01	1.0409E+00	3.3386E-02	2.9729E-03	3.9943E-04	6.7327E-05	1.3003E-05
.5	3.1158E+01	---	1.8146E+00	4.8052E-02	4.1310E-03	5.4246E-04	9.0635E-05	1.7390E-05
1.	2.2036E+00	2.9917E+00	---	1.0691E-01	8.0901E-03	1.0186E-03	1.6477E-04	3.1173E-05
2.	1.9212E-01	2.1535E-01	2.9062E-01	---	3.6964E-02	3.8035E-03	5.6797E-04	1.0222E-04
3.	4.6503E-02	5.0326E-02	5.9778E-02	1.0048E-01	---	1.7247E-02	2.0791E-03	3.4827E-04
4.	1.6984E-02	1.7964E-02	2.0459E-02	2.8104E-02	4.6882E-02	---	9.6020E-03	1.2750E-03
5.	7.7820E-03	8.1587E-03	8.9959E-03	1.1408E-02	1.5362E-02	2.6101E-02	---	5.9780E-03
6.	4.0855E-03	4.2526E-03	4.6265E-03	5.5813E-03	6.9952E-03	9.4212E-03	1.6250E-02	---
8.	1.4760E-03	1.5253E-03	1.6296E-03	1.8626E-03	2.1671E-03	2.5855E-03	3.2217E-03	4.3725E-03
10.	6.7149E-04	6.8711E-04	7.2059E-04	8.0359E-04	9.0475E-04	1.0308E-03	1.1946E-03	1.4216E-03

Table 5.11 I_{23} for Ar

μ/λ	0.25	0.5	1.	2.	3.	4.	5.	6.
-8.	7.6558E-03	9.6078E-04	8.7709E-05	4.5716E-06	5.2021E-07	8.0879E-08	1.4980E-08	3.1391E-09
-6.	6.4112E-02	7.9916E-03	7.3333E-04	3.7919E-05	4.2086E-06	6.5429E-07	1.2081E-07	2.5065E-08
-4.	5.5892E-01	6.9415E-02	6.2789E-03	3.1874E-04	3.4769E-05	5.3589E-06	9.8341E-07	2.0335E-07
-2.	5.3260E+00	6.5507E-01	5.7240E-02	2.8314E-03	2.9905E-04	4.4954E-05	8.1547E-06	1.6625E-06
0.	1.3467E+02	1.0779E+01	7.1186E-01	2.8391E-02	2.7693E-03	3.9915E-04	7.0274E-05	1.3986E-05
.25	---	2.3594E+01	1.0818E+00	3.8971E-02	3.6997E-03	5.2843E-04	9.2399E-05	1.8325E-05
.5	3.0296E+01	---	1.8242E+00	5.4138E-02	4.9688E-03	7.0286E-04	1.2185E-04	2.4038E-05
1.	2.2902E+00	3.0078E+00	---	1.1265E-01	9.1580E-03	1.2504E-03	2.1265E-04	4.1529E-05
2.	2.2426E-01	2.4263E-01	3.0623E-01	---	3.7402E-02	4.2109E-03	6.7015E-04	1.2651E-04
3.	5.7874E-02	6.0533E-02	6.7669E-02	1.0167E-01	---	1.7701E-02	2.2760E-03	3.9905E-04
4.	2.2470E-02	2.3276E-02	2.5115E-02	3.1115E-02	4.8117E-02	---	9.8123E-03	1.3675E-03
5.	1.0580E-02	1.0969E-02	1.1510E-02	1.3460E-02	1.6818E-02	2.6673E-02	---	6.0313E-03
6.	5.7575E-03	5.8819E-03	6.1634E-03	6.9075E-03	8.0151E-03	1.0105E-02	1.6395E-02	---
8.	2.1735E-03	2.2101E-03	2.2850E-03	2.4756E-03	2.6983E-03	3.0093E-03	3.5112E-03	4.4963E-03
10.	1.0255E-03	1.0410E-03	1.0667E-03	1.1222E-03	1.1926E-03	1.2854E-03	1.4094E-03	1.5878E-03

Table 5.12 I_{23} for Kr

μ/λ	0.25	0.5	1.	2.	3.	4.	5.	6.
-8.	2.7691E-03	3.6695E-04	3.6295E-05	2.0295E-06	2.3859E-07	3.8265E-08	7.2542E-09	1.5369E-09
-6.	2.8445E-02	3.6437E-03	3.4951E-04	1.8765E-05	2.1354E-06	3.3510E-07	6.2795E-08	1.3181E-08
-4.	2.9628E-01	3.7202E-02	3.4294E-03	1.7577E-04	1.9354E-05	2.9844E-06	5.4874E-07	1.1368E-07
-2.	3.4208E+00	4.0999E-01	3.6111E-02	1.7256E-03	1.8485E-04	2.7270E-05	4.8827E-06	9.9266E-07
0.	1.0040E+02	8.0358E+00	5.1379E-01	1.9614E-02	1.8759E-03	2.6220E-04	4.5322E-05	8.9606E-06
.25	---	1.7583E+01	7.8680E-01	2.7204E-02	2.5310E-03	3.4979E-04	6.0151E-05	1.1954E-05
.5	2.2577E+01	---	1.3433E+00	3.8346E-02	3.4444E-03	4.6743E-04	7.9998E-05	1.5678E-05
1.	1.6657E+00	2.2147E+00	---	8.1016E-02	6.5386E-03	8.4651E-04	1.4196E-04	2.7431E-05
2.	1.5655E-01	1.7185E-01	2.2186E-01	---	2.7606E-02	2.9680E-03	4.5908E-04	8.5873E-05
3.	3.9592E-02	4.1961E-02	4.8314E-02	7.5041E-02	---	1.2963E-02	1.6192E-03	2.7917E-04
4.	1.4873E-02	1.5479E-02	1.7003E-02	2.1931E-02	3.5237E-02	---	7.2077E-03	9.6508E-04
5.	6.9526E-03	7.2011E-03	7.7517E-03	9.2209E-03	1.1964E-02	1.9593E-02	---	4.4248E-03
6.	3.7244E-03	3.8362E-03	4.0711E-03	4.6889E-03	5.6074E-03	7.2788E-03	1.2028E-02	---
8.	1.3714E-03	1.4043E-03	1.4741E-03	1.6318E-03	1.8345E-03	2.1076E-03	2.5237E-03	3.2975E-03
10.	6.3272E-04	6.4466E-04	6.6948E-04	7.2637E-04	7.9355E-04	8.7546E-04	9.7989E-04	1.1294E-03

Table 5.13 $I_{23} \equiv I_{23}(\lambda, \mu)$ for Xe

μ/λ	0.25	0.5	1.	2.	3.	4.	5.	6.
-8.	4.2429E-04	6.4079E-05	7.6141E-06	5.2126E-07	6.9181E-08	1.1796E-08	2.3558E-09	5.1864E-10
-6.	6.4840E-03	6.9581E-04	9.7677E-05	5.8271E-06	7.3004E-07	1.2007E-07	2.3091E-08	4.9520E-09
-4.	1.0219E-01	1.3186E-02	1.2937E-03	6.8997E-05	7.8985E-06	1.2359E-06	2.3119E-07	4.8092E-08
-2.	1.7717E+00	2.1382E-01	1.8442E-02	8.6401E-04	9.0501E-05	1.3337E-05	2.3668E-06	4.7378E-07
0.	7.4122E+01	5.8326E+00	3.5017E-01	1.2391E-02	1.1239E-03	1.5127E-04	2.5152E-05	4.8404E-06
.25	---	1.2965E+01	5.5620E-01	1.7585E-02	1.5519E-03	2.0589E-04	3.4053E-05	6.4716E-06
.5	1.6647E+01	---	9.7691E-01	2.5617E-02	2.1427E-03	2.8092E-04	4.6134E-05	8.7099E-06
1.	1.1775E+00	1.6107E+00	---	5.7316E-02	4.2518E-03	5.2599E-04	8.4686E-05	1.5785E-05
2.	1.0120E-01	1.1481E-01	1.5580E-01	---	1.9728E-02	1.9974E-03	2.9326E-04	5.2866E-05
3.	2.4276E-02	2.6103E-02	3.1417E-02	5.3625E-02	---	9.3058E-03	1.1107E-03	1.8226E-04
4.	8.7546E-03	9.3028E-03	1.0565E-02	1.4759E-02	2.5296E-02	---	5.1711E-03	6.8257E-04
5.	3.9364E-03	4.1529E-03	4.6237E-03	5.8902E-03	8.2071E-03	1.4056E-02	---	3.2108E-03
6.	2.0333E-03	2.1312E-03	2.3426E-03	2.8864E-03	3.6608E-03	5.0436E-03	8.7280E-03	---
8.	7.2688E-04	7.5268E-04	8.0942E-04	9.4422E-04	1.1196E-03	1.3504E-03	1.7088E-03	2.3345E-03
10.	3.2339E-04	3.3205E-04	3.5453E-04	4.0173E-04	4.5821E-04	5.3177E-04	6.2254E-04	7.4939E-04

Table 5.14 $I_{\lambda\mu}$ for He

μ/λ	0.25	0.5	1.	2.	3.	4.	5.	6.
-8.	2.4663E-02	3.0266E-03	2.7083E-04	1.3601E-05	1.5048E-06	2.3269E-07	4.3400E-08	9.1336E-09
-6.	1.4712E-01	1.8217E-02	1.6540E-03	8.4904E-05	9.5497E-06	1.4963E-06	2.8213E-07	5.9917E-08
-4.	7.9399E-01	1.0037E-01	9.3989E-03	5.0294E-04	5.8193E-05	9.3126E-06	1.7852E-06	3.8425E-07
-2.	3.4327E+00	4.6006E-01	4.6594E-02	2.7269E-03	3.3272E-04	5.5205E-05	1.0869E-05	2.3877E-06
0.	1.3172E+01	1.7162E+00	1.7609E-01	1.2522E-02	1.7051E-03	3.0267E-04	6.2401E-05	1.4170E-05
.25	---	3.7339E+00	2.2089E-01	1.4964E-02	2.0693E-03	3.7166E-04	7.7198E-05	1.7628E-05
.5	4.7937E+00	---	3.2180E-01	1.7919E-02	2.5059E-03	4.5530E-04	9.5343E-05	2.1905E-05
1.	4.6694E-01	5.2984E-01	---	2.7135E-02	3.6646E-03	6.7953E-04	1.4487E-04	3.3703E-05
2.	8.6151E-02	8.0222E-02	7.3639E-02	---	8.8158E-03	1.4989E-03	3.2809E-04	7.8537E-05
3.	3.2368E-02	3.0516E-02	2.7076E-02	2.4003E-02	---	3.9488E-03	7.4462E-04	1.7982E-04
4.	1.5801E-02	1.5079E-02	1.3650E-02	1.1070E-02	1.0730E-02	---	2.0999E-03	4.1935E-04
5.	8.9222E-03	8.5844E-03	7.9089E-03	6.5930E-03	5.5073E-03	5.6991E-03	---	1.2532E-03
6.	5.5388E-03	5.3596E-03	5.0023E-03	4.2881E-03	3.6119E-03	3.1016E-03	3.4080E-03	---
8.	2.5674E-03	2.5034E-03	2.3754E-03	2.1170E-03	1.8590E-03	1.6075E-03	1.3808E-03	1.2448E-03
10.	1.3966E-03	1.3684E-03	1.3117E-03	1.1970E-03	1.0816E-03	9.6601E-04	8.5190E-04	7.4415E-04

Table 5.15 $I_{\lambda\mu}$ for Ne

λ/μ	0.25	0.5	1.	2.	3.	4.	5.	6.
-8.	1.9920E-02	2.7528E-03	2.8738E-04	1.7123E-05	2.0946E-06	3.4643E-07	6.7872E-08	1.4827E-08
-6.	2.1025E-01	2.7533E-02	2.6883E-03	1.4941E-04	1.7586E-05	2.8385E-06	5.4660E-07	1.1732E-07
-4.	2.0767E+00	2.6035E-01	2.4123E-02	1.2702E-03	1.4493E-04	2.2906E-05	4.3462E-06	9.2802E-07
-2.	1.8041E+01	2.2330E+00	2.0239E-01	1.0344E-02	1.1599E-03	1.8083E-04	3.4009E-05	7.2007E-06
0.	2.1411E+02	2.0323E+01	1.6391E+00	8.0806E-02	8.9472E-03	1.3918E-03	2.6067E-04	5.4989E-05
.25	---	3.7494E+01	2.2443E+00	1.0469E-01	1.1547E-02	1.7921E-03	3.3576E-04	7.0818E-05
.5	4.8144E+01	---	3.3252E+00	1.3660E-01	1.4926E-02	2.3075E-03	4.3230E-04	9.1194E-05
1.	4.7512E+00	5.4824E+00	---	2.4289E-01	2.5044E-02	3.8390E-03	7.1587E-04	1.5094E-04
2.	6.0242E-01	6.1219E-01	6.6025E-01	---	7.8144E-02	1.0823E-02	1.9761E-03	4.1344E-04
3.	1.8062E-01	1.8193E-01	1.8505E-01	2.1242E-01	---	3.4573E-02	5.5723E-03	1.1391E-03
4.	7.6202E-02	7.6413E-02	7.7109E-02	7.9969E-02	9.3980E-02	---	1.8402E-02	3.2384E-03
5.	3.8809E-02	3.8915E-02	3.9085E-02	3.9691E-02	4.1174E-02	5.0022E-02	---	1.1025E-02
6.	2.2251E-02	2.2305E-02	2.2401E-02	2.2573E-02	2.2880E-02	2.3929E-02	2.9970E-02	---
8.	9.2028E-03	9.2265E-03	9.2655E-03	9.3042E-03	9.3250E-03	9.3624E-03	9.5224E-03	1.0159E-02
10.	4.6272E-03	4.6344E-03	4.6463E-03	4.6683E-03	4.6778E-03	4.6771E-03	4.6762E-03	4.6997E-03

Table 5.16 $I_{\lambda\mu}$ for Ar

μ/λ	0.25	0.5	1.	2.	3.	4.	5.	6.
-8.	3.4713E-02	4.5767E-03	4.5349E-04	2.6401E-05	3.2273E-06	5.3092E-07	1.0315E-07	2.2445E-08
-6.	3.3205E-01	4.3717E-02	4.3213E-03	2.4401E-04	2.8737E-05	4.6497E-06	8.9008E-07	1.9056E-07
-4.	3.6490E+00	4.6653E-01	4.3832E-02	2.3220E-03	2.6226E-04	4.1293E-05	7.7518E-06	1.6360E-06
-2.	4.3750E+01	5.3028E+00	4.6130E-01	2.2674E-02	2.4352E-03	3.7001E-04	6.7935E-05	1.4061E-05
0.	5.6916E+02	6.3049E+01	4.8799E+00	2.1873E-01	2.2492E-02	3.3210E-03	5.9583E-04	1.2088E-04
.25	---	1.1604E+02	6.8057E+00	2.9136E-01	2.9679E-02	4.3688E-03	7.8136E-04	1.5832E-04
.5	1.4900E+02	---	1.0216E+01	3.8936E-01	3.9189E-02	5.7537E-03	1.0254E-03	2.0722E-04
1.	1.4408E+01	1.5843E+01	---	7.2103E-01	6.8662E-02	9.9681E-03	1.7645E-03	3.5505E-04
2.	1.6767E+00	1.7450E+00	1.9600E+00	---	2.2935E-01	3.0343E-02	5.2462E-03	1.0438E-03
3.	4.6426E-01	4.7742E-01	5.0735E-01	6.2345E-01	---	1.0375E-01	1.5918E-02	3.0767E-03
4.	1.8576E-01	1.9054E-01	2.0021E-01	2.2420E-01	2.8202E-01	---	5.5656E-02	9.3332E-03
5.	9.0313E-02	9.2300E-02	9.6336E-02	1.0537E-01	1.1762E-01	1.5129E-01	---	3.3333E-02
6.	4.9741E-02	5.0705E-02	5.2594E-02	5.6989E-02	6.1797E-02	6.8964E-02	9.0607E-02	---
8.	1.9366E-02	1.9685E-02	2.0317E-02	2.1672E-02	2.3031E-02	2.4474E-02	2.6287E-02	2.9443E-02
10.	9.3320E-03	9.4712E-03	9.7229E-03	1.0229E-02	1.0762E-02	1.1330E-02	1.1902E-02	1.2619E-02

Table 5.17 $I_{\lambda\mu}$ for Kr

μ/λ	0.25	0.5	1.	2.	3.	4.	5.	6.
-8.	2.4742E-02	3.2969E-03	3.3106E-04	1.9130E-05	2.3160E-06	3.8095E-07	7.3950E-08	1.5964E-08
-6.	2.5592E-01	3.3208E-02	3.2695E-03	1.8331E-04	2.1559E-05	3.4709E-06	6.6423E-07	1.4196E-07
-4.	2.7802E+00	3.5868E-01	3.4336E-02	1.8408E-03	2.0857E-04	3.2780E-05	6.1251E-06	1.2861E-06
-2.	3.9749E+01	4.8145E+00	4.2564E-01	2.0449E-02	2.1932E-03	3.2553E-04	5.8620E-05	1.1977E-05
0.	1.1284E+03	1.0149E+02	6.9317E+00	2.6551E-01	2.5014E-02	3.4568E-03	5.9247E-04	1.1649E-04
.25	---	1.9192E+02	1.0229E+01	3.7012E-01	3.4134E-02	4.6663E-03	7.9449E-04	1.5548E-04
.5	2.4643E+02	---	1.6151E+01	5.1962E-01	4.6710E-02	6.3046E-03	1.0669E-03	2.0751E-04
1.	2.1659E+01	2.6629E+01	---	1.0570E+00	8.9143E-02	1.1599E-02	1.9279E-03	3.6977E-04
2.	2.1299E+00	2.3288E+00	2.8750E+00	---	3.4726E-01	4.0479E-02	6.3724E-03	1.1901E-03
3.	5.3395E-01	5.6892E-01	6.5868E-01	9.4395E-01	---	1.5853E-01	2.1927E-02	3.8965E-03
4.	1.9842E-01	2.0878E-01	2.3297E-01	2.9910E-01	4.3093E-01	---	8.6140E-02	1.3227E-02
5.	9.1831E-02	9.6041E-02	1.0526E-01	1.2799E-01	1.6202E-01	2.3415E-01	---	5.1966E-02
6.	4.8851E-02	5.0777E-02	5.4879E-02	6.4978E-02	7.8263E-02	9.7736E-02	1.4126E-01	---
8.	1.7908E-02	1.8474E-02	1.9681E-02	2.2424E-02	2.5793E-02	2.9959E-02	3.5383E-02	4.3534E-02
10.	8.2525E-03	8.4630E-03	8.9061E-03	9.9142E-03	1.1097E-02	1.2494E-02	1.4160E-02	1.6251E-02

Table 5.18 $I_{\lambda\mu}$ for Xe

μ/λ	0.25	0.5	1.	2.	3.	4.	5.	6.
-8.	7.0855E-03	1.0732E-03	1.2859E-04	8.9673E-06	1.2095E-06	2.0948E-07	4.2311E-08	9.4129E-09
-6.	1.0842E-01	1.5060E-02	1.6636E-03	1.0180E-04	1.2989E-05	2.1688E-06	4.2250E-07	9.1577E-08
-4.	1.7225E+00	2.2527E-01	2.2601E-02	1.2438E-03	1.4511E-04	2.3015E-05	4.3491E-06	9.1300E-07
-2.	3.2517E+01	4.0029E+00	3.5177E-01	1.6724E-02	1.7627E-03	2.6086E-04	4.6502E-05	9.3841E-06
0.	1.5501E+03	1.3073E+02	7.9778E+00	2.7306E-01	2.4165E-02	3.2014E-03	5.2794E-04	1.0101E-04
.25	---	2.6163E+02	1.2542E+01	3.9382E-01	3.3854E-02	4.4093E-03	7.2134E-04	1.3625E-04
.5	3.3594E+02	---	2.1027E+01	5.7827E-01	4.7450E-02	6.0899E-03	9.8655E-04	1.8464E-04
1.	2.6551E+01	3.4668E+01	---	1.2835E+00	9.6002E-02	1.1680E-02	1.8481E-03	3.4063E-04
2.	2.2663E+00	2.5916E+00	3.4889E+00	---	4.3451E-01	4.5525E-02	6.6437E-03	1.1796E-03
3.	5.2956E-01	5.7806E-01	7.0937E-01	1.1811E+00	---	2.0158E-01	2.5387E-02	4.1810E-03
4.	1.8752E-01	2.0167E-01	2.3460E-01	3.3638E-01	5.4794E-01	---	1.1049E-01	1.5619E-02
5.	8.3375E-02	8.8807E-02	1.0090E-01	1.3344E-01	1.8758E-01	3.0034E-01	---	6.7718E-02
6.	4.2809E-02	4.5228E-02	5.0562E-02	6.4405E-02	8.3978E-02	1.1541E-01	1.8408E-01	---
8.	1.5166E-02	1.5804E-02	1.7219E-02	2.0650E-02	2.5176E-02	3.1152E-02	3.9819E-02	5.3225E-02
10.	6.7350E-03	6.9546E-03	7.4951E-03	8.6844E-03	1.0148E-02	1.2051E-02	1.4431E-02	1.7626E-02

(c) $\rho(\lambda)$

The quasi-equilibrium distribution function satisfies the integral equation (3-21) which becomes, with the introduction of the variables λ, μ

$$\rho(\lambda)\int_{-\infty}^{\omega} d\mu\ K_{\lambda\mu} = \int_{-\infty}^{s} d\mu\ \rho(\mu)\ K_{\lambda\mu} \tag{5-10a}$$

to be solved subjected to the boundary conditions

$$\rho(\dot{x}) = \begin{cases} 0 & s \leq x \\ <1 & 0<x<s \\ 1 & -\infty<x\leq 0 \end{cases} \tag{5-10b}$$

Since only the integration over μ is performed, the constant and the factor H_R can be eliminated from (5-9a) so that

$$\rho(\lambda)\int_{-\infty}^{\omega} d\mu\ I(\lambda,\mu) = \int_{-\infty}^{s} d\mu\ \rho(\mu)\ I(\lambda,\mu) \tag{5-10c}$$

where $I(\lambda, \mu)$ are defined in (5-8b) and their components I_{13}, I_{23} have been tabulated. We define, for convenience, two terms I^+, I^- as following

$$I^+(\lambda) = \int_{o}^{\omega} I(\lambda,\mu)d\mu \tag{5-11a}$$

$$I^-(\lambda) = \int_{-\infty}^{o} I(\lambda,\mu)d\mu$$

so that equations (5-10c) becomes

$$\rho(\lambda)\left(I^{-}(\lambda)+I^{+}(\lambda)\right)=I^{-}(\lambda)+\int_{o}^{s}\rho(\mu)\,I(\lambda,\mu)d\mu \quad (5\text{-}12a)$$

where the boundary condition of $\rho=1$ for $-\infty<\mu\leq 0$ has been applied to the integral on the right hand side. Here I^{+} and I^{-} can be prepared separately from the tables of I_{13}, I_{23} or calculated directly. In any case we can now solve ρ by transforming the integral (5-12a) into a quadrature form assuming that the mesh is fine enough to assure convergence. Specifically we use the Simpson Quadrature such that

$$\int_{o}^{s}\rho(\lambda)I(\lambda,\mu)d\mu=\sum_{j=0}^{m}\rho_{j}\,I(\lambda,jh)\,\frac{h}{3}\,C_{j} \quad (5\text{-}12b)$$

where

$$C_{j}=\begin{cases}1 & j=0 \text{ or } m\\ 4 & j=\text{odd}\\ 2 & j=\text{even}\end{cases},$$

h is the mesh size such that mh=s where m is an even number. In other words we break the interval (0,s) into m (even number) equal parts and use Simpson's rule to approximate the integral. By applying the same technique to I^{+} one finds that $\rho(\lambda)I^{+}(\lambda)$ as a Simpson's sum on the left hand side has one term $\lambda=\mu$ identical to the term on

the right hand side so that they cancel each other. Thus (5-12a) becomes

$$\rho_i(I_1^- + I_1^{+'}) = I_i^- + \frac{h}{3} I_{oi} + \sum_{j=1}^{m-1} \frac{h}{3} I_{ij} C_j \rho_j \qquad (5\text{-}12d)$$

where use of $\rho_m = 0$ ($\rho(s)=0$) and omission of the diagonal term in both $\rho_i I_i^{+'}$ and the sum have been made so that

$\sum_{j=1}^{m-1'}$ means no $\lambda = \mu$ term is included. Note also that I_{io} corresponds to the matrix element for $\mu = 0$ for a given λ. Equation (5-12d) can be put into matrix form

$$A_{ij} \rho_j = B_i \qquad (5\text{-}12e)$$

where

$$B_i = -I_i^- - \frac{h}{3} I_{io} \qquad (5\text{-}12f)$$

$$A_{ii} = =-I_i^- - I_i^{+'} \qquad (5\text{-}12g)$$

and

$$A_{ij} = \frac{h}{3} I_{ij} C_j \quad j \neq i \qquad (5\text{-}12h)$$

The solution ρ is given by the matrix equation

$$\rho_i = (A^{-1}_{ij}) B_j \qquad (5\text{-}12i)$$

Thus the procedure is to choose the mesh size h, prepare the corresponding matrix elements and carry out the matrix inversion. The solution can be improved successively by refining the mesh size h to ensure the convergence of all elements involved. In practice finer mesh implies larger dimensions of the matrix involved and also many more I_{13}, I_{23} elements are needed, thereby drastically increasing the computing time. We find that the mesh=1/16 is sufficient for our purpose of calculation.

It is obvious that ρ as a function of λ varies from one gas to another because of the corresponding change of the physical parameters. Nevertheless for the five cases under study, they are very close to each other, as can be seen from Table 5.20 and the figures of ρ (Fig 5.9 for Ar and 5.18 for Kr). This implies that the quasi-equilibrium distributions are not very sensitive to the change of the physical systems.

Table 5.19 $\rho(\lambda)$ for the recombination cases

λ/$\rho(\lambda)$	He	Ne	Ar	Kr	Xe
0.	1.	1.	1.	1.	1.
.25	9.9188E-01	9.9312E-01	9.9350E-01	9.9380E-01	9.9399E-01
.5	9.5810E-01	9.6367E-01	9.6511E-01	9.6616E-01	9.6670E-01
.75	9.0363E-01	9.1412E-01	9.1723E-01	9.1883E-01	9.1967E-01
1.	8.3550E-01	8.5009E-01	8.5461E-01	8.5685E-01	8.5786E-01
1.5	6.8382E-01	7.0234E-01	7.0828E-01	7.1129E-01	7.1221E-01
2.	5.3601E-01	5.5510E-01	5.6140E-01	5.6361E-01	5.6392E-01
2.5	4.1290E-01	4.2597E-01	4.2986E-01	4.3196E-01	4.3172E-01
3.	3.1200E-01	3.2040E-01	3.2243E-01	3.2320E-01	3.2246E-01
3.5	2.3362E-01	2.3758E-01	2.3864E-01	2.3782E-01	2.3664E-01
4.	1.7412E-01	1.7452E-01	1.7494E-01	1.7294E-01	1.7142E-01
4.5	1.2959E-01	1.2747E-01	1.2731E-01	1.2480E-01	1.2294E-01
5.	9.6497E-02	9.2836E-02	9.2279E-02	8.9519E-02	8.7556E-02
6.	5.3919E-02	4.9187E-02	4.8169E-02	4.5597E-02	4.3836E-02
7.	3.0504E-02	2.6167E-02	2.5088E-02	2.3082E-02	2.1711E-02
8.	1.7271E-02	1.3855E-02	1.2987E-02	1.1547E-02	1.0576E-02
9.	9.2755E-03	6.9582E-03	6.3572E-03	5.4431E-03	4.8238E-03
9.5	6.2335E-03	4.5283E-03	4.0734E-03	3.4146E-03	2.9706E-03
9.75	4.7114E-03	3.3492E-03	2.9808E-03	2.4743E-03	2.1311E-03
10.	0.	0.	0.	0.	0.

(d) Expression of α_R

From (a), (b), (c) we have now all the information needed for the calculation of α_R. Note also that (5-8d) can be put into the following form with I^-

$$\alpha_R = C_\alpha \Big(\int_\nu^\omega d\lambda \; e^\lambda \; (1-\rho(\lambda)) I^{(-)}(\lambda) + \int_\nu^\omega d\lambda \; e^\lambda \int_o^\nu d\mu \; (\rho(\mu) - \rho(\lambda)) \; I(\lambda,\mu) \Big) . \qquad (5\text{-}13)$$

Once I_{13}, I_{23} are tabulated and $\rho(\lambda)$ calculated, α_R is simple to calculate. The results for He, Ne, Ar, Kr and Xe are all in the order of 10^{-6} cm^3/sec and given in Table 5.20. Tests of variation over values of ν in the range (0, s) have been made and show no change in recombination corfficient α_R as expected.

Table 5.20 α_R and α_R/α_T

X	α_R/N_3^* (a)	$a_R \times 10$ (b)	RATIO α_R/α_T
He	4.641	9.355292	0.3480
Ne	2.990	2.132735	0.4478
Ar	4.515	0.908544	0.4985
Kr	3.882	0.713207	0.4870
Xe	3.661	0.673910	0.4982

(a) in unit of 10^{-6} cm^3/sec. see also C_α in (5-8f).

(b) see a_R in (5-15c).

5.3 Comparison with the Thomson Treatment

Recall that the expression of the recombination rate coefficient α_T for ions in their parent gas, is given by (2-5 and 2-6)

$$\alpha_T = \frac{4\pi}{3} r_T^3 \bar{v} N_3 (2q^+) \qquad (5\text{-}14a)$$

$$= \frac{64\pi}{81} N_3 q^+ \frac{e^6}{(k\theta)^{5/2}} \left(\frac{8(1+a')}{m_1}\right)^{1/2} . \qquad (5\text{-}14b)$$

Here a'=1 in Thomson's treatment of equal masses, we have

$$\alpha_T = \frac{256\pi}{81} q^+ N_3 \frac{e^6}{(k\theta)^{5/2}(m_1)^{\frac{1}{2}}} \qquad (5\text{-}15c)$$

$$= \frac{256\pi \cdot e^6}{81 \cdot k^3\theta^3} N_3 \frac{\pi^{\frac{1}{2}}}{m_1^*} \frac{e}{1600} \frac{(1.66047\times10^{-24})^{-1}}{k_m N_L}$$

after a substitution of q^+ in (5-5c). While according to (5-8e) and (5-8f) and(5-15a) the rate coefficient becomes

$$\alpha_R = \alpha_T a_R \left(\int_\nu^\omega d\lambda\, e^\lambda \int_{-\infty}^{\nu} d\mu \,(\rho(\mu) - \rho(\lambda)) \cdot \right.$$

$$\left. \left[C_{13} I_{13}(\lambda,\mu) + C_{23} I_{23}(\lambda,\mu) \right] \right) \qquad (5\text{-}15b)$$

where

$$a_R = 2.995374\times10^{-3} k_m (m_1^*)^{\frac{1}{2}} (1+a)^2 / a^{3/2} \qquad (5\text{-}15c)$$

The results of the ratio to the Thomson's values are given in Table 5.20. We see that Thomson's model overestimates α_R by about a factor of 2 compared with those from the more detailed calculation. Considering its simplicity in arriving at the estimated values of α_T this is not too much an error.

5.4 Bottleneck Model

The basic expression for the rate of recombination is given by (3-19) or (3-16). While the energy change rate $K_{if}dE_f$ for de-excitation between the neighboring levels increases rapidly with increasing effective quantum number n (i.e., with decreasing binding, smaller λ), the equilibrium populations (3-13) of the excited states (X^+Y^-) decrease with increasing n. Hence the total effective rate for de-excitation will exhibit a minimum for a particular level n* with negative energy E* ($=-\lambda^* k\theta$). Ion-pairs more tightly bound than E* have much greater probability of undergoing further de-excitation to the level for recombination stabilization than those of being excited above the minimum rate state

n^*. Thus the recombination rate is given as the total de-excitation rate pass level n^* which is therefore known as the recombination bottleneck. It is then a sufficient approximation to assume that

$$\rho(x) = \begin{cases} 1 & E \geq E^* \quad (x \leq \lambda^*) \\ 0 & E < E^* \quad (\lambda^* < x) \end{cases} \tag{5-16a}$$

Thus the recombination coefficient is, from (3-16)

$$\alpha^{BT}(\lambda^*) = N_3\left[\pi e^3/(4k^3\theta^3)\right] \int_{\lambda^*}^{\omega} d\lambda \, \frac{e^{\lambda}}{\lambda^{5/2}} \int_{-\infty}^{\lambda^*} d\mu \, \kappa(\lambda,\mu) \tag{5-16b}$$

or from (5-15b)

$$\alpha^{BT}(\lambda^*) = \alpha_T \, a_R \int_{\lambda^*}^{\omega} d\lambda e^{\lambda} \int_{-\infty}^{\lambda^*} d\mu \, (C_{13}I_{13} + C_{23}I_{23}) \tag{5-16c}$$

$$= \alpha_T a_R \, \alpha_o^{BT}$$

where

$$\left(\frac{d\alpha^{BT}}{d\lambda}\right)_{\lambda=\lambda^*} = 0 \tag{5-16d}$$

Calculation of (5-16c) can be performed numerically for each case studied by simultaneously changing the lower limit of λ integration and upper limit of μ integration. The results of the ratio of the minimum rate coefficient to α_T are listed in Table 5.21.

Table 5.21

RESULTS of BTL : Recombination

X	λ^*	α^{BT}/N_3^*	α_o^{BT}	α^{BT}/α_T
He	1.875	9.719	0.7790	0.7288
Ne	2.	7.271	5.1053	1.0888
Ar	2.	11.604	14.1024	1.2812
Kr	2.	10.931	19.224	1.3711
Xe	2.	11.153	22.526	1.5180

(a) α^{BT}/N^* is in unit of $10^{-6} cm^3/sec$

(b) $\alpha^{BT}/\alpha_T = a_R \alpha_o^{BT}$, see a_R in Table 5.20

5.5 Remarks

For each of the five cases of rare-gas halide systems, the matrix elements of the direct collision κ_{23} are all very much alike as we can see from the figures of $F_R^{(2)}$. There is always a sharp peak around $\lambda = \mu$ (i.e., $E_i = E_f$). In fact it blows up at $\lambda = \mu$ though they are excluded in the figures. (The divergence at $\lambda = \mu$ is due to the contribution from the forward angle scattering at infinite impact parameter at which there is always no energy transfer in scattering). As pointed out earlier this indicates the failure of the classical treatment. In our treatment fortunately, as has been previously shown, these elastic collisions do not contribute.

In the five cases studied (He--Xe) the elements κ_{13} due to the charge-exchange are all very similar. But their characteristics are different from κ_{23} in that the peaks about the elastic point $\lambda = \mu$, in the figures of $F_R^{(1)}$, are finite and broad (the symmetric charge-exchange cross section appears only as a parameter).

For a given initial energy κ_{23} are always bigger than or equal to κ_{13} for all transitions. So the contributions from the direct collision to the total encounter rate coefficient (for a given energy change) are

as important as the SRCT part. The contribution to the reaction rate coefficient α_R from each mechanism can be calculated separately. Using κ_{13}(κ_{23} in the direct collision case) one can solve $\rho_{13}(\lambda)$ and $\rho_{23}(\lambda)$ then calculate α_{13} and α_{23}. If ρ_{13} and ρ_{23} are the same it is obvious that the total coefficient is the sum of the two, or $\alpha_R=\alpha_{13}+\alpha_{23}$. In the two cases tested (Ar and Kr) ρ_{13} and ρ_{23} are very close though not identical so $\alpha_{13}+\alpha_{23}$ are almost exactly equal to α_R. We also find that in these two cases the contribution from the direct collision is almost twice that from the charge exchange part.

In comparing different approximations we find in all cases that the Thomson's treatment and the BTL give bigger rate constant than the QEST (see tables 5.20 and 5.21). The QEST results are about $0.5\alpha_T$ while the BTL results range from $0.7\alpha_T$ to slighly greater than $1.5\alpha_T$ in the respective cases. As will be explicitly shown in section 7.8, α_R is smaller than α^{BT} because of the upflow processes.

Fig. 5.1 to 5.8 (Ar) and Fig. 5.10 to 5.17 (Kr) are some representative energy-change (encounter) coefficients $F_R^{(i)}(\sim\kappa_{i3})$ and $F_R(\lambda,\mu)$, as a function of final energy $E_f = -\lambda k\theta$. F_R, given by solid lines in graphs, is the sum of $F_R^{(1)}$ (for (1,3) encounter) and $F_R^{(2)}$ (for (2,3) encounter).

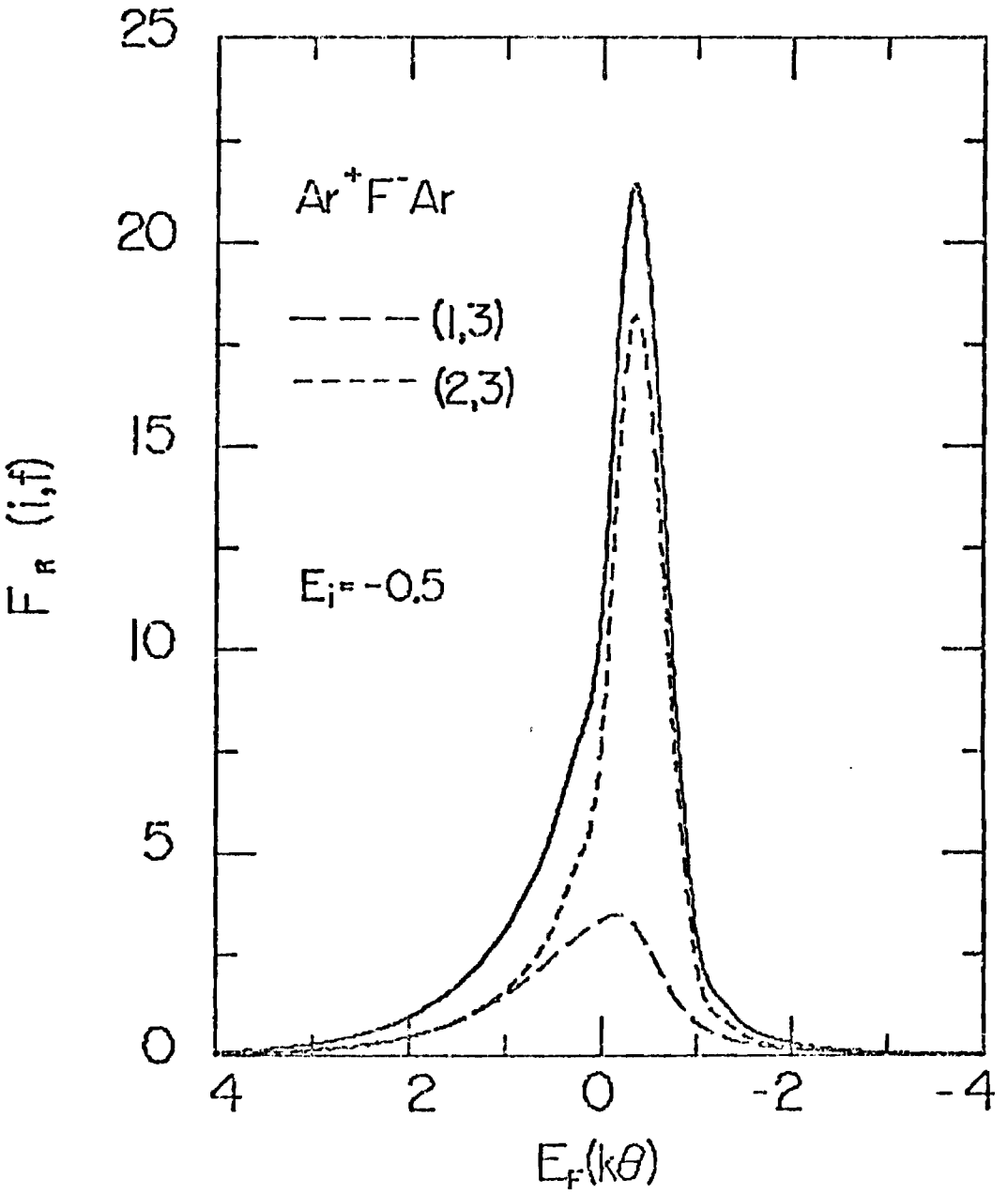

Fig 5.1

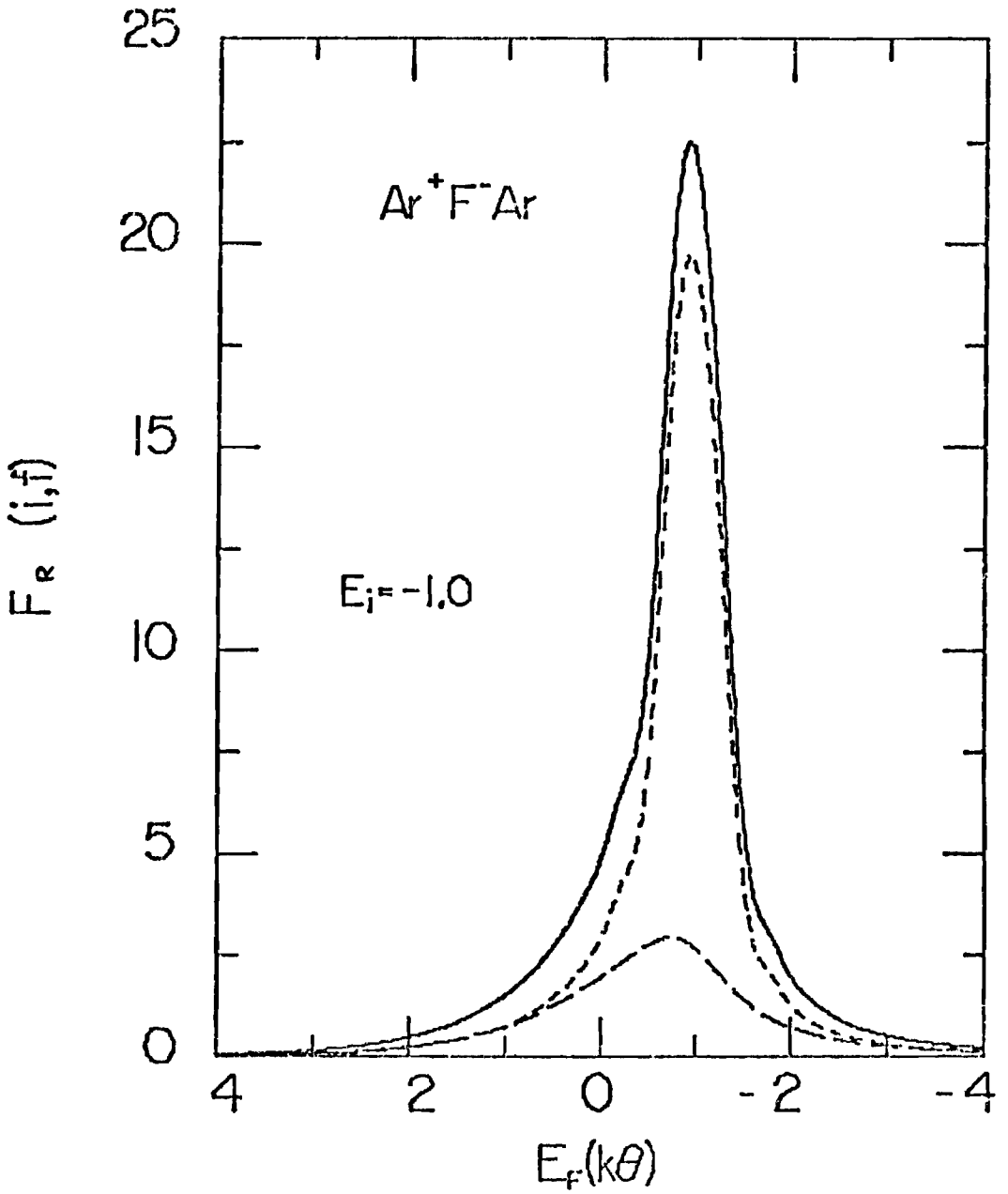

Fig 5.2

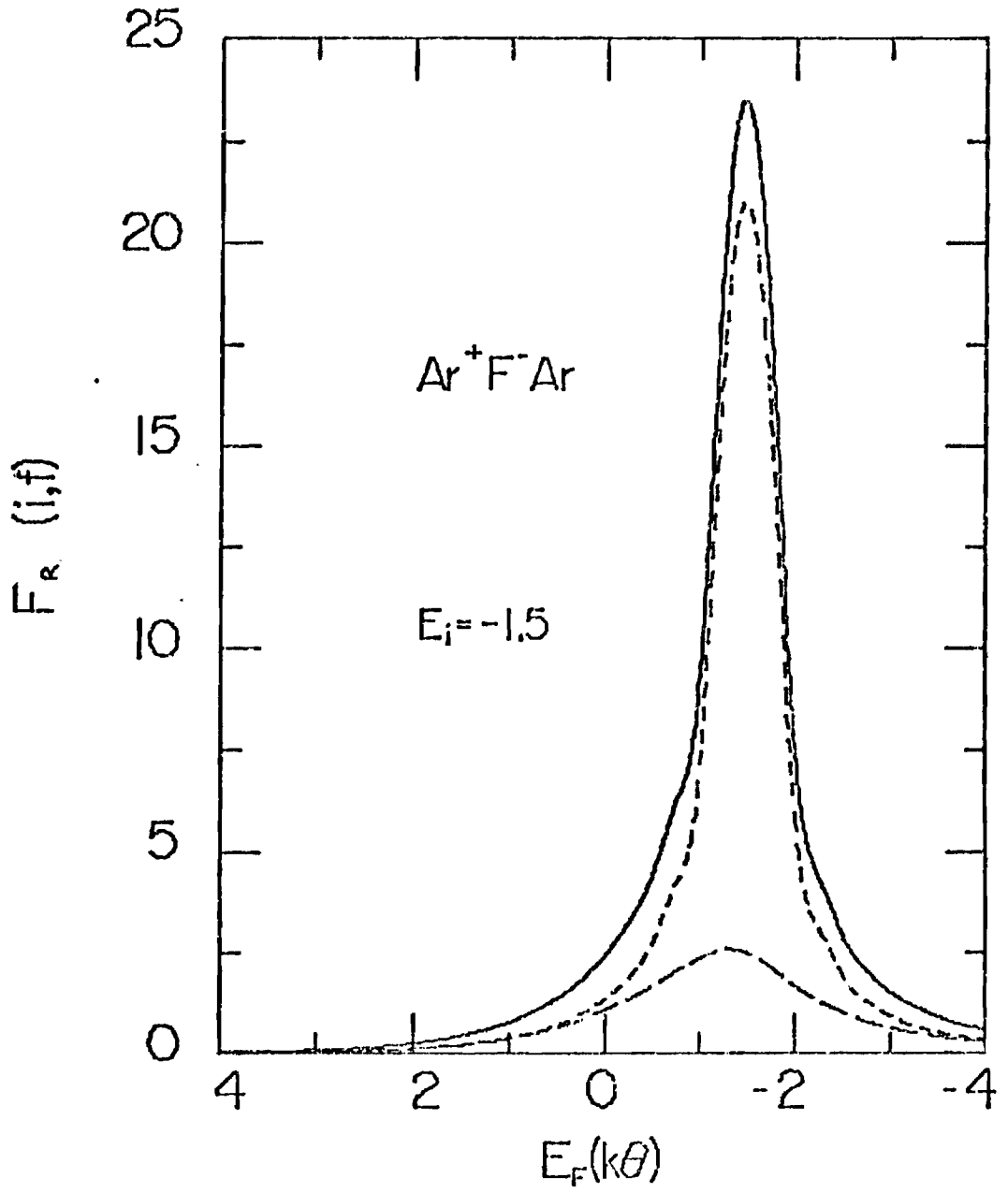

Fig 5.3

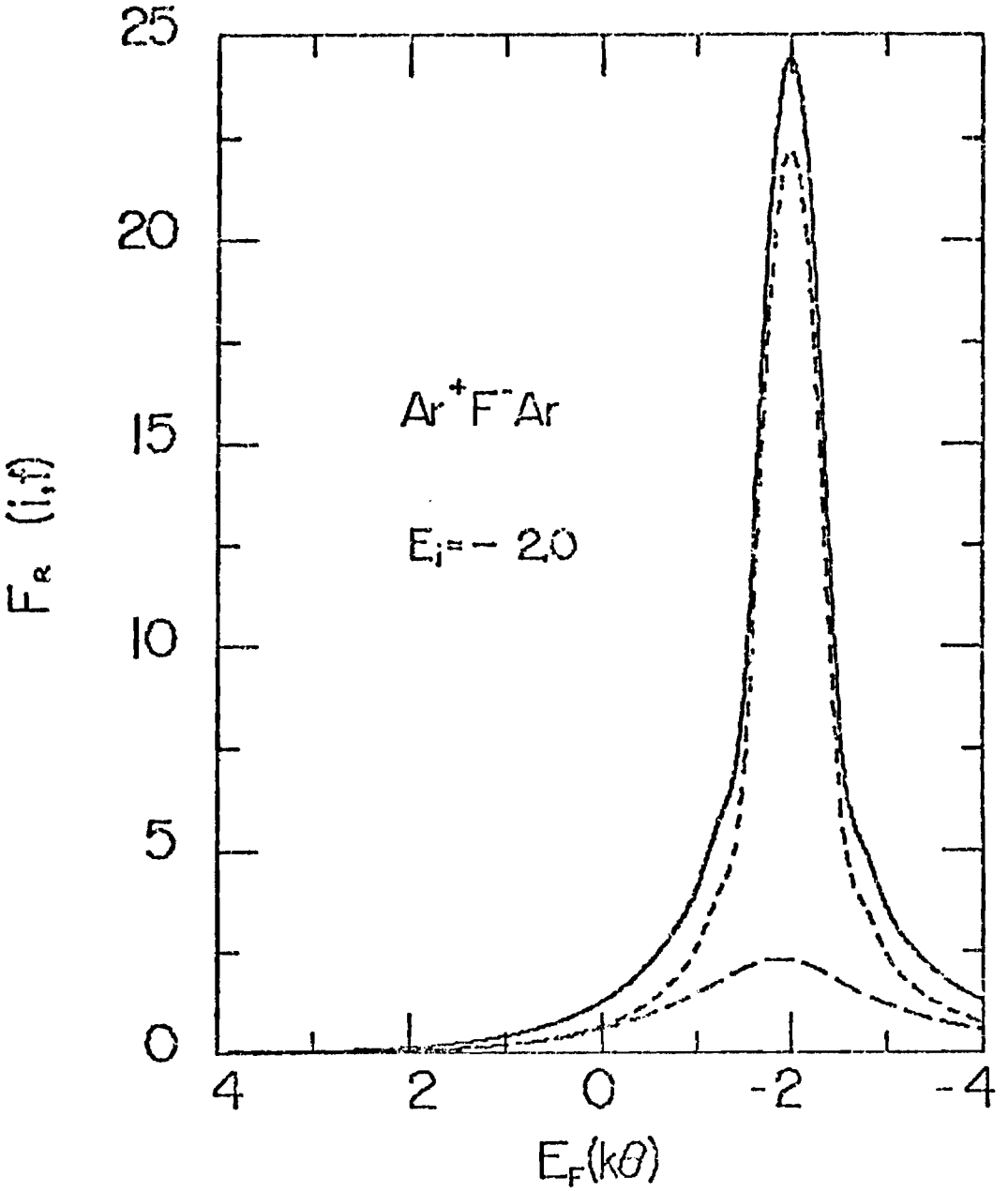

Fig 5.4

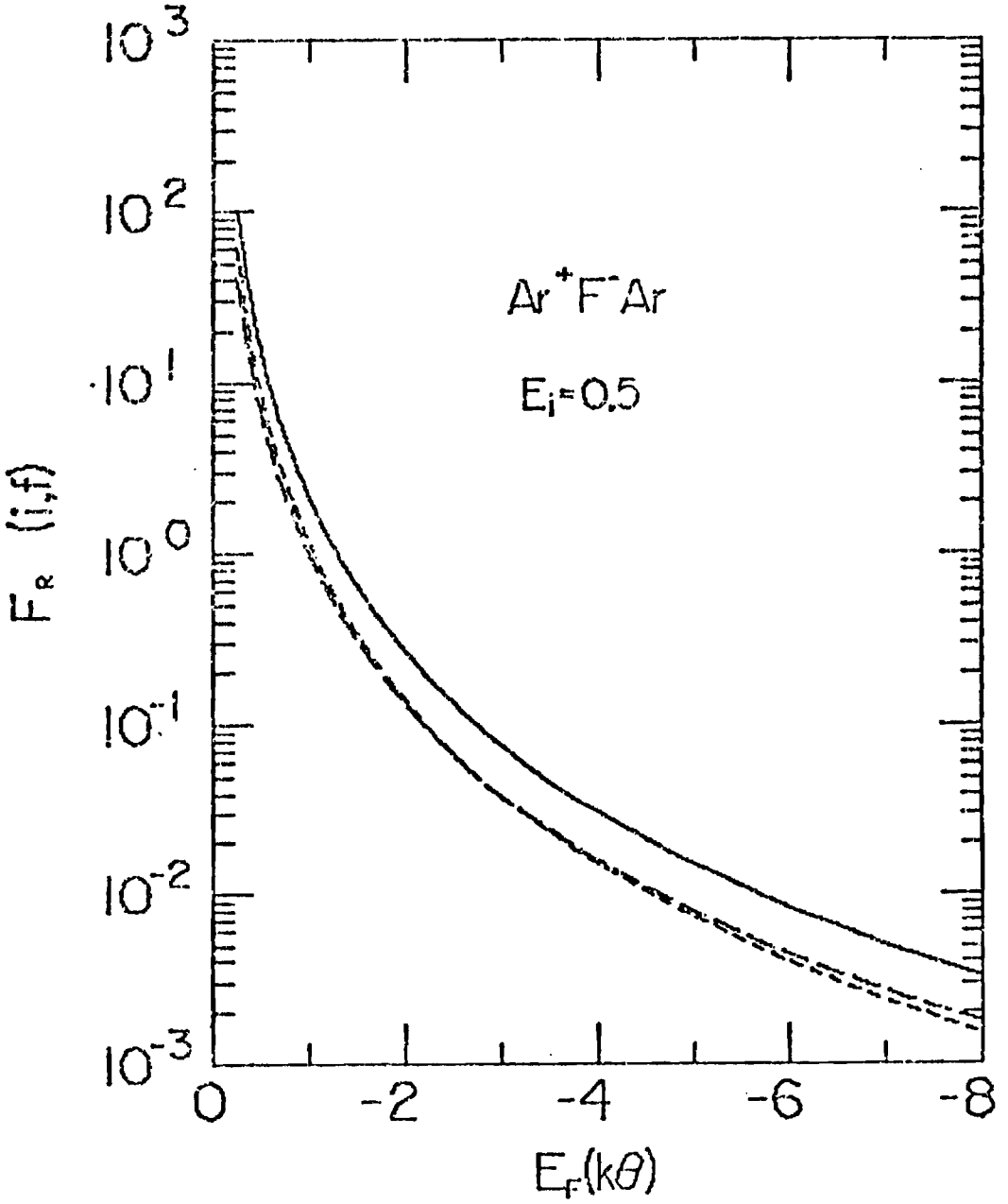

Fig 5.5

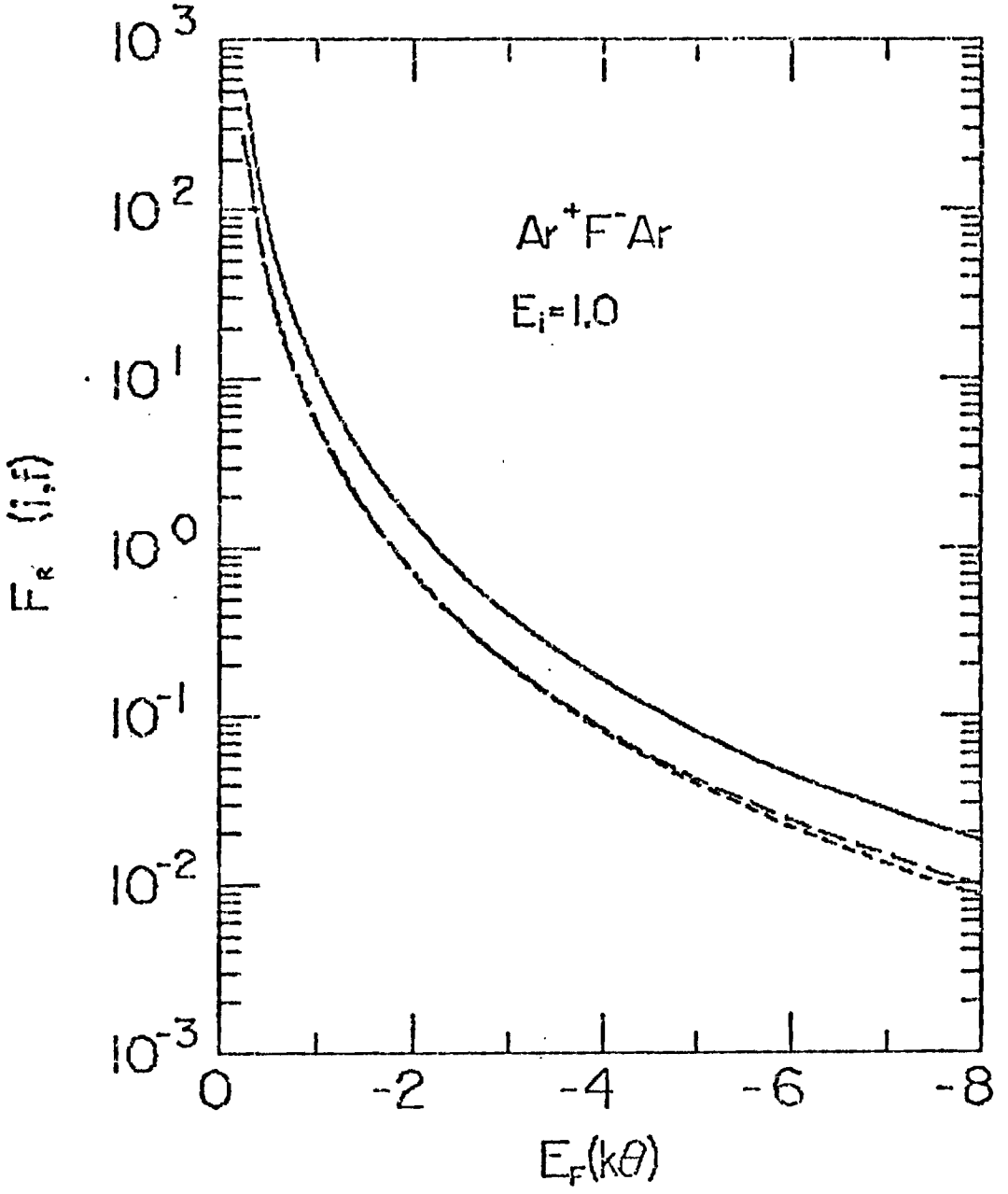

Fig 5.6

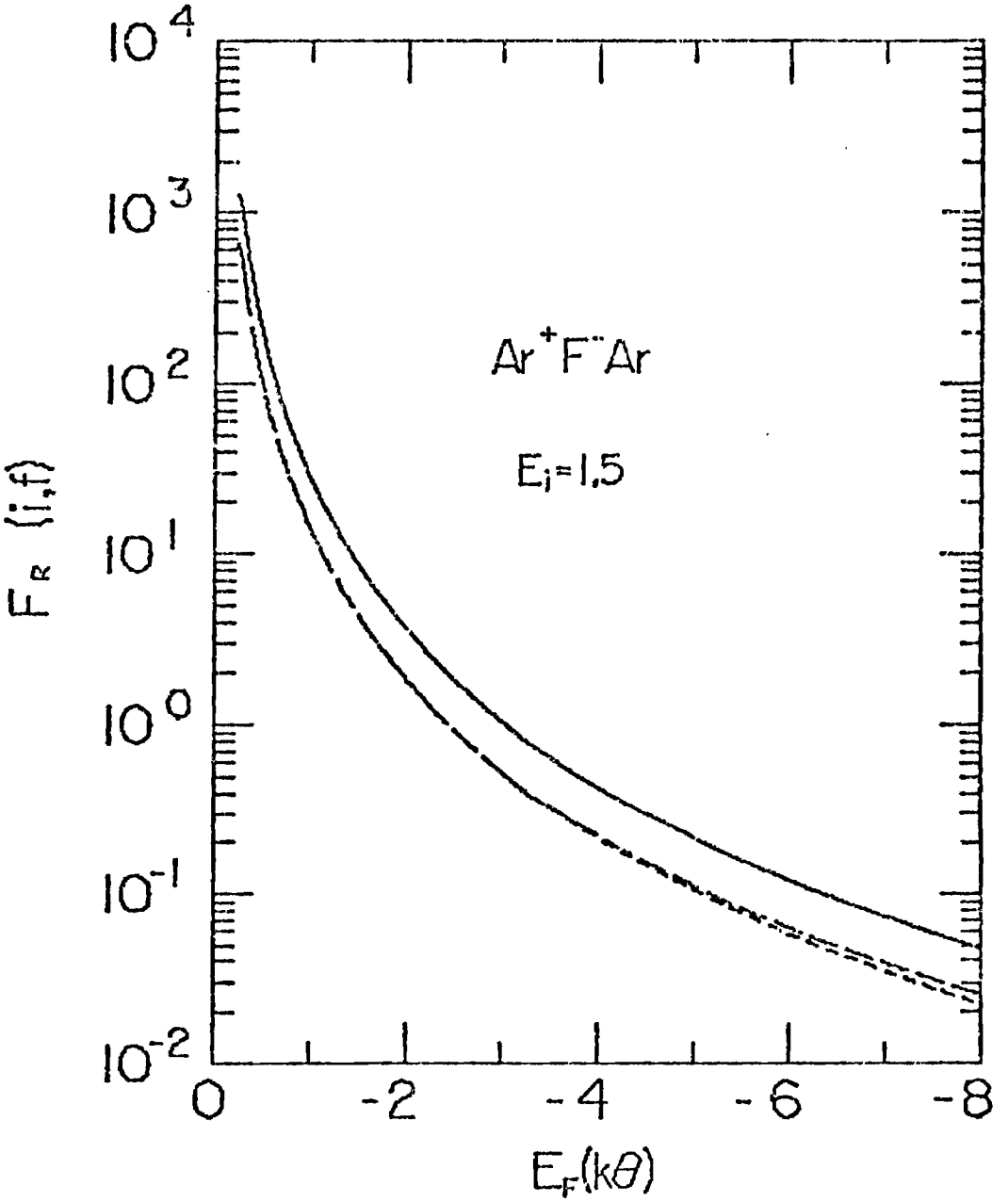

Fig 5.7

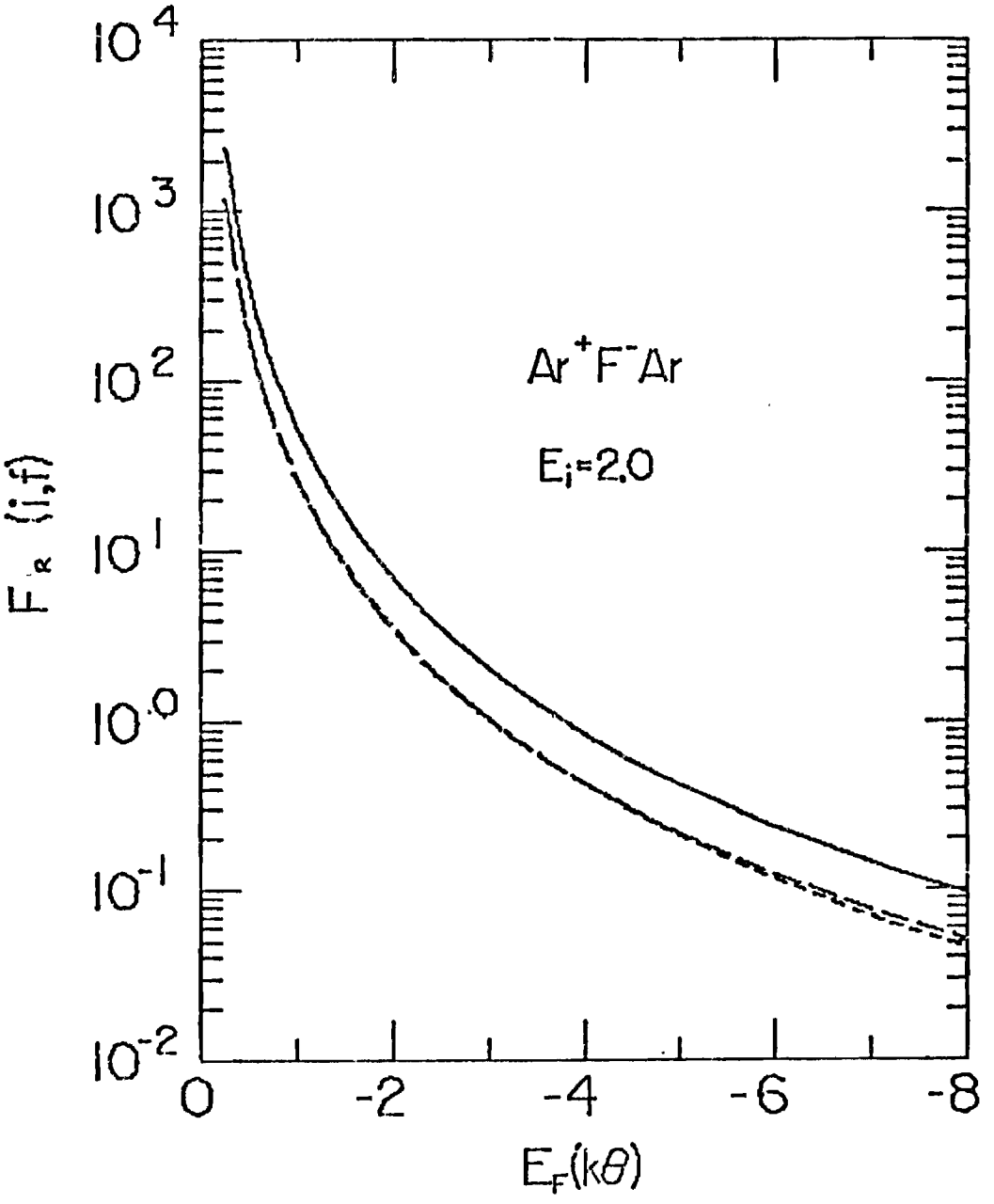
10^4
10^3
10^2
10^1
10^0
10^{-1}
10^{-2}
$F_\alpha(i,f)$
Ar^+F^-Ar
E_i=2.0
0
-2
-4
-6
-8
$E_F(k\theta)$

Fig 5.8

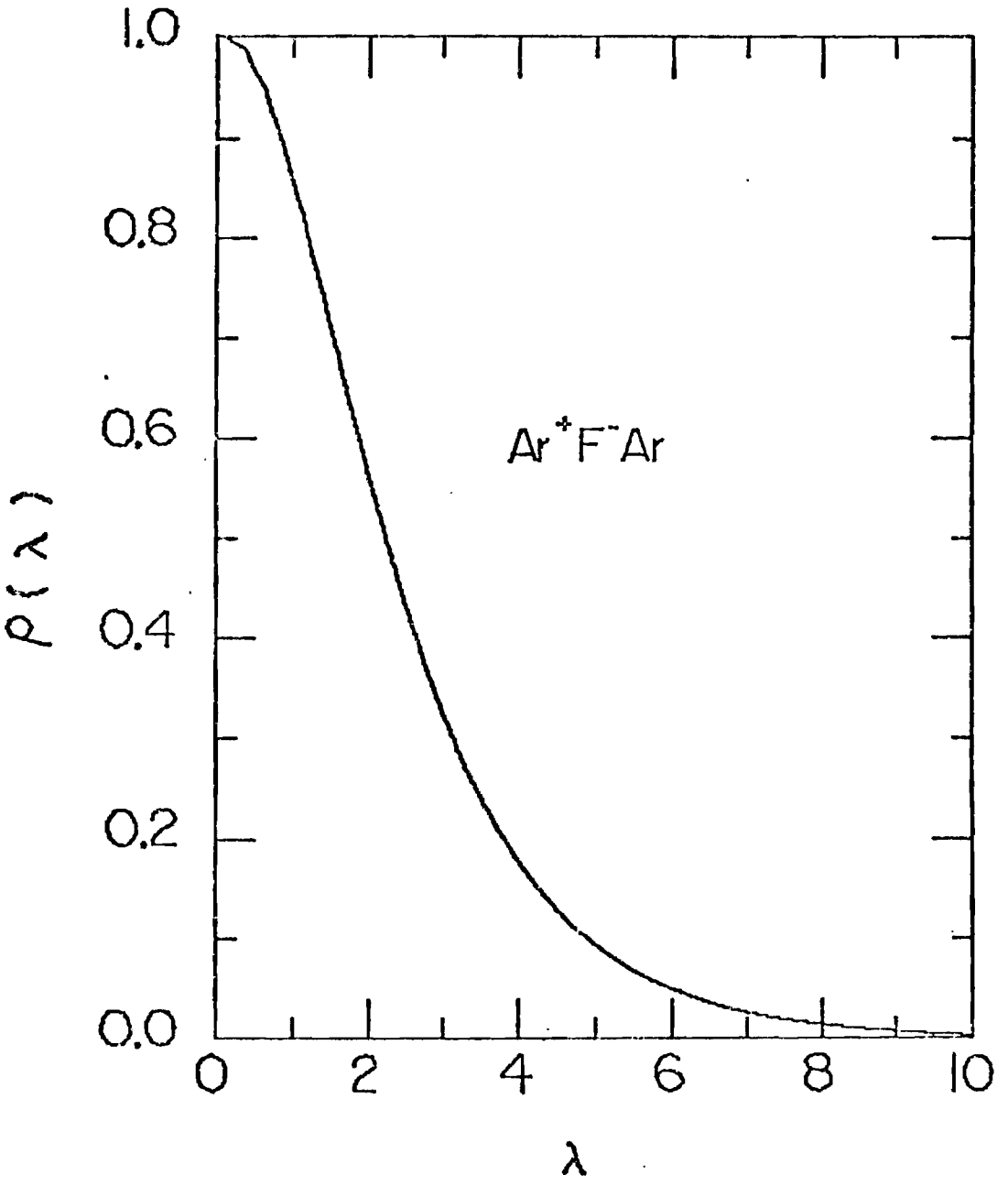

Fig 5.9

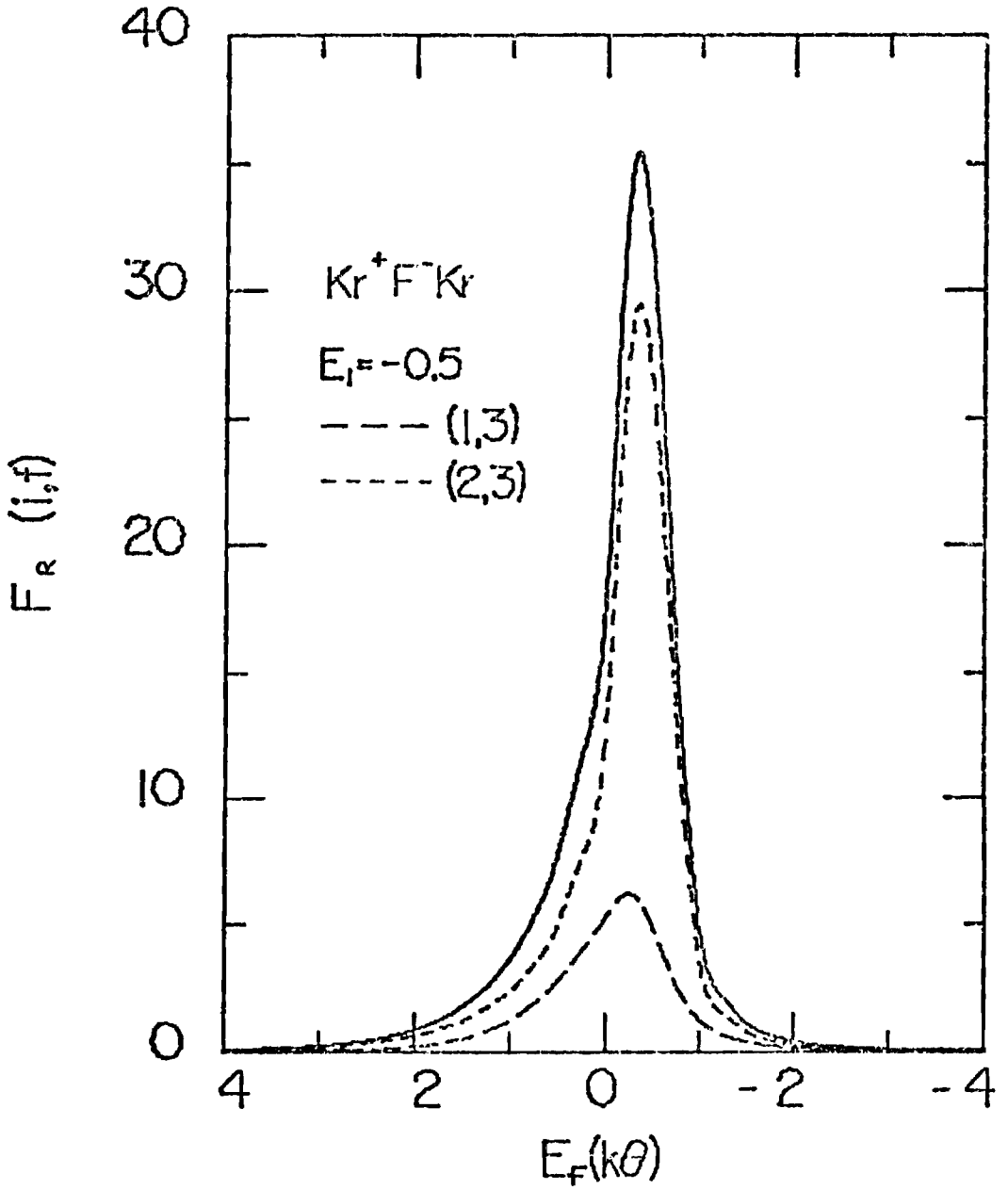

Fig 5.10

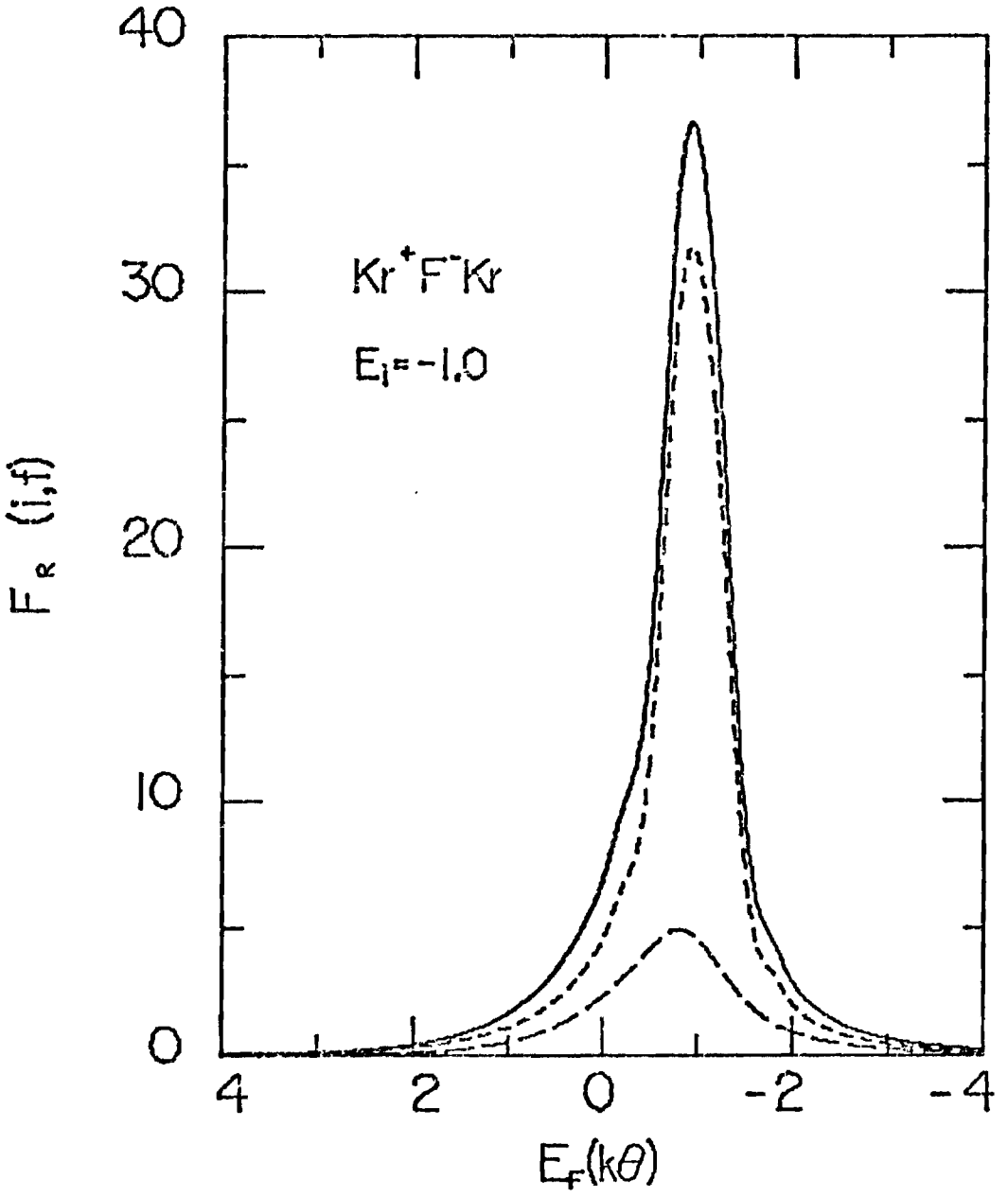

Fig 5.11

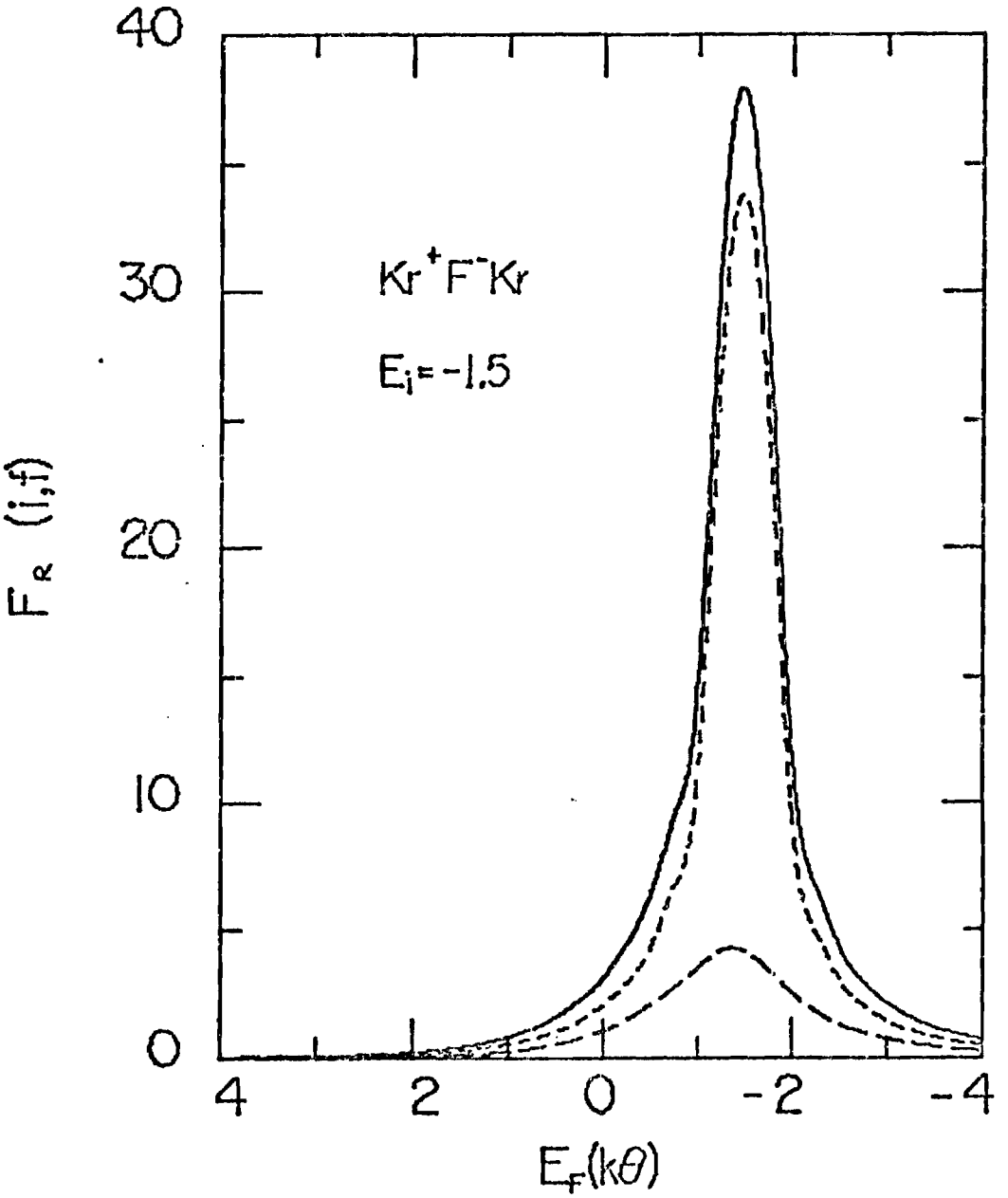

Fig 5.12

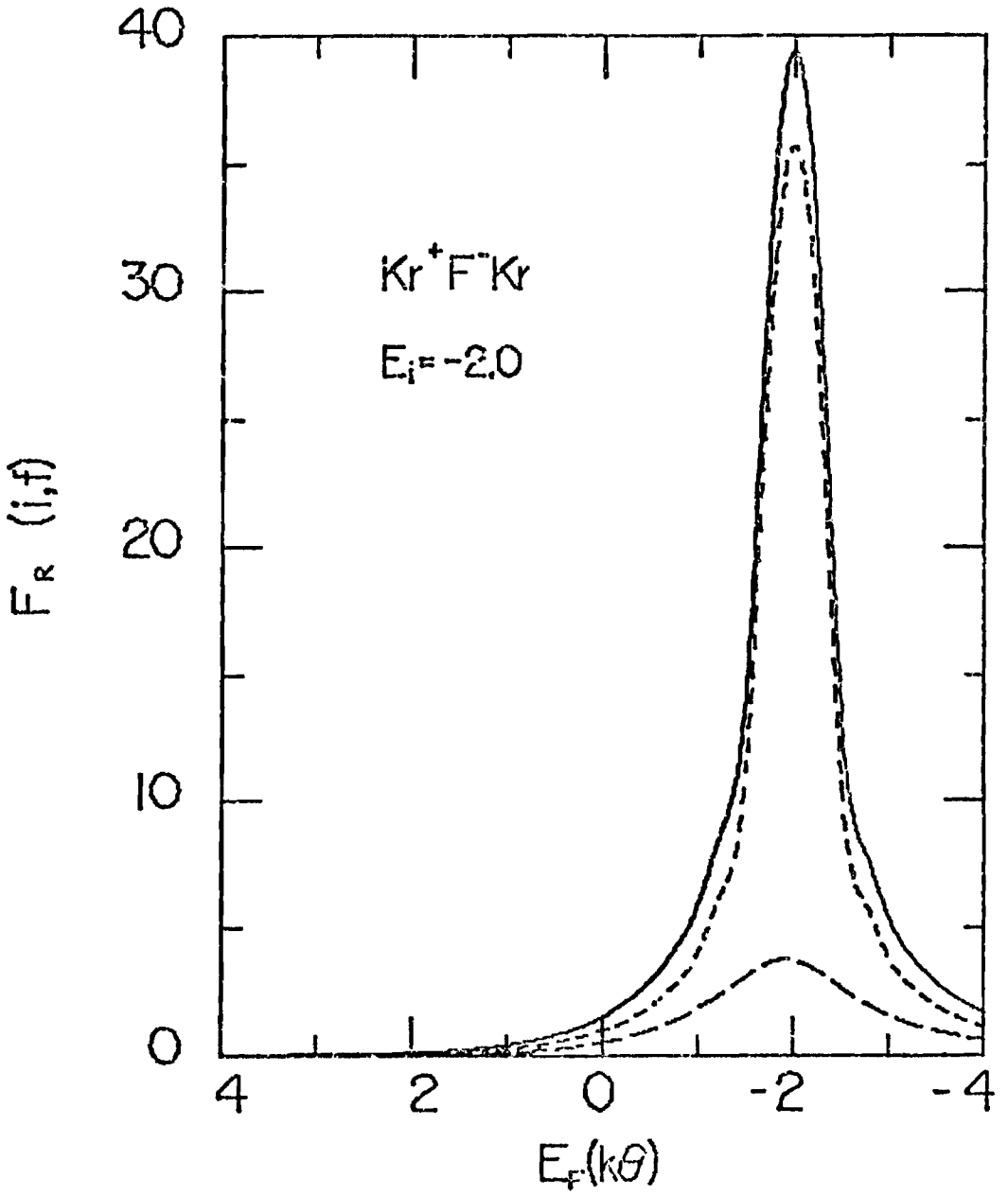

Fig 5.13

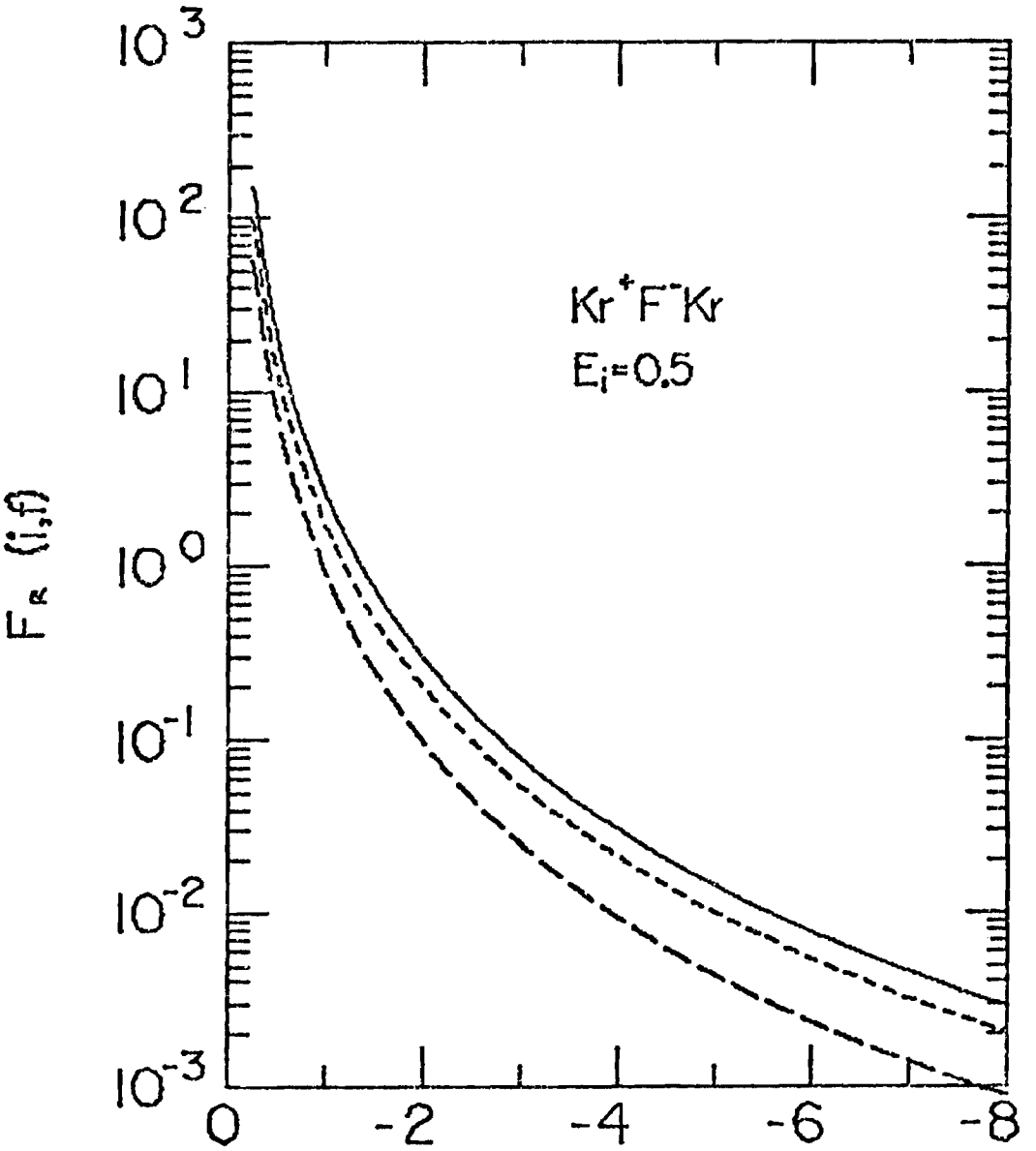

Fig 5.14

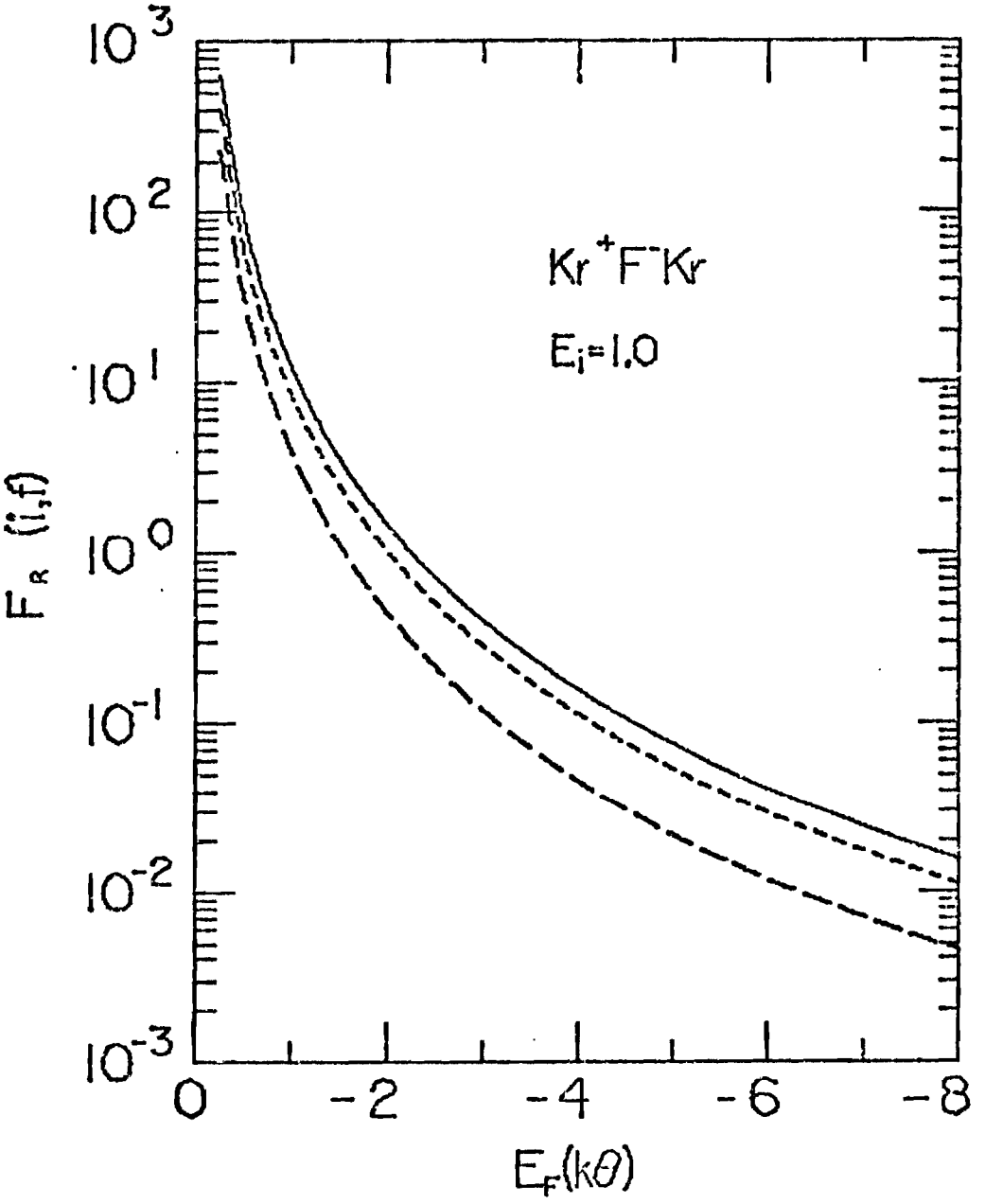

Fig 5.15

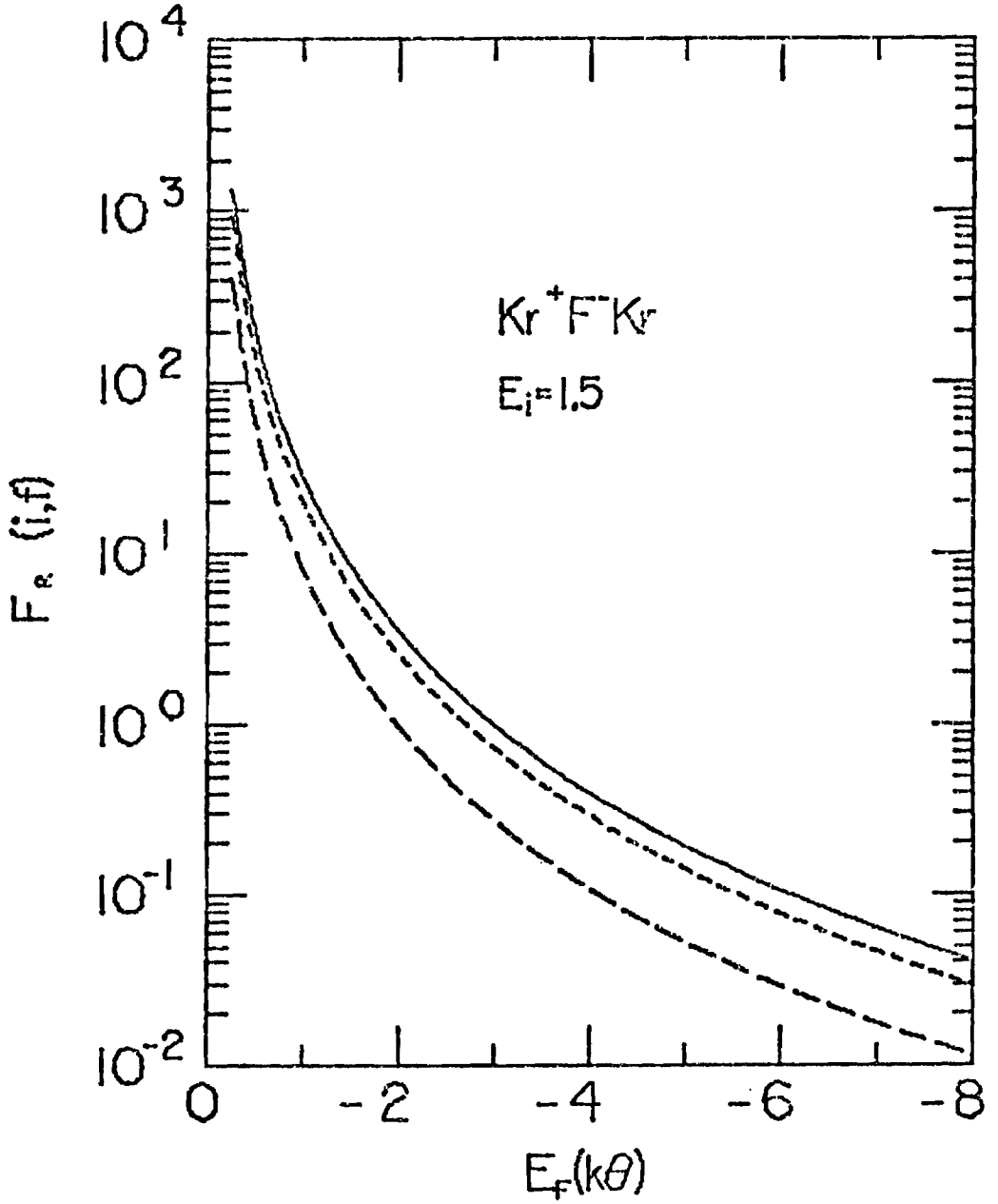

Fig 5.16

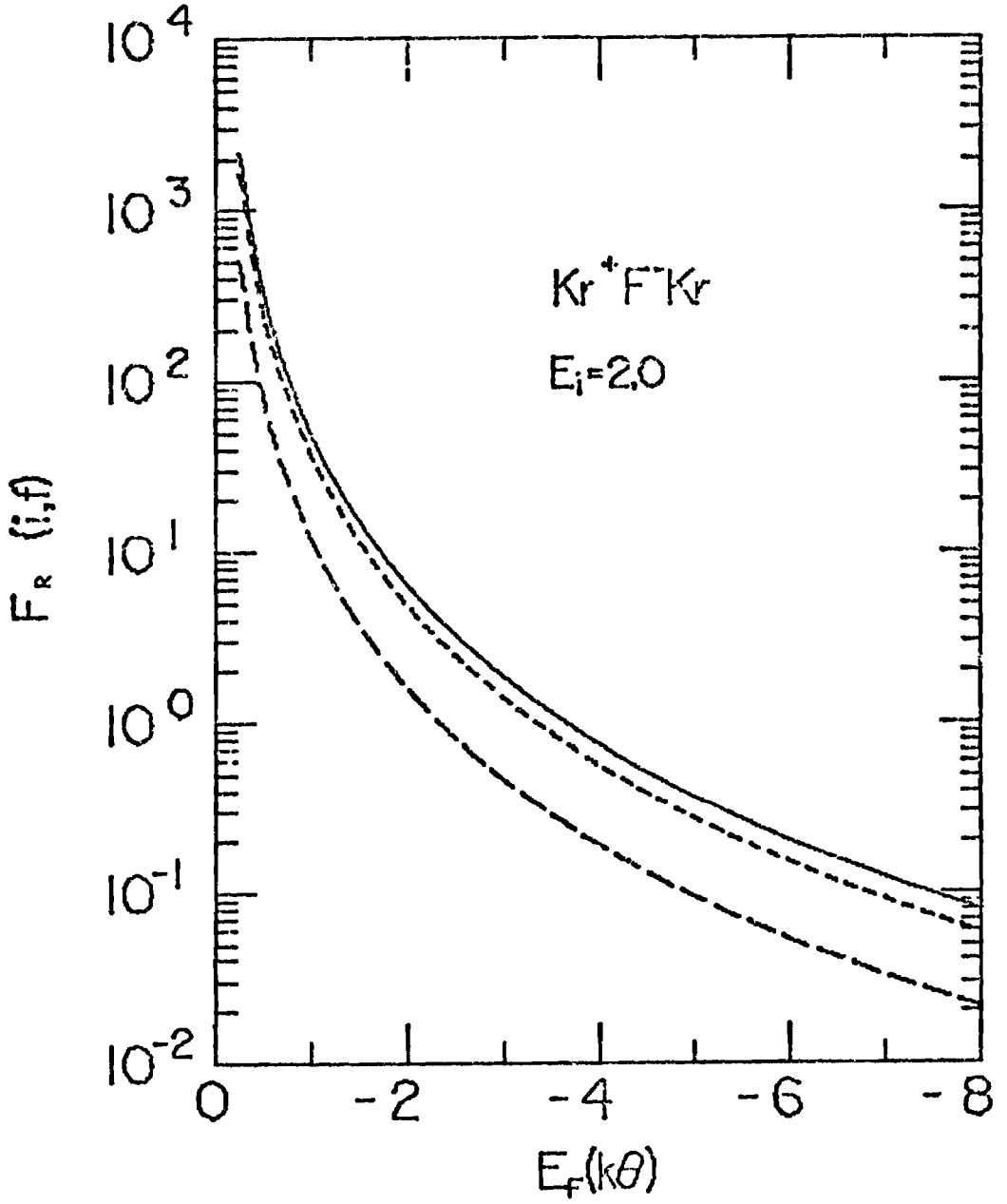

Fig 5.17

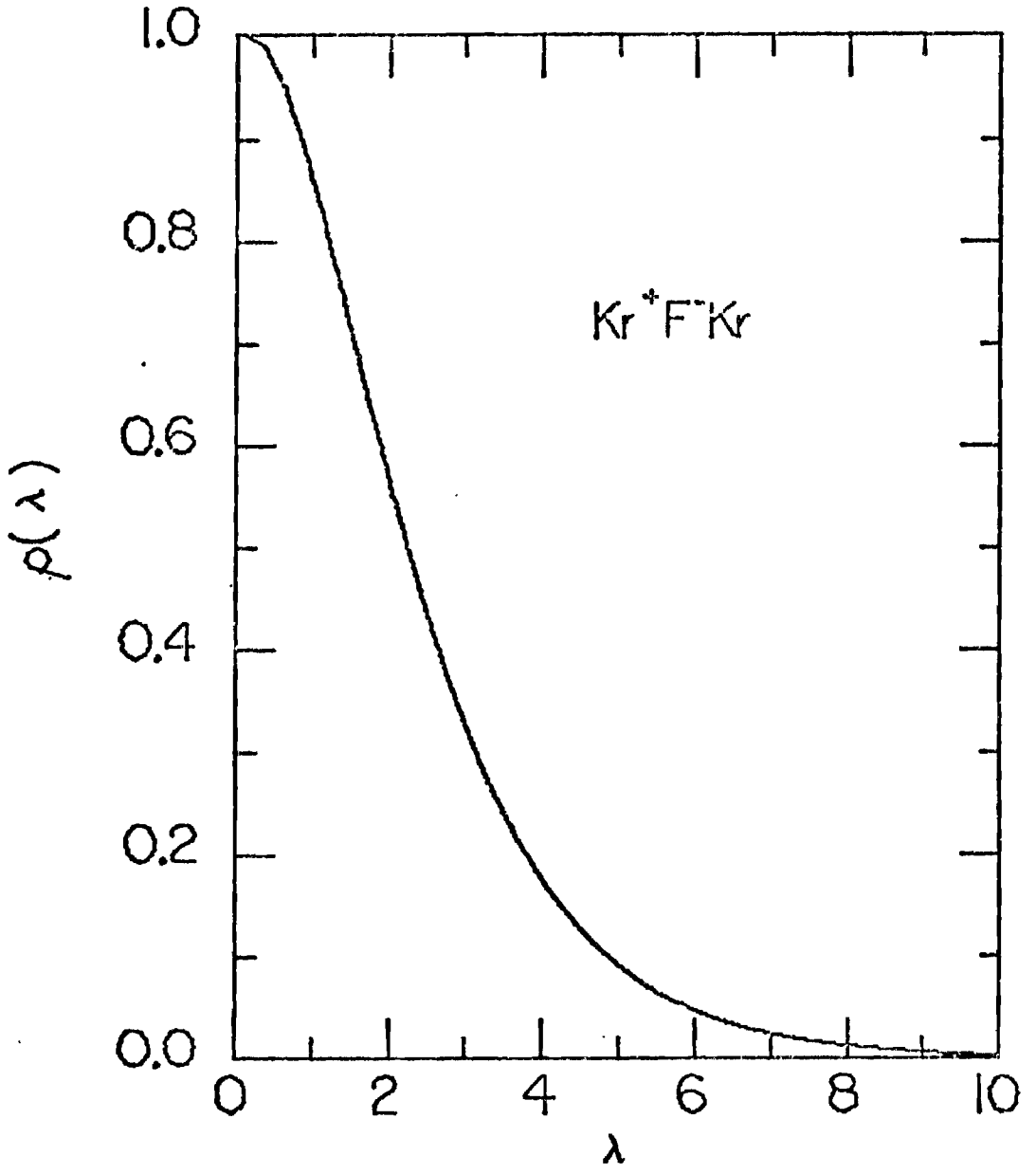

Fig 5.18

CHAPTER VI

MODIFIED NATANSON'S MODEL

IONIC-RECOMBINATION AT ALL GAS DENSITIES

6.1 Introduction

At low densities mutual neutralization and many single collisions of the ion-pairs with the neutral gas control the recombination. As the density increases the ion-pairs may undergo double or even multiple collisions with two or more gas molecules simultaneously. The density dependence of the recombination rate therefore departs from its linear dependence on N_3 (the neutral gas density) to dependence of higher power of N_3. Although it is possible to generalize the QEST of Bates and his

colleagues employed earlier to account for this simultaneous multiple collision, the effort needed and complexity involved for the resulting computational problem increases dramatically- it is plainly too cumbersome to be useful. Besides this difficulty the generalization is incomplete in that it neglects the fact that the initial approach of the ions eventually becomes limited by the speed of random diffusion and the attractive drift at higher gas densities. In fact it is so limited at high density that the recombination rate decreases as N_3^{-1} . A different scheme is needed.

To link the two physically distinct regions from low N_3 to high N_3, Bates and Flannery (1969) instead modified Natanson's successful treatment (of equal masses) which gave the correct behavior in the two extreme limits of N_3. They noted that the Natanson's result α_N could be expressed as

$$\alpha_N^{-1} = \alpha_{TN}^{-1} + \alpha_{LN}^{-1} \qquad (6\text{-}1)$$

where the added subscript N to α_T and α_L denoted the respective modifications of Natanson (1959) to the origional formula (2-2) of Thomson and (2-8) of Langevin.

The treatment (a) introduced a density dependent trapping radius r_N, (b) allowed for Coulombic trajectory (rather than a linear one) with an extra multiplicative 'focusing factor' $(1+e^2/r_N k\theta)=17/5$ and (c) acknowledged that ions with separation $(r_N+\lambda)$ just entering the collision sphere had a density factor $E \sim \exp(12r_N/\lambda)$, higher than at infinite separation. Analogous modification also applied to the Langevin process. The resulting α's were

$$\alpha_{TN} = C_o \pi r_N^2 P(r_N)(3k\theta/m_{12})^{\frac{1}{2}} E_o \qquad (6\text{-}2a)$$

where

$$C_o=17/5, \quad E_o=\exp(12r_N/\lambda) \qquad (6\text{-}2b)$$

$$r_N = \tfrac{1}{2}\lambda\left[\left(1+\frac{5e^2}{3k\theta\lambda}\right)^{\frac{1}{2}}-1\right] \rightarrow \begin{cases} r_N = \dfrac{5e^2}{12k\theta} & \text{low } N_3 \quad (6\text{-}2c) \\ r_N = \left(\dfrac{5e^2\lambda}{12k\theta}\right)^{\frac{1}{2}} & \text{high } N_3 \quad (6\text{-}2d) \end{cases}$$

for Thomson's case, and

$$\alpha_{LN} = \alpha_L(1-\exp(-12r_N/5\lambda))^{-1} \qquad (6\text{-}3)$$

for Langevin's case, λ being the mean free path of an ion in the gas. Through scaling of r_N by a multiplicative factor, they enforced the agreement of α_N at low density limit with results of the quasi-equilibrium treatment

which is more accurate. They then used formula (6-1) with the inclusion of mutual neutral neutralization α_M to the Thomson's 3-body collision expression of α_T i.e., using

$$\alpha'_{TN} = \alpha_{TN} + \alpha_M$$

rather than α_{TN} alone to calculate α_N. The results for oxygen ions (assumed to be O_2^+, O_4^+, O_2^+) recombining in O_2 were in good agreement at the low density limit with the measurements of McGowan (1964) and at high density region with Mächler's results (1936). We therefore apply their method to the rare-gas halide systems important in the kinetics of the excimer lasers. No inclusion of the mutual neutralization will be made in the following for the reason of simplicity.

6.2 α_{TN} and α_{LN} for Different Masses m_i and Mean Free Paths λ_i

For ions of different masses m_1 and m_2 and mean free paths λ_1 , λ_2 in a neutral gas of m_3, Natanson's results can be suitably generalized. Since it has already been

reported by Flannery (1978, F3), here we will only give a brief sketch of the modified expressions and apply them to several systems of current interest.

The new expression for the Thomson's part of α_N is

$$\alpha_{TN} = \left(\frac{8k\theta}{\pi m_{12}}\right)^{\frac{1}{2}} \left[r_1^2 W(x_1) C_1 E_1 + r_2^2 W(x_2) C_2 E_2 - r_s^2 W(y_1) W(y_2) S \right] \qquad (6\text{-}5a)$$

where

$$C_i = 1 + 3/2\, \delta_i \qquad (6\text{-}5b)$$

$$E_i = \exp(3r_i / 2\, \delta_i \lambda_i) \qquad (6\text{-}5c)$$

$$\delta_i = F_i / (1 - F_i) \qquad (6\text{-}5d)$$

$$F_i = 2m_1 m_2 m_3 (m_1 + m_2 + m_3) / (m_1 + m_2)^2 (m_i + m_3)^2 \qquad (6\text{-}5e)$$

and

$$x_i = r_i / \lambda_i, \qquad r_s = \text{min. of } (r_1, r_2)$$
$$y_i = r_s / \lambda_i, \qquad S = \text{min. of } (C_1 F_1, C_2 E_2). \qquad (6\text{-}6)$$

(6-5a) is obviously a revision of both the origional Thomson's formula (2-5) with (2-6) and Natanson's expression (6-2).

The modifications are severalfold: (a) Instead of having a common trapping radius r_T each ion, because of the mass difference, has its own trapping radius given by

$$r_i = \tfrac{1}{2}\lambda_i\left[\left(1 + \frac{8e^2\delta_i}{3k\theta\lambda_i}\right)^{\frac{1}{2}} - 1\right] \qquad i=1,2. \qquad (6\text{-}7)$$

This is the first modification so designed that arbitrary mass ions are incapable of separation to $\lambda_i + r_i$, where they suffer the next collision, rather than to infinity. (b) Coulombic rather than linear trajectories are involved so that there is an extra multiplicative focusing factor C_i for each ion:

$$C_i = 1 + \frac{1}{k\theta}\int_{r_i}^{r_i+\lambda_i} \frac{e^2}{r^2}\, dr \qquad (6\text{-}8)$$

(c) Introduction of δ_i reflects the effect due to masses difference. Note that for the equal masses case, we have $\delta_i=3/5$ instead of the value 5/8 needed to make the present expression reduce to Natanson's results. This deviation is due to Natanson's erroneous assumpton of isotropic scattering in both the laboratory and the ion-atom C.M. frame (Wadela and Bardsely, 1978). (d) The factors $E_i=\exp(e^2/(r+\lambda_i/2)k\theta)$ represent higer density for ions with separations $\lambda_i + r_i$ just before entering the collision sphere than at infinite separation. Also note that the average relative speed is used instead of the usual root

mean square speed of $(3k\vartheta/m_{12})^{\frac{1}{2}}$ in (6-2a).

An analogous modification of the Langevin's expression of (6-3) yields

$$\alpha_{LN} = 4\pi e \left[\frac{K_1}{1-E_1^{-1}} + \frac{K_2}{1-E_2^{-1}}\right] . \qquad (6\text{-}9)$$

The combination of (6-1), (6-5), (6-6) and (6-9) thus gives the total recombination rate coefficients α_N as a function of N_3 for any species.

The mechanism of energy reduction is mainly determined by the charge-transfer (SRCT) for ion with its neutral parents gas

$$X^+(\text{fast})+X(\text{slow}) \dashrightarrow X(\text{fast})+X^+(\text{slow}) \qquad (6\text{-}10a)$$

and by the elastic ecounters for

$$Y^-(\vec{v}_2)+X(\vec{v}_3) \dashrightarrow Y^-(\vec{v}_2')+X(\vec{v}_3') \qquad (6\text{-}10b)$$

where $Y \neq X$, in which the speeds of Y^- and X are changed from $\vec{v}_2$ and $\vec{v}_3$ to $\vec{v}_2'$ and $\vec{v}_3'$ respectively. As we discussed before the mean free path λ is related to the diffusion scattering cross section Q_D by $\lambda = 1/N_3 Q_D$. Since the charge-transfer cross section q^+ is half of the diffusion

cross section one can follow section 5.1 and express the mean free paths for the two processes above as

$$\lambda_i = \frac{1600}{e}\left(\frac{m_{i3}k_\theta}{2\pi}\right)^{\frac{1}{2}} k_m^{(i)} \frac{N_L}{N_3} \times \begin{cases} 2 & \text{charge exchange only} \\ 1 & \end{cases} \qquad (6\text{-}11)$$

where $k_m^{(i)}$ are the reduced measured mobilities of the ions in the neutral gas, m_{i3} the ion-neutral reduced mass, N_L the Loschmidt's number density. The extra factor 2 is only for the case in which the single strong ion-neutral (X^+-X) encounter is controlled by the symmetric charge-transfer.

We are now ready to apply these results to three representative cases of three-body recombination related to the rare-gas halide lasers. Since not all of the reduced mobilities $k_m^{(i)}$ are measured we use the polarization formula (DA,1958),

$$k_m^{(i)} \doteq 13.87/(p^* m^*)^{\frac{1}{2}} \ (\text{cm}^3/\text{vol-sec}) \qquad (6\text{-}12)$$

where p^* is the reduced neutral polarizability (in unit of 10^{-24}cm^3) and the the reduced mass of the ion-neutral is in O^{16} units as in section 5.1. The formula gives reasonable estimates of p^* for heavy rare gas.

6.3 Rare-Gas Atomic Ions X^+ with F^- in Dense X

The reaction we are considering is

$$X^+ + F^- + X \dashrightarrow (XF)^* + X$$
$$1 \quad 2 \quad 3$$

i.e., for all rare gases, X=He, Ne, Ar, Kr, Xe, at all gas densities. The (1,3) encounter is dominated by the symmetric charge-transfer so that the mean free path associated with it, i.e. λ_1, has a multiplicative factor of 2 (see (6-11)), while the (2,3) encounter is an elastic collision hence use λ_2 with factor unity.

The parameters involved are masses of each rare gas m^*_1, of fluorine m^*_2 and the reduced mobilities $k_m^{(1)}$ of (1,3) encounter, $k_m^{(2)}$ of (2,3) encounter. Table 5.1 gives m^*_1 and $k_m^{(1)}$, while $m^*_F = 18.9984$, and of course $m^*_3 = m^*_1$. For $k_m^{(1)}$, the measured values are available for He and Ar only (DAF 1, 2, 1977). The rest are estimated from (6-12) with atomic polarizabilities taken from tables of McDaniel and Mason (MM,1973). The parameters involved are summarized in Table 6.1. The results at room temperature ($\theta^* = 3$, i.e., 300 K), has been recently published in Applied Physics Letters 32, 327, 1978 and is reproduced in Appendix II. The original figure is now Fig 6.1.

Table 6.1

$m_2^* = m_F^* = 18.9984$

X	p^* (Å^3)	m_1^*	$k_m^{(1)}$	$k_m^{(2)}$
He	0.205	4.003	10.3	29.5 (e)
Ne	0.395	20.183	4.08	7.051
Ar	1.640	39.944	1.52	3.33 (e)
Kr	2.480	83.80	0.823	2.237
Xe	4.040	131.30	0.570	1.693

(e) measured values from reference DAF 1 & 2 (1977)

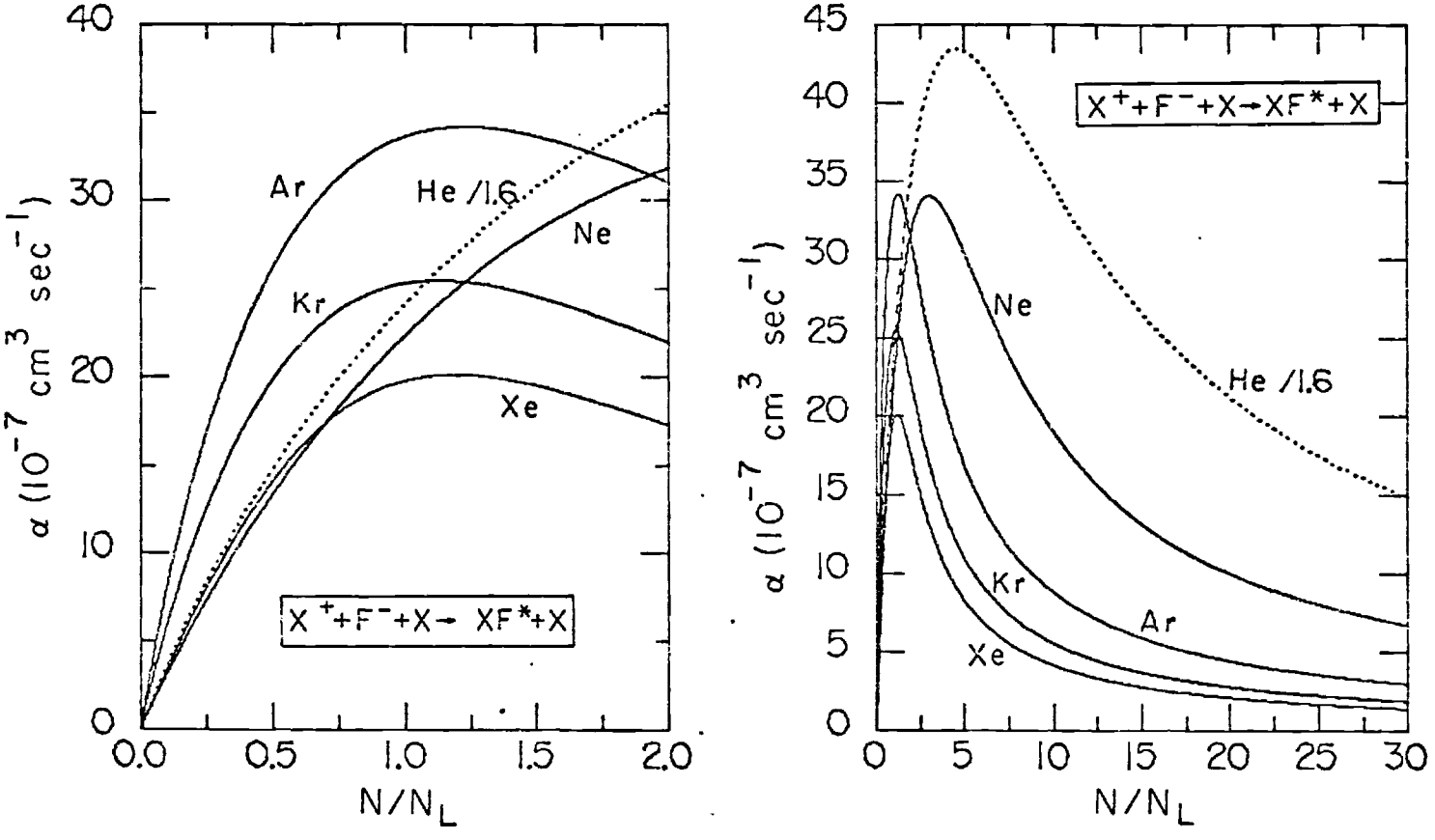
40
30
20
10
0
α (10⁻⁷ cm³ sec⁻¹)
Ar
He /1.6
Ne
Kr
Xe
X⁺+F⁻+X→ XF*+X
0.0
0.5
1.0
1.5
2.0
N/N_L
45
40
35
30
25
20
15
10
5
0
X⁺+F⁻+X→XF*+X
Ne
He /1.6
Kr
Ar
Xe
0
5
10
15
20
25
30
N/N_L

Fig. 6.1

6.4 Rare Gas Molecular Ion X_2^+ with F^- in Dense X

The corresponding molecular case of (5-1) is

$$X_2^+ + F^- + X \dashrightarrow (X_2F)^* + X \qquad (6\text{-}13)$$

1 2 3

which is believed to be important in the kinetics of rare-gas halide lasers as can be seen in Appendix III. Again X is used to label He, Ne, Ar, Kr and Xe.

From the point of view of the three-body recombination this differs from the previous atomic case in that the symmetric charge-transfer process is no longer involved since the partners of the (1,3) encounter have different masses. Therefore the expressions for the mean free paths, λ_1 of (1,3), and λ_2 of (2,3) both are associated with factor unity only.

Again the results for the system at room temperature ($\theta^*=3.$) have been published in Applied Physics Letters 32, 356, 1978, and is reproduced in Appendix III. The orginal figure is now Fig 6.2.

The parameters involved are displayed in Table 6.2.

Table 6.2

X	m*	$k_m^{(1)}$	$k_m^{(2)}$
He	4.003	16.7	29.5
Ne	20.183	6.16	7.051
Ar	39.944	1.83	3.33
Kr	83.80	1.22	2.237
Xe	131.30	0.80	1.693

a) $m_I^* = 2m_X^*$

b) $k_m^{(1)}$ here are for X_2^+ in X, while $k_m^{(2)}$ are for F^- in X as in the atomic case

c) $k_m^{(1)}$ are all taken from reference EL 1976, except the Xe case which is taken from reference BIC 1954.

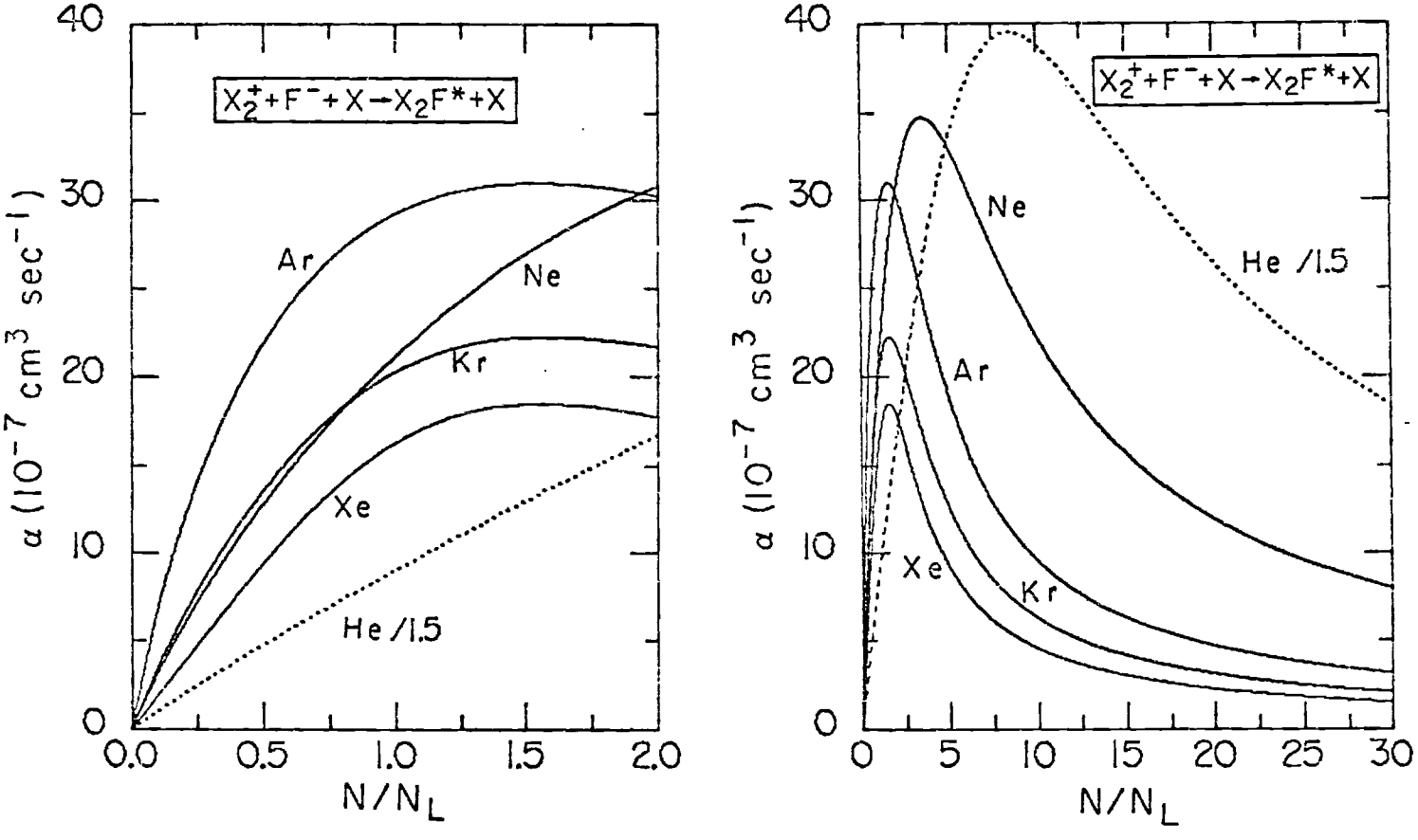
$X_2^+ + F^- + X \rightarrow X_2F^* + X$
Ar
Ne
Kr
Xe
He /1.5
$\alpha\ (10^{-7}\ cm^3\ sec^{-1})$
N/N_L
0
10
20
30
40
0.0
0.5
1.0
1.5
2.0
5
15
25

Fig. 6.2

6.5 Kr^+ and Kr_2^+ with F^- in dense buffer (lighter) Gas

In the previous two sections we have treated the recombinations that the rare-gas buffer is identical to the rare gas. However in most lasers of current interest, the dominant positives ions are likely to be heavy rare gas ions (e.g., Kr^+, Kr_2^+) which recombined with F^- in a lighter gas buffer such as He, Ne, Ar.

So we consider the following processes

$$\underset{1}{Kr^+} + \underset{2}{F^-} + \underset{3}{Y} \dashrightarrow (KrF)^* + Y \quad , \qquad (6\text{-}14)$$

$$\underset{1}{Kr_2^+} + \underset{2}{F^-} + \underset{3}{Y} \dashrightarrow (Kr_2F)^* + Y \qquad (6\text{-}15)$$

with Y=He, Ne, Ar, Xe. The case of Xe is for completeness. No symmetric charge-transfer case is involved. Since the masses involved are given previously ($m^*_{Kr_2} = 2m^*_{Kr}$) we only list the reduced mobilities in Table 6.3. In both cases $k_m^{(2)}$ for ion F^- are given in the third column, $k_m^{(1)}$ for Kr^+ are given in the first column while $k_m^{(1)}$ of Kr_2^+ are in the second column.

Results of this calculation have been accepted and scheduled to appear in Applied Physics Letters 33(7), 1 Oct 1978 and is reprocued in Appendix IV. The orginal

figure of the Kr^+ case is given in Fig 6.3, and that of Kr_2^+ in Fig 6.4.

Table 6.3

mobilities of Kr^+, Kr_2^+ and F^- in Y

$m^*_F = 18.9984$, $m^*_{Kr} = 83.80$, $m^*_{Kr_2} = 167.60$

Y	Kr^+	Kr_2^+(c)	F^-(d)
He	20.2(a)	15.50	29.5
Ne	5.47	5.20	7.95
Ar	2.30(b)	1.90	3.33
Xe	0.964	0.804	1.69

a) from reference CH 1963

b) from reference MCSE 1967

c) all calculated from formula (6-12) using p* in Table 6.1

d) see $k_m^{(2)}$ of Table 6.1

In concluding this section we like to point out that results for the ions Xe^+ and Xe_2^+ with F^- in He, Ne, Ar, Kr can also be obtained easily. As expected similar results compared to the previous cases have been obtained. Another interesting case, reported by Flannery (F3,1978), is the mercury ion Hg^+ with halogens ions (F^-, Cl^-, Br^-, I^-) in Ar obtained from exactly the same methods. A comarison with the case of Ar^+ with halogens in Ar has also been made.

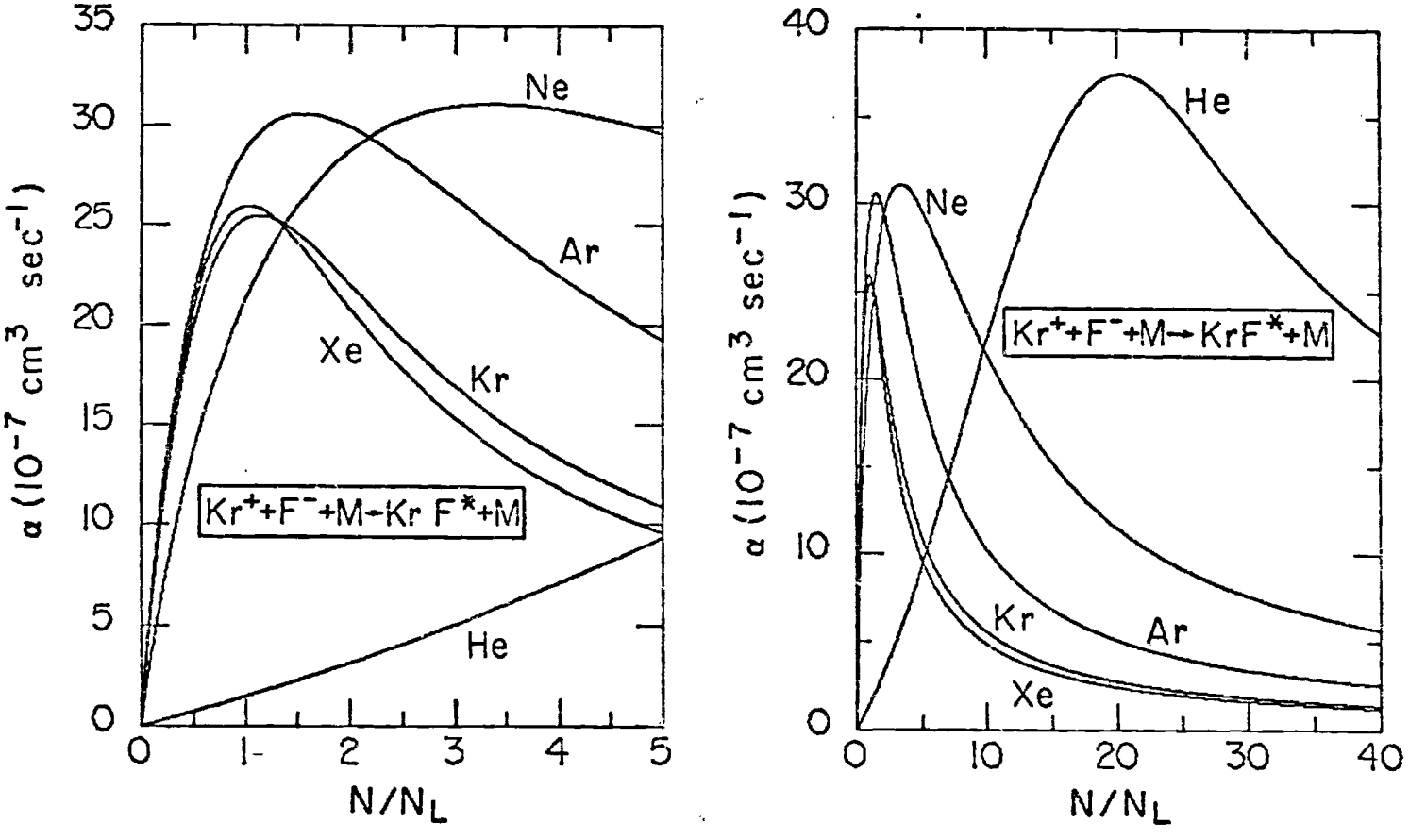

Fig. 6.3

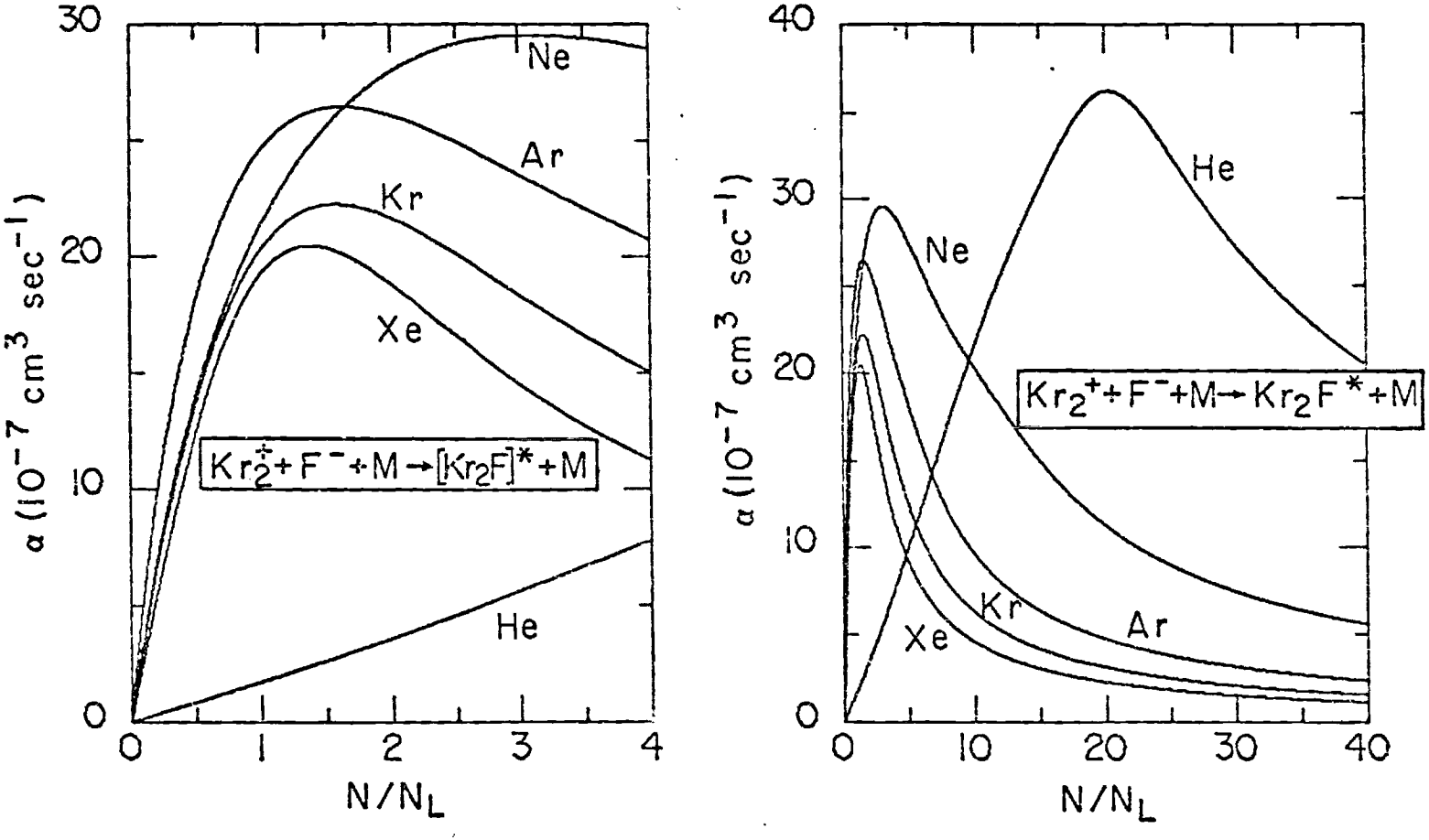
30
20
10
0
α (10⁻⁷ cm³ sec⁻¹)
Ne
Ar
Kr
Xe
He
Kr₂⁺ + F⁻ + M → [Kr₂F]* + M
0
1
2
3
4
N/N_L
40
30
20
10
0
α (10⁻⁷ cm³ sec⁻¹)
He
Ne
Kr₂⁺ + F⁻ + M → Kr₂F* + M
Xe
Kr
Ar
0
10
20
30
40
N/N_L

Fig. 6.4

CHAPTER VII

THREE-BODY ION-ATOM ASSOCIATION

Three body ion-atom association

$$X^{\pm} + Y + Z \longrightarrow XY^{\pm} + Z \qquad (7\text{-}1)$$

is generally not a rapid process at all. Under some circumstances however it is an important way of producing complex ions, in particular, by converting atomic ions into molecular ions, as one can see, e.g., in reaction (1-5a) for eventual recombination.

Although there have been several studies on the subject, as pointed out by Bates and McKibbin (1974) all of these treatments, mostly classical and one quantal, are subjected to much uncertainty (see the works cited in this reference).

Since it is such a difficult problem, we shall confine ourselves in this study to the problem of ion-atom association in their parent gas:

$$X^+ + X + X \longrightarrow X_2^+ + X \qquad (7\text{-}2)$$

By analogy to the recombination case one naturally considers this three-body process as one in which one member of the unbound ion-atom pair $(X^+ Y)$ collides with the third particle Z, thereby loses enough of their relative kinetic energy to form a bound molecular ion (here Z=Y=X, c.f. (7-1)).

We first follow Bates' early treatment (1950, B2), a modification of Thomson's theory of three-body recombination, as a 'guide', then adopt the quasi-equilibrium treatment (QEST) presented earlier for the recombination case, and finally make some investigation of the Bottleneck Treatment (BTL). The QEST is based on the fact that quasi-equilibrium of the

ion-atom pair $(X^+ X)$ is quickly established and that association proceeds via a net flow of the pairs down an energy ladder, until sufficiently strong binding is attained so that X_2^+ is incapable of further dissociation by the collision with the third body.

7.2 Thomson-Type Treatment

When the positive ion X^+ (particle 1), which is in thermal equilibrium with the neutral gas (particle 3) at temperature θ, approaches with a speed v_1 a neutral X (particle 2) to within a distance r, the kinetic energy of the relative motion increases from a thermal value $3k\theta/2$ to $(3k\theta/2 + pe^2/2r^4)$ with the interaction due to ion-induced dipole potential (p is the polairizability of the neutral atom).

We assume that all the kinetic energy gained $pe^2/2r^4$ is lost via a single, strong collision with a third neutral body. If this encounter occurs within a separation r such that the loss is greater than or equal to the initial thermal energy, i.e., the total energy of

the (1,2) relative motion becomes negative, the ion-atom pair is incapable of separation, thereby defining the trapping radius r_T

$$r_T = (pe^2/3k\theta)^{\frac{1}{4}} = (pe^2/m_{12}v_{12}^2)^{\frac{1}{4}} , \qquad (7\text{-}3)$$

where m_{12} is the reduced mass of the ion-atom pair.

The number density $N_1 (=N_+)$ of positive ions decreases with time according to the rate equation

$$dN_1/dt = -\alpha^A N_1 N_x = -K^A N_1 N_x^2 \qquad (7\text{-}4)$$

where $N_x (=N_2=N_3)$ is the neutral gas density, α^A is the coefficient of association, K^A defines the association rate. Thus as in the case of recombination, the simple model treatment predicts

$$\alpha_T^A = \pi r_T^2 \bar{v}_{12} P(r_T, N_x) \qquad (7\text{-}5)$$

for association, where $\bar{v}_{12}$ is the averaged ion-atom relative speed and where P is the density dependent probability that a ion-neutral collision occurs within a trapping radius. By analogy with the recombination this probability for a straight line trajectory is given by,

$$P(r_T N_x) = 1 - \tfrac{1}{2}\left(\frac{\lambda_+}{r_T}\right)^2 \left[1 - \left(1 + \frac{2r_T}{\lambda_+}\right) \exp\left(-\frac{2r_T}{\lambda_+}\right)\right] \qquad (7\text{-}6)$$

with the limits

$$P(r_T, N_x) \rightarrow \begin{cases} 1 & \text{high gas density, } N_x/N_L \rightarrow \infty \\ & \text{or } \lambda_+ \ll r_T \\ & \\ 4r_T/3\lambda_+ & \text{low density, } N_x/N_L \rightarrow 0 \\ & \text{or } \lambda_+ \gg r_T \end{cases} \tag{7-7}$$

where λ_+ is the mean free path of the ion X^+ in the gas.

Thus for low gas density, we have

$$\alpha_T^A = 4\pi r_T^3 \bar{v}_{12}/3\lambda_+ . \tag{7-8}$$

With the mean free path expressed in terms of the diffusion cross section Q_D, i.e.,

$$\lambda_+ = 1/N_x Q_D \tag{7-9a}$$

and the mean relative speed $\bar{v}_{12}$ given

$$\bar{v}_{12} = (8k\theta/m_{12}\pi)^{\frac{1}{2}} , \tag{7-9b}$$

the expression for ion-atom association is

$$\alpha_T^A = \frac{4\pi}{3}\left(\frac{p e^2}{3k\theta}\right)^{3/4}\left(\frac{8k\theta}{\pi m_{12}}\right)^{\frac{1}{2}} Q_D N_x \tag{7-10}$$

In terms of the measured mobility k_m, the explicit form of λ_+ is

$$\lambda_+ = \frac{16\bar{K}_{13}}{3e}\left(\frac{m_{13}k\theta}{2}\right)^{\frac{1}{2}} = \left(\frac{m_{13}k\theta}{2}\right)^{\frac{1}{2}} \frac{1600 k_m N_L}{e \quad N_x} \tag{7-11}$$

such that the rate coefficient in (7-8) becomes

$$\alpha_T^A = \frac{2\pi e}{300\ k_m^{(1)} m_1}\left(\frac{Pe^2}{3k\theta}\right)^{3/4} \frac{N_x}{N_L} \tag{7-12a}$$

$$= 2.58380 \times 10^{-29}\left(\frac{P^*}{\theta^*}\right)^{3/4} \frac{1}{m_1^* k_m^{(1)}} N_x \tag{7-12b}$$

where we use (i) the fact that all masses are equal, and (ii) that the physical parameters p*, θ^*, m*, are in the reduced units as in CHAP V.

Thus from knowledge of the mass m* and the polarizability p* one can estimate the rate constant of reaction K_T^A defined in (7-4),

$$K_T^A = \alpha_T^A / N_x \quad . \tag{7-12c}$$

For the rare-gas cases we have the results of K_T^A in Table 7.1.

We see from the table the agreement of K_T^A with the measured values is remarkble except the case of Kr. This indicates that formula (7-11a) or (7-11b) from the simple trapping-radius theory certainly provides useful and convenient estimates of the rate for the association of ions in their parent gases.

However, as in the case of three-body recombination, the artificial concept of trapping radius r_T is valuable only in that it provides some measure of the insight to a complicated series of events that result in association. A realistic assignment of r_T can be affected only after the detailed history of the ion-atom associating pair is established. Another shortcoming of this theory is that it neglects the effect of many weak collisions and further dissociative collision with the third body by the assumption that association results from a single, strong collision.

We thus follow the reasoning of the recombination case, develop a QEST which takes full account of the above problems, as already employed earlier. The success of Bates and Moeffett (1966), Bates and Flannery (1968) and our studies of recombination here should encourage this approach. So far the only work of association with the QEST is due to Bates and McKibbin (1974), in which they studied the problem of mercury ion Hg^+ with Hg in helium gas.

Table 7.1

Rates K_T^A (10^{-32} cm^6/sec) for the Ion-Atom Association

$$X^+ + X + X \rightarrow X_2^+ + X$$

X=He, Ne, Ar, Kr, Xe at 300°K

X	p^*(Å)^3 (a)	m^* (a)	k_m(1)	K_T^A(b)	K^A(expt)
He	0.205	4.003	10.3	8.38	10.8 (3.5-11) (d)
Ne	0.395	20.183	4.08	6.86	(5-9)
Ar	1.640	39.944	1.52	27.06	30 (c) (30-47) (e)
Kr	2.480	83.80	0.823	32.48	23 (c)
Xe	4.040	131.30	0.570	43.16	--

a) see Tables 5.1, 5.2 for references

b) K_T^A estimated from (7-12b); K^A, expt. values

c) Beaty & Patterson (1965, 1968)

d) Table ii of Bohme, Dunkin, Fehsenfeld & Ferguson (1969)

e) Gaur & Chanin (1969)

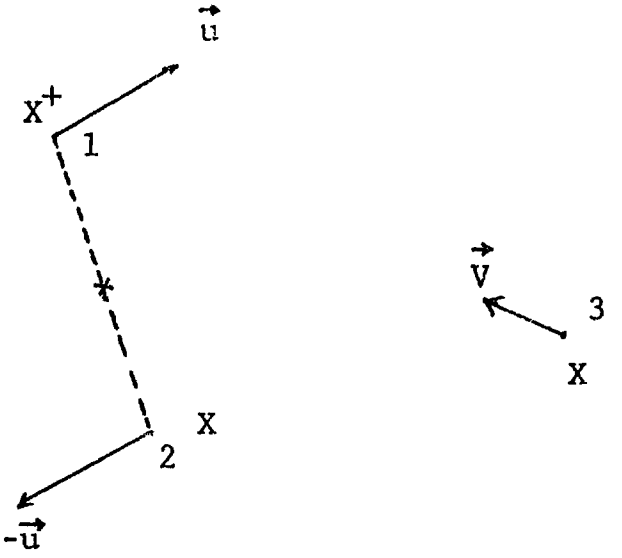

(a) before (1,3) charge-exchange

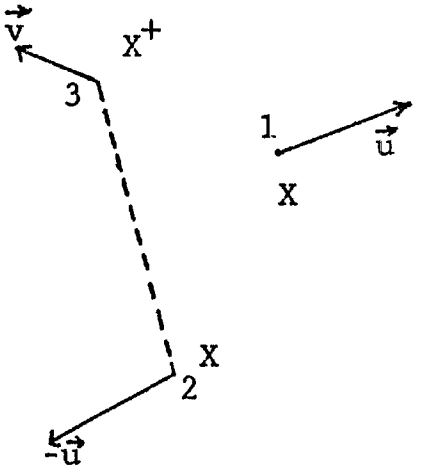

(b) after charge-exchange

Fig. 7.1 Association $X^+_1 + X_2 + X_3 \rightarrow X_2^+ + X$

7.3 Quasi-Equilibrium Statistical Treatment

Unlike the recombination case, the energy reduction of the associating ion-atom pair in the following process,

$$\underset{1}{X^+} + \underset{2}{X} + \underset{3}{X} \longrightarrow (X^+ + X)^* + X \longrightarrow X_2^+ + X \qquad (7\text{-}13)$$

involving particles denoted by 1, 2 and 3, is brought about only via the symmetrical resonance charge-transfer (SRCT) collision,

$$X^+(\text{fast}) + X(\text{slow}) \longrightarrow X(\text{fast}) + X^+(\text{slow}). \qquad (7\text{-}14)$$

The SRCT simply interchanges the velocity vector of the ion with the thermal velocity vector of the neutral. Thus the initial fast ion $X^+(1)$ is converted via (7-14) into a slow ion $X^+(3)$ which may then be trapped in the (2,3) mutual field. The neutral particle 2 sits as a spectator during the process of charge-transfer. Further collisions with the neutral can occur causing even further deactivation or dissociation of the ion-atom pair.

The two essential ingredients for a realistic description of process (7-13) are then (i) the determination of the encounter rate coefficient $K(E_i, E_f)$ for the rate of the collisions

$$(X^+ + X)_{E_i} + X \dashrightarrow (X^+ + X)_{E_f} + X \qquad (7\text{-}15)$$

which changes the internal energy of the associating ion-atom pair from a initial value of E_i to a final value of E_f, and (ii) the formulation of the subsequent course of the deactivation events with time in terms of $K(E_i, E_f)$.

We will develop (i) and (ii) in the following two sections.

7.4 Expression of $K(E_i, E_f)$

The expression of $K(E_i, E_f)$ follows exactly as the case of recombination except that here only the charge transfer (SRCT) part contributes, there is no elastic collision. The development is simplified further for the reason that all masses are equal.

Consider the three particles 1, 2, 3 of (7-13) with initial velocities $\vec{u}$, $-\vec{u}$, $\vec{v}$ respectively in the C.M. frame of the initial (1,2) system. The velocities before and after the (1,3) charge-exchange collision are shown in Fig 7.1. The initial kinetic energy of the ion-neutral

(1,2) pair T_1, and the final relative kinetic energy of the ion-neutral (2,3) pair T_f, are given by

$$T_i = m_{12} \vec{g}_i^{\,2}/2 = m\vec{u}^{\,2} \qquad (7\text{-}16a)$$

$$T_f = m_{23} \vec{g}_f^{\,2}/2 = m(\vec{u}+\vec{v})^2/4 \qquad (7\text{-}16b)$$

where m is the mass of the atom (or ion). Under the Impulse Approximation which leaves both the relative separation of the ion-atom pair and the velocity of the spectator 2 unchanged, the change of the internal energy of the pair from E_i to E_f is just $T_f - T_i$, or

$$\Delta = E_f - E_i = T_f - T_i = m(\vec{v}^{\,2} - 3\vec{u}^{\,2} + 2uv\cos\psi)/4 \qquad (7\text{-}17)$$

where ψ is the angle between $\vec{v}$ and $\vec{u}$.

From the obvious limits of the relative speed g ($|v-u| \leq g \leq v+u$) and the reality of the limits of v_1, v_2 of v, for a given Δ and u, satisfying

$$v^2 \pm 2uv - (3u^2 + 4\Delta/m) = 0 \qquad (7\text{-}18a)$$

such that

$$v_{2,1} = 2(u^2 + \Delta/m)^{\frac{1}{2}} \pm u \qquad (7\text{-}18b)$$

we have the requirement

$$u^2 + \frac{\Delta}{m} \geq 0$$

or (7-19)

$$u^2_{min} = 0 \quad \text{or} \quad \Delta \geq 0, \text{ excitation}$$
$$u^2_{min} = -\frac{\Delta}{m} \quad \text{or} \quad \Delta < 0, \text{ de-excitation} .$$

Let q^+ be the charge-transfer cross section for (7-14) at (1,3) relative speed $|v-u|$ so that the rate of encounters with $\chi=\cos\psi$ to be within $d\chi$ about χ is

$$dK = |\vec{v}-\vec{u}|\, q^+ \, d\chi/2 \quad . \tag{7-20a}$$

From (7-17) we have, for a given initial internal energy E_i and $\vec{u}$, $\vec{v}$,

$$d\chi = dE_f \, 2/muv \tag{7-20b}$$

so that

$$dK = dE_f q^+ |\vec{v}-\vec{u}|/muv \quad . \tag{7-20c}$$

Insert in (7-20c), the expression from (7-17)

$$2uv\cos\psi = 4\Delta/m + 3u^2 - v^2 \tag{7-20d}$$

we obtain

$$dK = \sqrt{2} \; q^+ (v^2 - u^2 - 2\Delta/m)^{\frac{1}{2}} \, dE_f/muv \tag{7-21a}$$

for the partial encounter rate coefficient for a given $\vec{u}$,

$\vec{v}$, Δ . From expression (7-21a) we see a further restriction on the minimum of v

$$v^2 \geq u^2 + 2\Delta/m \ . \qquad (7\text{-}21b)$$

After integration over distributions $\mathcal{J}(u)$ of u and $\mathcal{G}(v)$ of v we have the encounter rate coefficient changing the pair energy from E_i to (E_f, E_f+dE_f)

$$dE_f \ K(E_i,E_f) = dE_f \ \frac{\sqrt{2}q^+}{m} \int du \int dv \ \frac{\mathcal{J}(u)}{k} \ \frac{\mathcal{G}(v)}{v} \left(v^2-u^2-\frac{2\Delta}{m}\right)^{\frac{1}{2}} . \qquad (7\text{-}22)$$

Assuming the (1,2) system has a microcanonical distribution, one has (see CHAPTER IV)

$$\mathcal{J}(u)\,du = \frac{1}{C(E_i)} \ (E_i-V)^{\frac{1}{2}} \ r^2\,dr \qquad (7\text{-}23a)$$

where $C(E_i) = \int dr \ r^2(E_i-V)^{\frac{1}{2}}$,

with the interaction potential between ion and the neutral atom

$$V=-pe^2/2r^4 \qquad (7\text{-}23c)$$

where r is the ion-atom separation. From Appendix A, for the polarization potential we have

$$C(E_i) = \left(\frac{pe^2}{2k\theta}\right)^{3/4} \frac{(k\theta)^{\frac{1}{2}}}{4|E_i/k\theta|^{\frac{1}{4}}} B(\tfrac{3}{2},\tfrac{1}{4}) \qquad (7\text{-}24a)$$

$$= \left(\frac{pe^2}{2k\theta}\right)^{3/4} (k\theta)^{\frac{1}{2}}/H_A$$

where

$$H_A = 4\lambda^{\frac{1}{4}}/B(3/2,1/4) \qquad (7\text{-}24b)$$

From the fact that $E_i = T_i + V_i$ and,

$u = ((E_i - V)/m)^{\frac{1}{2}}$

we have, from (7-23a)

$$\mathcal{J}(u)du/u = m^{\frac{1}{2}} r^2 dr/C(E_i) \qquad (7\text{-}24c)$$

We assume that the C.M. of (1,2) is in thermal equlibrium with 3 at temperature θ, such that the distribution of speed v is

$$\mathcal{J}(v)dv = 4\pi v^2 dv(\mu'/2\,k\theta)^{3/2} e^{-\mu' v^2/2k\theta} \qquad (7\text{-}25a)$$

where

$$\mu' = m_3(m_1 + m_2)/(m_1 + m_2 + m_3) = 2m/3 \qquad (7\text{-}25b)$$

since all masses are equal. Hence

$$\mathcal{J}(v)dv/v = 4\pi v dv\,(m/3\pi k\theta)^{3/2} e^{-mv^2/3k\theta} \qquad (7\text{-}25c)$$

To simplify things further we define x, y, z, λ, μ as before

$$x=T_i/k\theta = (E_1-V)/k\theta = -\lambda + 1/z$$

$$y=mv^2/3k\theta$$

$$z=r(2k\theta/pe^2)^{\frac{1}{4}}$$

$$\lambda = -E_i/k\theta \ , \qquad \mu=-E_f/k\theta \ . \tag{7-26}$$

Eq. (7-22) then becomes

$$K(E_i,E_f)dE_f = dE_f \frac{2\sqrt{2}\ q^+}{C(E_i)}\left(\frac{pe^2}{2k\theta}\right)^{3/4}\frac{1}{\sqrt{\pi m}}$$

$$x\int_{Z\ min}^{Z\ max} dz\ z^2 \int_{y_-}^{y_+} dy\ e^{-y}\left[y-\frac{x}{3}-\frac{2}{3}(\lambda-\mu)\right]^{\frac{1}{2}} \tag{7-27a}$$

where

$$Z_{min}=0, \qquad Z_{max}=\text{min. of } (1/\lambda^{\frac{1}{4}}\ ,\ 1/\lambda^{\frac{1}{4}}) \tag{7-27b}$$

and

$$y_{\pm}=\frac{1}{3}\left[5x+4(\lambda-\mu) \pm 4\sqrt{x(x-\lambda-\mu)}\right] \tag{7-27c}$$

with the condition $x+\lambda-\mu>0$, or

$$1/z^4 \geq \mu \tag{7-27d}$$

which is compatible with (7-27b). After a substitution

$$Y=y-x/3-2(\lambda-\mu)/3$$

and an integration over Y, $K(E_i,E_f)$ in (7-27a) is further

simplified

$$K(E_i,E_f)dE_f = dE_f \frac{(2)^{\frac{1}{2}} q^+}{C(E_i)}\left(\frac{pe^2}{2k\theta}\right)^{3/4}\frac{1}{\sqrt{m}}\int_0^{Z_{max}} dz\, z^2\, I_0 \qquad (7\text{-}28a)$$

where

$$I_0 = \exp\left[-(x+2(\lambda-\mu))/3\right]\left[\operatorname{erf}(\sqrt{Y_+})-\operatorname{erf}(\sqrt{Y_-})\right.$$
$$\left.\frac{2}{\sqrt{\pi}}\left(\sqrt{Y_+}\,e^{-Y_+}-\sqrt{Y_-}\,e^{-Y_-}\right)\right], \qquad (7\text{-}28b)$$

$$Y_{\pm} = 2\left((x)^{\frac{1}{2}}+(x+\lambda-\mu)^{\frac{1}{2}}\right)^2/3 \qquad (7\text{-}28c)$$

and erf(x), the error function defined before ((4-60b)), x defined in (7-26).

$K(E_i,E_f)$ can also be expressed in another form by cancelling the factor from $C(E_i)$ in (7-24a),

$$K(E_i,E_f) = \left(\frac{2}{mk\theta}\right)^{\frac{1}{2}} q^+ \frac{4}{B(\frac{3}{2},\frac{1}{4})} F_A(\lambda,\mu) \qquad (7\text{-}28d)$$

where

$$F_A(\lambda,\mu) \equiv \lambda^{\frac{1}{4}} F(\lambda,\mu) = \lambda^{\frac{1}{4}}\int_0^{Z_{max}} dz\, z^2 I_0 \,. \qquad (7\text{-}28e)$$

Since $K(E_i, E_f)$ is the encounter rate coefficient of transition from energy E_i to E_f, F_A is the 'system independent' rate coefficient as all the system parameters have been factored out resulting in great simplification for later calculation. Table 7.2 list some values of

$F_A(\lambda,\mu)$, including the bound-bound transition ($\lambda > 0$, $\mu > 0$) and the bound-free transition ($\lambda > 0$, $\mu < 0$). As expected there is a peak value in the neighborhood of $\lambda = \mu$ for elastic transition. The decays in their values with increasing $\lambda - \mu$ are much faster in the bound-free case than the bound-bound transition as can be seen in Fig 7.2. Also shown in Fig 7.3 are the free-bound transition elements obtained from applying the detailed balance relation to the generated table of F_A for $\lambda > 0$. In this case the elements all decay as $|\mu|$ is increased since transition involving larger energy changes are becoming less probable. Also listed in Table 7.2 are some values of $F_{AC}(\lambda)$,

$$F_{AC}(\lambda) = \int_{-\infty}^{\circ} d\mu\ F(\lambda,\mu) \tag{7-28f}$$

which is effectivly the contribution to depleting a given bound state λ via bound-free transition.

To conclude this section we note that

$$\kappa(\lambda,\mu)d\mu = K(E_i,E_f)dE_f = K(E_i,E_f)k\theta d\mu \tag{7-29a}$$

so that

$$\kappa(\lambda,\mu) = K(E_i,E_f)k\theta \tag{7-29b}$$

Table 7.2 $F_A(\lambda,\mu) = \lambda^{\frac{1}{4}}F(\lambda,\mu)$

λ	0.5	1.0	1.5	2.0	3.0	4.0	5.0
-5.0	1.954E-03	8.294E-04	3.970E-04	2.014E-04	5.693E-05	1.728E-05	5.471E-06
-4.0	5.216E-03	2.183E-03	1.039E-03	5.259E-04	1.486E-04	4.515E-05	1.432E-05
-3.0	1.348E-02	5.604E-03	2.665E-03	1.350E-03	3.827E-04	1.168E-04	3.717E-05
-2.0	3.305E-02	1.384E-02	6.632E-03	3.382E-03	9.691E-04	2.982E-04	9.551E-05
-1.5	5.016E-02	2.130E-02	1.030E-02	5.287E-03	1.529E-03	4.735E-04	1.524E-04
-1.0	7.366E-02	3.211E-02	1.576E-02	8.175E-03	2.396E-03	7.483E-04	2.423E-04
-.5	1.029E-01	4.705E-02	2.367E-02	1.247E-02	3.724E-03	1.176E-03	3.835E-04
0.0	1.321E-01	6.610E-02	3.462E-02	1.867E-02	5.725E-03	1.835E-03	6.042E-04
.5	1.422E-01	8.677E-02	4.875E-02	2.727E-02	8.687E-03	2.839E-03	9.464E-04
1.0	1.203E-01	1.002E-01	6.467E-02	3.844E-02	1.296E-02	4.349E-03	1.472E-03
1.5	1.007E-01	9.635E-02	7.709E-02	5.132E-02	1.889E-02	6.578E-03	2.272E-03
2.0	8.641E-02	8.787E-02	7.874E-02	6.232E-02	2.667E-02	9.788E-03	3.471E-03
3.0	6.762E-02	7.275E-02	7.119E-02	6.550E-02	4.449E-02	2.013E-02	7.778E-03
4.0	5.591E-02	6.177E-02	6.271E-02	6.082E-02	5.092E-02	3.413E-02	1.599E-02
5.0	4.790E-02	5.375E-02	5.568E-02	5.544E-02	5.058E-02	4.109E-02	2.739E-02
$F_{AC}(\lambda)$	2.261E-01	8.463E-02	3.790E-02	1.839E-02	4.901E-03	1.429E-03	4.382E-04

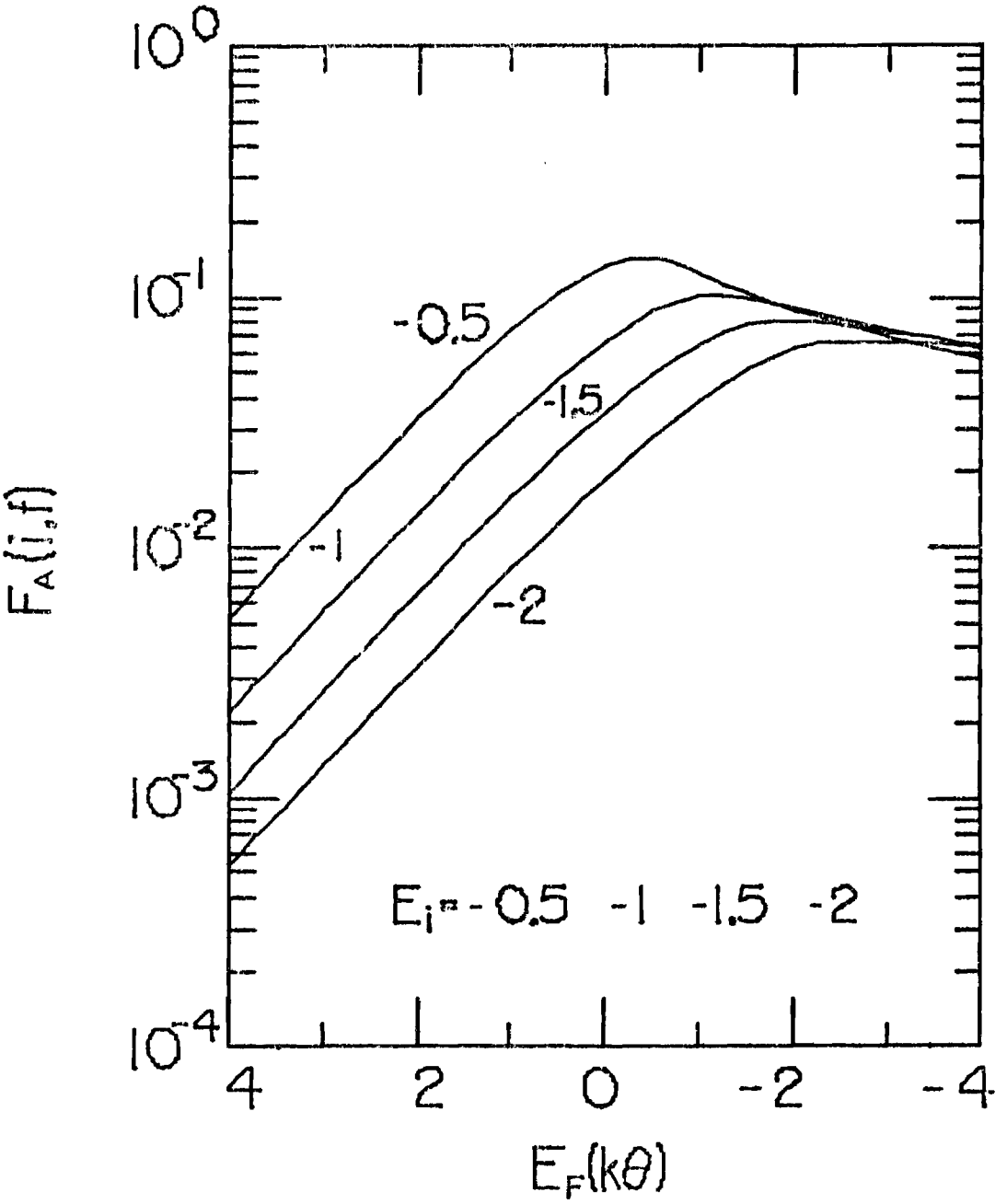

Fig. 7.2

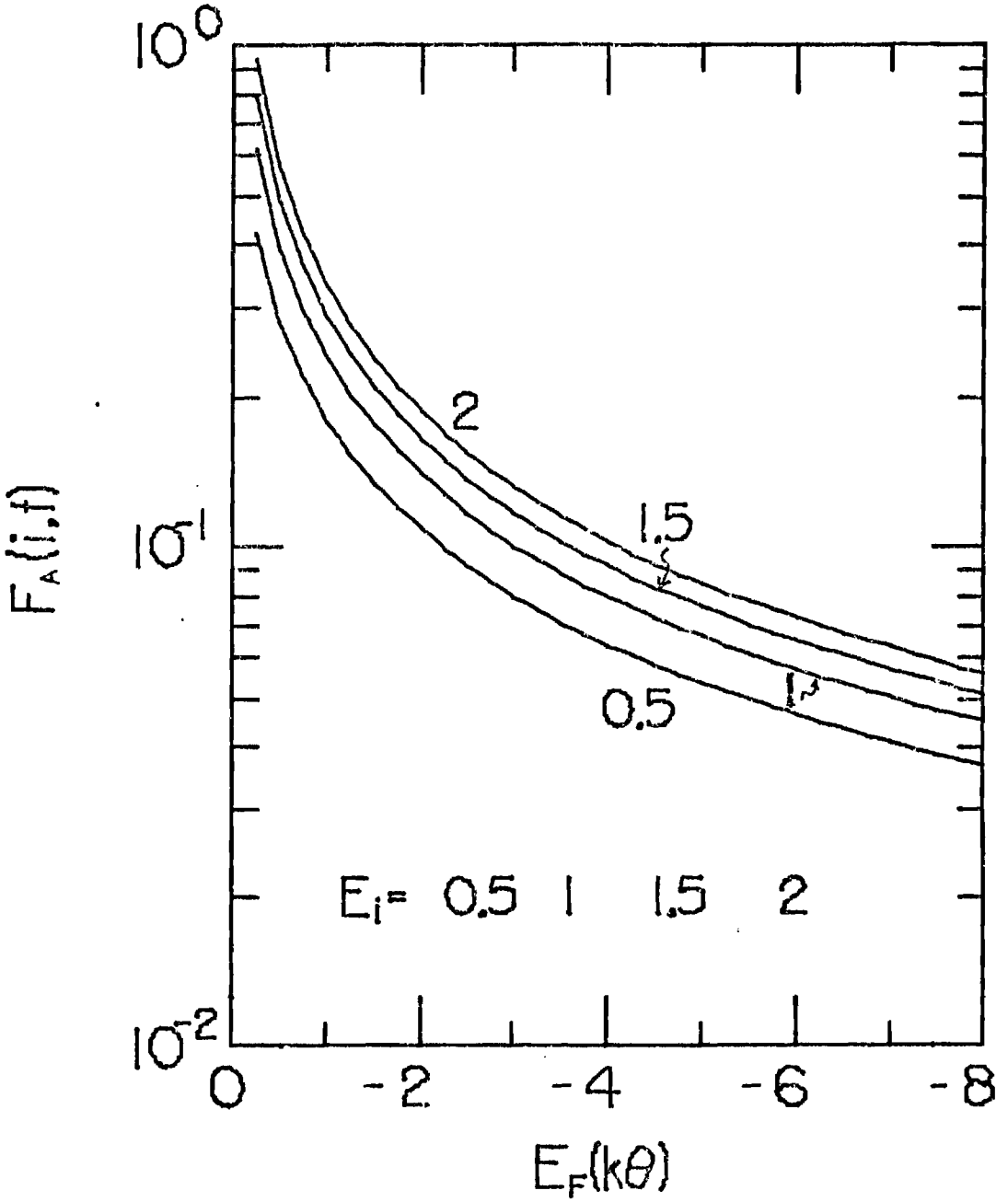

Fig. 7.3

7.5 Reaction Rate Coefficient α_A

From the total number density $n(E_i)dE_i$ of the associating ion-atom pairs with internal energy in the interval (E_i, E_i+dE_i), a number $n(E_i)dE_i(K(E_i,E_f)dE_f N_x)$ has formed in (E_f, E_f+dE_f) as a result of a single collision with N_x neutral gas atom in unit volume. The association rate is then the balance of the downward and upward transitions of these pairs passing some negative energy level E_o,

$$\begin{aligned}\alpha_A N_1 N_2 &= R\downarrow - R\uparrow \\ &= N_3\Big[\int_{E_o}^{\infty} n(E_i)dE_i \int_{E_D}^{E_o} dE_f\ K(E_i,E_f) \\ &\quad - \int_{E_D}^{E_o} dE_f\ n(E_f) \int_{E_o}^{\infty} K(E_f,E_i)dE_i\Big] .\end{aligned} \tag{7-30}$$

This is formally exactly the same as (3-7) in recombination case, except here we have $N_2=N_3=N_x$ and the greatest binding energy E_D is for the polarization potential. The schematic energy levels diagram in Fig 3.1 is still suitable for our reference here provided that E_D, E_s are different from the previous case.

Under the thermodynamic equilibrium condition of the ion-atom pair, detailed balance is satisfied, i.e.,

$$n_T(E_i)\ K(E_i,\ E_f) = N_T(E_f)\ K(E_f,\ E_i)\ . \tag{7-31}$$

From the definition of the normalized distribution function

$$\rho_i = n_i/(n_T)_i, \qquad \rho_f = n_f/(n_T)_f \tag{7-32}$$

and with the help of (7-31), the rate coefficient α_A of (7-30) is now

$$\alpha_A = N_x \int_{E_o}^{\infty} dE_f \int_{E_D}^{E_o} dE_i \frac{n_T(E_i)}{N_1 N_x} (\rho_f - \rho_i) K_{if} \tag{7-33a}$$

where dummy indices i, f have been interchanged as in (3-9), and $N_1=N_+$, $N_x=N_2=N_3$ have been substituted.

The number density $n_T(E_i)$ of the ion-atom pairs in the thermal equilibrium at temperature θ with the neutral gas N_x is, from Appendix I

$$\frac{n_T(E_i)dE_i}{N_i N_x} = \frac{g(E_i)dE_i\, e^{-E_i/k\theta}}{(2\pi m_{12} k\theta)^{3/2}} \tag{7-33b}$$

assuming both ion-atom pair and atom are structureless ($\omega_A=\omega_{AB}=\omega_{AB}=1$). Using the result of Appendix A, we have the equilibrium population

$$\frac{n_T(E_i)dE_i}{N_1 N_x} = \frac{8\pi^{\frac{1}{2}} C(E_i)dE_i}{(k\theta)^{3/2}}\, e^{-E_i/k\theta} \tag{7-33c}$$

$$= 2\left(\frac{pe^2}{2}\right)^{3/4} \frac{\pi^{\frac{1}{2}} e^{\lambda}}{k^3 \theta^3 \lambda^{\frac{1}{4}}} B\left(\frac{3}{2}, \frac{1}{4}\right) d\lambda .$$

Also noting that $m_1=m_2=m_3$ we have α_A from (7-33a),

$$\alpha_A = N_x 8\left(\frac{\pi}{k\theta}\right)^{\frac{1}{2}} \int_{-\infty}^{\nu} d\mu \int_{\nu}^{\omega} d\lambda \; C(E_i)(\rho_f - \rho_i)\kappa(\lambda,\mu) \qquad (7\text{-}34)$$

$$= N_x 3q^+\left(\frac{2\pi}{m}\right)^{\frac{1}{2}} \left(\frac{pe^2}{2}\right)^{3/4} \frac{1}{(k\theta)^{\frac{1}{4}}} \int_{\nu}^{\omega} d\lambda e^{\lambda} \int_{-\infty}^{\nu} d\mu(\rho(\mu)-\rho(\lambda))F(\lambda,\mu)$$

$$\equiv N_x a_A \int_{\nu}^{\omega} d\lambda \; e^{\lambda} \int_{-\infty}^{\nu} d\mu(\rho(\mu)-\rho(\lambda)) \; F(\lambda,\mu)$$

with the integration variables E_i, E_f changing to λ, μ and the definition of $F(\lambda, \mu)$ in (8-28e). We finally have a complete expression of the association rate coefficient α_A from (7-34) together with (7-28) and (7-26) provided that the distribution function $\rho(x)$ is known. The characteristics of each individual systems studied are from the atomic mass m, atomic polarizability p and its charge-exchange cross section q^+ (hence the measured mobility $k_m^{(1)}$).

As we shall see in the following section $\rho(x)$ is more or less independent of the system parameters since all variables involved have already been scaled. So in the case of association of ions in their parent gas a fairly 'constant' triple integral (over λ, μ, z) provided that the maximum binding energy - $\omega k\theta$ and the 'sink' $-s\,k\theta$ do not have much variation over the systems studied.

To compare the expression α_A in (7-34) with that of Thomson's model, we again recall the fact that the charge-transfer cross section q^+ is half of that of diffusion: $Q_D=2q^+$, so the constant factor of α_A, i.e., in (7-34) becomes

$$a_A = 4\sqrt{2}\ Q_D(\pi/m)^{\frac{1}{2}}(p e^2/2)^{3/4}/(k\theta)^{\frac{1}{4}} \qquad (7.35a)$$

The factor a_A is converted to

$$a_A = 9\ \alpha_T^A/4N_x(6)^{\frac{1}{4}} \qquad (7\text{-}35b)$$

when compared to α_T^A in (7-10), or becomes

$$a_A = \sqrt{2}\,\pi E\left(\frac{pe^2}{2k}\right)^{3/4}/[200m\ N_L k_m^{(1)}] \qquad (7\text{-}35c)$$

$$= 3.714528 \times 10^{-29}(p^*/\theta^*)^{3/4}/m_1^* k_m^{(1)} \qquad (7\text{-}35d)$$

with the parameters expressed in the proper reduced units. We will use (7-35b) and (7-35d) in the expression of α_A, which in terms of a_A is now

$$\alpha_A = N_x a_A \alpha_o \equiv N_x a_A \int_\nu^\omega d\lambda\ e^{\lambda\int_{-\infty}^{\nu} d\mu(\rho(\mu)-\rho(\lambda))F(\lambda,\mu)}. \qquad (7\text{-}36)$$

7.6 Quasi-Equilibrium Distribution $\rho(x)$

The determination of ρ, the quasi-equilibrium distribution for the association process, follows exactly the same lines as the corresponding case of the three-body recombination. So we will give only a few important points here.

When the association is proceeding, the number density $n(E_i)$ of all ion-atom pairs with energy E_i is governed by equation (3-18), where $E_s=-sk\theta$ is now the negative energy level at which the association is stabilized, or the 'sink'. In terms of the normalized distribution ρ, (3-18) becomes (3-19) subject to boundary conditions (3-20) or (5-9b).

In the association, as in the recombination, a quasi-equilibrium distribution of the excited ion-atom pairs is estabilished almost immediately and while the rates of formation or destruction of these states are rapid (c.f. Table 7.2) the overall population ρ of a given events changes only slowly in comparison to the rate of association. Thus the quasi-equilibrium distribution ρ is, after taking $\partial\rho/\partial t=0$, the solution of the integral equation

$$\rho(\lambda)\int_{-\infty}^{\omega}\kappa(\lambda,\mu)d\mu = \int_{-\infty}^{s}\rho(\mu)\,\kappa(\lambda,\mu)d\mu \qquad (7\text{-}37a)$$

in terms of the reduced energy variable (λ , μ). This equation is simplified further to

$$\rho(\lambda)\int_{-\infty}^{\omega}F(\lambda,\mu)d\mu = \int_{-\infty}^{s}\rho(\mu)\;F(\lambda,\mu)\;d\mu \qquad (7\text{-}37b)$$

where $F(\lambda,\mu)$ has been defined in (7-28e), and is the main part of $F_A(\lambda,\mu)$ without system dependent factors $(2/m)^{\frac{1}{2}}\;q^{+}$ and H_A. In solving $\rho(\lambda)$, one needs the table of $F(\lambda,\mu)$ only. The numerical procedure is identical to the recombination case. The result for the chosen 'sink' $s=10$, and $\omega=12$ for maximum binding energy is given in Table 7.3 and shown in Fig 7.4.

Unlike the recombination case here the distribution function drops quickly from the initial value of unity at $\lambda=0$ to 0.2988 at $\lambda=0.5$ compare to the value of 0.9673, e.g., in the case of recombination of Kr. This reflects the nature of $1/r^4$ interaction in the association and the first difficulty of the QEST without including the centrifugal potential due to orbital angular momentum. In fact we expect a physical distribution of $\rho(x)$ decreasing

from 1 at x=0 to 0 at x=s smoothly as the case of recombination. With many tries we make the choice of s=10 and ω =12 such that ρ (1/16)=0.605 and $\rho(9.9375)=7.343\times10^{-4}$. Other choices of (s, ω) either cause too sharp a drop of ρ when x is close to zero and/or too slow a decay of ρ to zero when x are close to s.

Table 7.3 $\rho(\lambda)$ for Association

λ	$\rho(\lambda)$	λ	$\rho(\lambda)$
0.	1.	3.	3.3202E-02
.0625	6.0542E-01	3.5	2.3066E-02
.125	5.2010E-01	4.	1.6276E-02
.1875	4.6206E-01	4.5	1.1660E-02
.25	4.1715E-01	5.	8.4795E-03
.5	2.9881E-01	6.	4.6915E-03
.75	2.2607E-01	7.	2.7514E-03
1.	1.7565E-01	8.	1.6985E-03
1.25	1.3873E-01	9.	1.0890E-03
1.5	1.1083E-01	9.5	8.8028E-04
2.	7.2507E-02	9.75	7.9304E-04
2.5	4.8598E-02	10.	0.

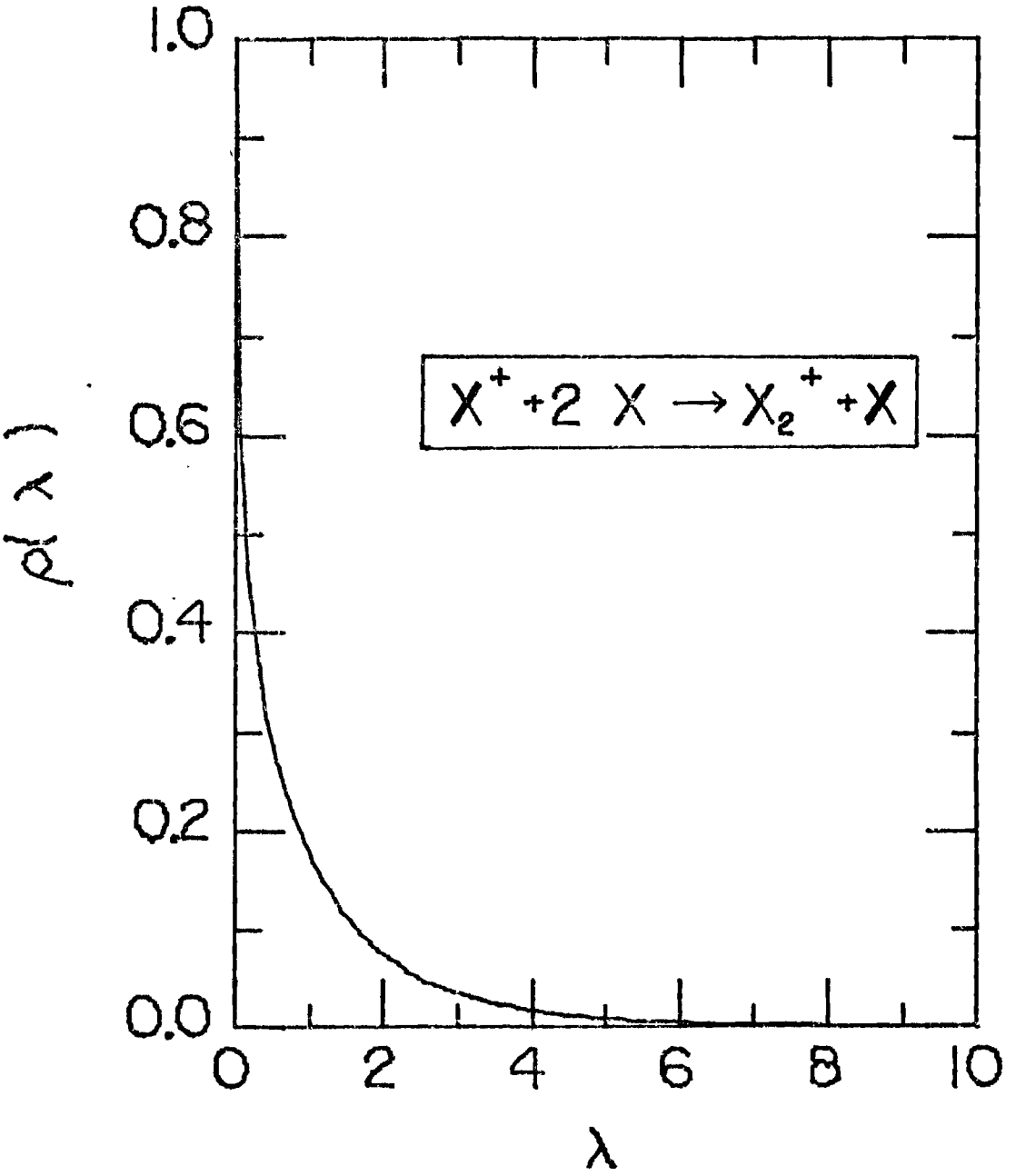

Fig. 7.4

7.7 Results of the QEST of Association

With the tables of $F(\lambda, \mu)$ and $\rho(\lambda)$ ready we can now calculate the association rate coefficient α_A using (7-36) with the aid of (7-35d). For the five cases considerded (He, Ne, Ar, Kr and Xe) we take same values of ω and s: s=10, and ω=12 for convenience with the mesh of 1/16. The result of integration over λ and μ is α =1.01616. Taking the system parameters from Table 7.1, the rate constants α_A / N_x for each system are calculated and listed in Table 7.4.

We also note that from (7-36) and (7-35b) the ratio of the rate constant α_A to that of Thomson's is

$$\alpha_A / \alpha_T^A = 9\alpha_o / 4(6)^{\frac{1}{4}} = 1.46085 \qquad (7\text{-}38)$$

i.e. the present treatment gives almost one and a half of the value of the rate constant from Thomson's treatment. While the Thomson's approach underestimates the rate constant (c.f. expt. values in Table 7.1) because of the exclusion of many processes like multiple collisions, bound-bound transtions etc., the present method gives higher values of the rate constant for perhaps different reasons. Though the resonance charge exchange is 'the' mechanism for ions associating in their parent gas, the ion-atom pairs neverthless are in relative orbital motion.

The centrifugal orbital potential barrier is of longer range than the polarized potential therefore should be included in the mutual potential. This in turn modifies the distrbution function and perhaps the charge-exchange cross section. From previous experience (BMC1, 1974) this inclusion of A.M. may reduce the final result of the rate constant. Since the inclusion of the orbital potential is in itself an interesting subject, obviously very complicated, and outside our scope of consideration we will not dwell further. To conclude our study of the association problem we will now investigate the applicability of the Bottlenek Approximation in our final section.

Table 7.4

Association Rate Constant

	a_A	α_A/N_x
He	1.20408	1.2235
Ne	0.985972	1.0019
Ar	3.88956	3.9524
Kr	4.66936	4.7448
Xe	6.20453	6.3048

N.B. a_A and α_A/N_x are all in unit of 10^{-31} cm^6/sec.

7.8 Bottleneck Treatment

The basic expression for the association rate coefficient α_A is given in (7-33a) or (7-34). While the collisional rate $K_{if}dE_f$ for de-excitation between the neighboring levels decreases rapidly with increasing binding, i.e., with greater λ (see Fig 7.2 and 7.3 where $E_i = -\lambda k\theta$, and Table 7.2) the equilibrium population (7-33c) of the excited (X^+-X) bound states increases rapidly with increasing binding. Hence the total effective rate for de-excitation will exhibit a minimum for a particular level λ^* with the negative energy $E^* = -\lambda^* k\theta$. Ion-atom pairs more tightly bound than E^* have much greater possibility of undergoing further de-excitations to the level for the stabilization of the association than of being excited above the minimum rate state λ^*. Thus the association rate is given as the total de-excitation rate past λ^* which is therefore the corresponding 'association bottleneck' as the recombination case. It is then sufficient to assume in (7-23a) or (7-34), as in CHAP. 5,

$$\rho(x) = \begin{cases} 1 & E \geq E^* \quad (x \leq \lambda^*) \\ 0 & E^* > E \quad (\lambda^* < x) \end{cases} \tag{7-39}$$

so the association rate coefficient (7-33a) reduces to

$$\alpha_A^{BT} = N_x \int_{E^*}^{\infty} dE_f \int_{E_D}^{E^*} dE_i \; \frac{n_T(E_i)}{N_+ N_x} K_{if} \qquad (7\text{-}40a)$$

where E* is the energy level such that

$$d\alpha_A^{BT}/dE^* = 0 \qquad (7\text{-}40b)$$

i.e., giving minimum α_A^{BT}. Numerically one can vary E* to get the minimumu of α_A^{BT}. Using (7-33c) and changing the variable of integration, (7-40a) can be written as

$$\alpha_A^{BT} = N_x \, a_A \int_{\lambda^*}^{\omega} d\lambda e^{\lambda} \int_{-\infty}^{\lambda^*} F(\lambda, \mu) d\mu$$

$$= N_x \, a_A \, \alpha_o^{BT} \qquad (7\text{-}41a)$$

where a_A is given in (7-35). Before we check the results of the variation of the two dimensional integration over λ^* in Table 7.5, we note that the ratio of α_A^{BT} to the Thomson's is given by

$$\alpha_A^{BT}/\alpha_T^A = 9 \, \alpha_o^{BT}(\lambda^*)/4(6)^{\frac{1}{4}} = 1.565085 \, \alpha_o^{BT}(\lambda^*) \qquad (7\text{-}41b)$$

from (7-35b) and (7-41a).

Unless the minimum α_o^{BT} is really small the bottleneck rate is always greater than the Thomson's rates. From Table 7.5 we see that the real λ^* to give minimum of α_o^{BT} (=1.2186) is λ^*=0.1 at which α_A^{BT} is 20% greater than the rate from the QEST. Since the values of α_A in the QEST is

independent of the choice of ν as long as $0 \leq \nu \leq s$, i.e., in the range of stabilization, we may take $\nu = \lambda^*$ in (7-36) so that

$$\alpha_o' = \int_{\lambda^*}^{\omega} d\lambda e^{\lambda} \int_{-\infty}^{\lambda^*} d\mu \left[\rho(\mu) - \rho(\lambda) \right] F(\lambda, \mu)$$

$$= \int_{\lambda^*}^{\omega} d\lambda e^{\lambda} \int_{-\infty}^{\lambda^*} \rho(\mu) F(\lambda, \mu) d\mu - \int_{\lambda^*}^{\omega} d\lambda e^{\lambda} \rho(\lambda) \int_{-\infty}^{\lambda^*} d\mu F(\lambda, \mu) \quad . \qquad (7\text{-}42)$$

While the first term, with $\rho \leq 1$, is smaller than α_o^{BT}, the second double integral is always positive. We see that in any case the BTL always gives higher rate than that from the QEST. This is also true for the case of recombination as can be easily seen from the identical formulation of the QEST in the two processes. So one should use the QEST if possible unless it is too complicated for numerical calculation or other considerations. In the latter situation the BTL neverthless still gives an upper bound of the rate coefficint which is bigger than the result from QEST (by a factor of 2 in the recombination case, by 20% in the case of association here). When the up-flow (or excitation) processes are less significant, the BTL may have better agreement with that of the more elaborate QEST.

Table 7.5 BTL in Association

λ^*	α_o^{BT}	λ^*	α_o^{BT}
0.01	1.2575	0.10	1.2186[a]
0.02	1.2453	0.11	1.2188
0.03	1.2371	0.12	1.2193
0.04	1.2311	0.15	1.2231
0.05	1.2268	0.18	1.2294
0.06	1.2236	0.20	1.2347
0.07	1.2213	0.30	1.2719
0.08	1.2198	0.50	1.3831
0.09	1.2190	1.00	1.8186

(a) minimum of α_o^{BT} .

APPENDIX A

THE THERMODYNAMIC-EQUILIBRIUM DISTRIBUTION

Following the 1973 paper of Bates and McKibben, the ratio of the thermodynamic equilibrium distribution function of the bound pair AB in the the reaction

$A+B \dashrightarrow AB$

to the number densities of A and B is given by (see also, Fowler, 1936)

$$\frac{N_{AB}}{N_A N_B} = \frac{\omega_{AB}}{\omega_A \omega_B} \Omega h^3 \exp(-E/k\theta)/(2\pi\mu_{AB}k\theta)^{3/2} \qquad (1)$$

where

(i) N_{AB}, N_A, N_B are particle density of (AB), A, B respectively.

(ii) ω's are statistical weight of the internal degree of freedom (e.g. electon spin, nuclear spin, vibration, rotation etc.). ω is unity for 'structureless' molecule which is the case we assumed for both recombination and association.

(iii) θ : temperature of the system

(iv) E : binding energy of AB, μ_{AB} its reduced mass.

(v)

$$\Omega h^3 = g(E) = \int d\Gamma \delta(E-H) \quad \Gamma: \text{phase space}$$

is the statistical weight of the binding 'molecule' AB, assuming a microcanonical distribution. We will evaluate this factor in the following.

With the Hamiltionian of the AB system

$$H=p^2/2\mu_{AB} + V(r) \ , \tag{3}$$

one has

$$g(E)=(4\pi)^2 \int\int dr\ r^2\ dp p^2 \delta(E-H)$$

or

$$g(E)=16\pi^2(2\mu_{AB}^3)^{\frac{1}{2}} \int dr\ r^2(E-V)^{\frac{1}{2}} \ . \tag{4}$$

Let

$$C(E) = \int dr\ r^2(E-V)^{\frac{1}{2}} \ . \tag{5}$$

We see C(E) depends on the interaction potential between A and B.

Before we evaluate C(E) for the two cases in which we are interested note that (i) in terms of C(E) now becomes

$$\frac{N_{AB}}{N_A N_B} = \frac{8\pi^{\frac{1}{2}} C(E)}{(k\theta)^{3/2}} \exp(-E/k\theta) \qquad (6)$$

Although the factor C(E) in the final expression of reaction rate coefficient is cancelled, it is still interesting and worthwhile to investigate them for the reason that the encounter rate coefficient K_{if} is proportional to C(E).

Case 1: Recombination , $A=X^+$, $B=Y^-$, the interaction $V=-e^2/r$ is purely Coulombic. We expect the energy level be hydrogenic $E_n=-(e^2/a_o)/(2n^2)$ where $a_o=\hbar^2/\mu_{AB}e^2$, level n has n^2 degeneracy. Putting in V and carrying out the r integration we have

$$C(E) = \int dr\ r^2(E + \frac{e^2}{r})^{\frac{1}{2}} = e^6 B(\frac{3}{2},\frac{5}{2})/|E|^{5/2} \qquad (7)$$

$$= \pi e^6/16\ |E|^{5/2} = e^6/H_R(k,\theta)^{5/2}$$

where

$$H_R = 16\lambda^{5/2}/\pi \ . \qquad (8)$$

Case 2: Association, $A=X^+$, $B=Y$, $V=-pe^2/2r^4$ pure polarized potential, for a ion with an atom (neutral). We have

$$C(E) = \int dr\ r^2 (E + \frac{pe^2}{2r^4})^{\frac{1}{2}} = (\frac{pe^2}{2})^{3/4} \frac{B(\frac{3}{2}, \frac{1}{4})}{4|E|^{\frac{1}{4}}} \qquad (9)$$

$$= (pe^2/2)^{3/4} / H_A (k\theta)^{\frac{1}{4}}$$

where

$$H_A = 4\lambda^{\frac{1}{4}} / B(3/2,\ 1/4)\ . \qquad (10)$$

In both (8) and (10),

$$B(\tfrac{\mu}{2}, \tfrac{\nu}{2}) = 2 \int_0^{\frac{\pi}{2}} \sin^{\mu-1} \cos^{\nu-1} \theta d\theta = \frac{\Gamma(\frac{\mu}{2}, \frac{\nu}{2})}{\Gamma(\frac{\mu+\nu}{2})} \qquad (11)$$

is the Beta function which can in turn be expressed in terms of Gamma function, $\Gamma(x)$.

APPENDIX B

Ionic Recombination of Rare-Gas Atomic Ions X^+ with F^- in a Dense Gas X

This is a reprint of an anticle appeared in Applied Physics Letter Vol 32, page 327-329, March 1978.

Ionic recombination of rare-gas atomic ions X^+ with F^- in a dense-gas X[a)]

M. R. Flannery[b)]

Joint Institute for Laboratory Astrophysics, University of Colorado and National Bureau of Standards, Boulder, Colorado 80309

T. P. Yang

School of Physics, Georgia Institute of Technology, Atlanta, Georgia 30332
(Received 17 October 1977; accepted for publication 5 January 1978)

Rates for the recombination processes $X^+ + F^- + X \rightarrow XF^* + X$, ($X \equiv$ He, Ne, Ar, Kr, Xe) at 300 K are calculated for pressures of the background gas X in the range ~0.1–50 atm. Rates as high as $(2\text{–}7)\times 10^{-6}$ cm^{3}sec^{-1} are obtained for pressures 1–5 atm of Xe→He, and in general decrease with increasing ionic mass, except at low gas densities.

PACS numbers: 34.50.Lf, 34.70.+e

Laser action has been obtained in many experiments[1] based on the excitation of rare-gas X-fluorine F_2 mixtures at $\frac{1}{2}$–2 atm by high-energy electron beams. The lasing transitions originate on excited molecular states of XF^* [$2\,^2\Pi$ and $2\,^2\Sigma$ without spin-orbit coupling, as in Hund's case (a), or III $\frac{1}{2}$, II $\frac{3}{2}$ and IV $\frac{1}{2}$ with spin-orbit coupling, as in Hund's case (c)] predominantly ionic in character at intermediate nuclear separations (2–10 Å), and they terminate on the dissociative or slightly bound $X\,^2\Sigma^+$ and $1\,^2\Pi$ states with covalent products $X + F(^2P_{1/2,3/2})$. Efficient scaling of these lasers to high average power requires detailed knowledge of the mechanisms for the production and quenching of these excited states. These states for high-density gas mixtures are formed directly[1–3] by the *ionic recombination process*

$$X^+ + F^- + X \rightarrow XF^* + X \quad (X \equiv \mathrm{He, Ne, Ar, Kr, Xe}) \qquad (1)$$

involving positive ions X^+ produced by *electron-impact ionization*

$$\tilde{e} + X^{(*)} \rightarrow \tilde{e} + X^+ + e_s \qquad (2)$$

of rare-gas atoms in their ground and metastable states and negative ions F^- formed by *dissociative attachment*

$$e_s + F_2 \rightarrow F + F^- \qquad (3)$$

of the slow ejected electrons e_s in reaction (2) with F_2.

Various theories of ionic recombination have been reviewed recently by Flannery.[3,4] The treatments range from the simplistic models of Langevin,[5] Thomson,[6] and Natanson[7] to the more elaborate quasiequilibrium statistical approaches of Bates and Flannery[8] who have shown for equal mass constituents that the former simple methods are capable of predicting α, the recombination coefficient, to within a factor of 2 when compared with their more detailed treatment.

In the absence of any information on reaction (1), the purpose of this letter is to provide α as a function of gas density N with the aid of a modification[9] to the original formula of Natanson for all N. Application of the more accurate low-density quasiequilibrium treatment of Bates and Flannery[8] is at present under way but is extremely time consuming.

In the low-density limit, deactivation of the ion pair is brought about by collision with the third (gas) bodies. As the ions approach from infinity to a distance R of one another under their mutual Coulombic field, Thomson[6] assumed that the gain (e^2/R) in kinetic energy of the ion pair over the original thermal value $(\frac{3}{2}kT)$ at temperature T is completely lost via a *single strong* collision with the neutral, with the possibility, therefore, that bound ion pairs (with negative relative energy) can be formed for ion-ion separations $R \leq R_T = (2e^2/3kT)$. Eventual electron transfer in the bound systems completes the recombination. Thus Thomson's approximation[6] to the recombination rate at gas density N yields

$$\alpha_T\ (\mathrm{cm^3\,sec^{-1}}) = (\pi R_T^2)(3kT/M_{12})^{1/2} P(R_T, N), \qquad (4)$$

where P is the density-dependent probability for a collision between a neutral and a pair of ±ive ions with reduced mass M_{12} and separation $R \leq R_T$. The probability for a single ion-neutral encounter within R_T is,[10] for a straight-line trajectory,

$$w(x_i) = 1 - (1/2x_i^2)[1 - \exp(-2x_i)(1 + 2x_i)], \qquad x_i = \lambda_i/R_T,\ i = 1, 2 \qquad (5)$$

where λ_i $(i = 1, 2)$ are the mean free paths of the ±ive in the gas. Thus, the overall probability P that an ion pair with separation $\leq R_T$ collides with the neutral is

$$P(R_T, N) = w(x_1) + w(x_2) - w(x_1)w(x_2) \rightarrow \tfrac{4}{3}R_T(\lambda_1^{-1} + \lambda_2^{-1}), \quad \text{low } N; \qquad \rightarrow 1, \quad \text{high } N \qquad (6)$$

since $w(x_1)w(x_2)$, the chance that both ions collide simultaneously with the neutral has already been counted twice in $w(x_1) + w(x_2)$.

In the limit of high gas densities N, however, the Thomson formula is invalid since the speed of approach of the ions becomes limited by the speed of diffusion and

a)Work sponsored by U.S. Energy Research and Development Administration, Division of Laser Fusion, under contract E(40-1)-5002.
b)Visiting Fellow, 1977–1978 on leave from Georgia Institute of Technology.

 0003-6951/78/2205 0327$00.50

random drift. In this region, the recombination rate is controlled by the mobilities, K_1 and K_2, of the two ions in the gas and is given by[5,11]

$$\alpha_L = 4\pi e(K_1 + K_2), \tag{7}$$

a result originally due to Langevin[5] (without knowledge of the quantum process), but presented rather elegantly by Bates.[11]

Since λ^* and $K_{1,2}$ vary as N^{-1}, the recombination rate α increases as N for low gas densities N and decreases N^{-1} in the limit of high N. A unified theoretical treatment linking the (microscopic) low-density regime regime with the (macroscopic) high-density region is difficult but Bates and Flannery[9] have shown that the result of Natanson,[7] who gave a solution to the problem, could be written as

$$\alpha_N^{-1} = \alpha_{TN}^{-1} + \alpha_{LN}^{-1} \tag{8}$$

where the added subscript N to α_T and α_L denote the respective modifications of Natanson to the equations [(4) and (7)] of Thomson and Langevin, respectively. For ions of mass M_1 and M_2 and mean free paths λ_1 and λ_2 in a gas of mass M_3, the Natanson result can be suitably generalized to give[12]

$$\alpha_{TN} = \pi[r_1^2 w(x_1) C_1 E_1 + r_2^2 w(x_2) C_2 E_2 - r_s^2 w(y_1) w(y_2) S] \times (8kT/\pi M_{12})^{1/2}, \tag{9}$$

where

$$C_i = 1 + \frac{3}{2\delta_i}, \quad E_i = \exp\frac{3r_i}{2\delta_i\lambda_i}, \qquad \delta_i = \frac{F_i}{(1-F_i)}, \quad F_i = \frac{2M_1M_2M_3(M_1+M_2+M_3)}{(M_1+M_2)^2(M_i+M_3)^2} \tag{10}$$

and where

$$x_i = r_i/\lambda_i, \quad r_s = \min(r_1, r_2), \qquad y_i = r_s/\lambda_i, \quad S = \min(C_1E_1, C_2E_2). \tag{11}$$

This result differs from the original formula (4) of Thomson in that (a) it introduces different mass-dependent and density-dependent trapping radii,

$$r_i = \frac{1}{2}\lambda_i\left[\left(1 + \frac{8e^2\delta_i}{3kT\lambda_i}\right)^{1/2} - 1\right], \quad i = 1, 2 \tag{12}$$

designed so that arbitrary mass ions are incapable of separation to $(r_i + \lambda_i)$, where they suffer their next collision, rather than to infinity; (b) it makes allowance for Coulombic rather than linear trajectories by the introduction of a multiplicative focusing factor $C_i = [1 + (1/kT)\int_{r_i}^{r_i+\lambda_i} e^2\,dr/r^2]$; (c) it acknowledges that ions with separations $(r_i + \lambda_i)$ just before entering the collision sphere have densities a factor of $E_i = \exp[e^2/(r_i + \lambda_i)kT]$ higher than at infinite separation; and (d) it acknowledges different masses by the introduction of a mass-variable parameter δ_i. (The original Natanson formula[7] for equal mass is obtained by setting $\delta_i = \frac{1}{2}$). An analogous modification of the Langevin formula (7) yields,

$$\alpha_{LN} = 4\pi e[K_1/(1 - E_1^{-1}) + K_2/(1 - E_2^{-1})]. \tag{13}$$

Thus the combination (8) of Eqs. (9) and (13) yields α_N as a function of the neutral-gas density N, for arbitrary species.

For atomic neutrals X, the energy reduction is mainly determined by the *symmetrical resonance charge-transfer process*

$$X^+(\text{fast}) + X(\text{slow}) \rightarrow X(\text{fast}) + X^+(\text{slow}) \tag{14}$$

for the positive ions, and by the elastic encounters

$$Y^-(v_3) + X(v_3) \rightarrow Y^-(v_3') + X(v_3') \tag{15}$$

in which the speeds of Y^- and X are changed from v_3 and v_3 to v_3' and v_3', respectively. Since the cross section for $(X^+$-$X)$ diffusion is twice that for process (14), then the mean free paths $\lambda_{1,2}$ in Eqs. (11) and (12) for the positive and negative ions can be obtained from the expression[4]

$$\lambda_i = (1600/e)(M_{i3}kT/2\pi)^{1/2}K_i(N_L/N)\times\begin{cases}2, & i=1\\ 1, & i=2\end{cases}, \tag{16}$$

where K_i are the reduced measured mobilities[13–15] (in $\text{cm}^2/\text{V sec}$) of the ions in the neutral gas, M_{i3} is the ion-neutral reduced mass, and N_L is Loschmidt's number density (2.69×10^{19} cm^{-3} at STP). The factor of 2 in Eq. (16) specifically acknowledges the fact that the single strong ion-neutral $(X^+$-$X)$ encounter required in this theory for recombination is controlled by the charge-transfer process (14).

While measured values of K_i are in general used here in Eqs. (9)–(13), the polarization formula[16]

$$K_i = 13.87[p(\text{Å}^3)M_{i3}(\text{O}^{16})]^{-1/2}\ \text{cm}^2/\text{V sec} \tag{17}$$

in terms of the polarizability p of the neutral, and of the ion-neutral reduced mass M_{i3} provides reasonable estimates, especially for the heavier rare gases.

Accordingly, the recombination coefficients α are here determined for processes (1) as a function of neutral-gas density N with the aid of formulas (8)–(13) and (16). While the recombination, in principle, populates all the excited molecular states, we assume that the branching ratio to the lowest excited states $2\,^2\Sigma$ and $2\,^2\Pi$ (with ionic character) is effectively unity.[17] The results are displayed in Fig. 1 which exhibits the characterisitic N^1 increase of α at low densities N, followed by maxima $(2.0–7.0)\times10^{-6}$ $\text{cm}^3\,\text{sec}^{-1}$ in the range 1–5 atm, and the predicted

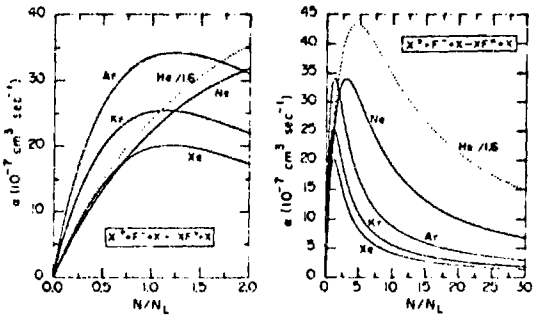

FIG. 1. Ionic recombination coefficients α ($\text{cm}^3\,\text{sec}^{-1}$) for the processes $X^+ + F^- + X \rightarrow XF^* + X$ (X = He, Ne, Ar, Kr, Xe) as a function of neutral-gas density N (in units of Loschmidt's number N_L, 2.69×10^{19} cm^{-3}). Gas X as indicated on each curve. Note the rates for the He case have been divided by 1.6.

N^{-1} decrease in the high-density limit. Here, α as in Eq. (7) is directly proportional to the sum of the mobilities and hence decreases systematically as the gas is varied from He-Xe.

The low gas-density limit to Eq. (9) is

$$\alpha = \tfrac{1}{3}\pi (C_1\delta_1^2/\lambda_1 + C_2\delta_2^2)(2e^2/3kT)^{\frac{1}{2}} \times (8kT/\pi M_{12})^{1/2} \qquad (18)$$

exhibiting a more complex variation with masses which tends to overcome the implicit variation of the mobilities. The relatively larger rates α displayed for He originate from the fact that $M_1 < M_2$ (with consequent greater approach speed) and, at higher N, from much larger mobilities in He. As the gas is varied from He-Xe, the maximum decreases and shifts from ~5 atm towards smaller pressure (1.2 atm), an effect due to the competition between slower approach speeds and lower mobilities.

Finally, it is worth noting that results we recently obtained from the more elaborate quasiequilibrium treatment at *low gas densities alone* yields $\alpha = 3.00\times10^{-6}(N/N_L)$ and $3.66\times10^{-6}(N/N_L)$ for the Ne and Xe cases, to be compared with the corresponding values $3.31\times10^{-6}(N/N_L)$ and $3.78\times10^{-6}(N/N_L)$ of the present treatment in the low-density limit, thereby indicating that the present model yields fairly accurate results for different ionic mass ratios. Also results obtained from Eq. (9) with $\delta_i = \frac{2}{3}$, the original value of Natanson,[7] were within 20% of those in Fig. 1 for densities $N > N_L$.

So that the present results be used in the kinetic codes for the modeling of rare-gas—halide lasers, we have presented in Table I the calculated recombination coefficients α over a wide range (~0.1—50 atm) of pressure. Note that in the high-density limit, the N^{-1} dependence of α is exhibited.

TABLE I. Three-body recombination rates α (10^{-6} cm^3 sec^{-1}) for the processes $X^+ + F^- + X \rightarrow XF^* + X$, ($X$ = He, Ne, Ar, Kr, Xe) as a function of gas density N at 300 K. Low-density limit is $\alpha_0 N/N_L$ (10^{-6} cm^3 sec^{-1}).

N/N_L[a]	He	Ne	Ar	Kr	Xe
0.1	0.591	0.315	0.817	0.597	0.351
0.2	1.110	0.601	1.434	1.061	0.662
0.4	1.990	1.107	2.312	1.739	1.193
0.6	2.717	1.541	2.867	2.173	1.592
0.8	3.333	1.913	3.197	2.420	1.849
1.0	3.864	2.232	3.364	2.528	1.978
1.2	4.327	2.502	3.417[b]	2.541[b]	2.010[b]
1.4	4.732	2.728	3.393	2.492	1.978
1.6	5.088	2.914	3.321	2.409	1.909
1.8	5.400	3.064	3.219	2.306	1.820
2.0	5.674	3.180	3.101	2.197	1.725
2.2	5.912	3.269	2.976	2.086	1.629
2.4	6.118	3.332	2.850	1.979	1.536
2.6	6.296	3.373	2.725	1.877	1.449
2.8	6.447	3.395	2.605	1.781	1.369
3.0	6.574	3.402[b]	2.491	1.692	1.294
3.5	6.801	3.366	2.233	1.495	1.134
4.0	6.920	3.277	2.013	1.334	1.005
4.5	6.958[b]	3.160	1.827	1.200	0.900
5	6.933	3.028	1.669	1.089	0.813
6	6.756	2.755	1.417	0.916	0.681
7	6.485	2.499	1.228	0.789	0.585
8	6.174	2.270	1.082	0.692	0.512
9	5.853	2.071	0.966	0.616	0.455
10	5.541	1.899	0.872	0.554	0.410
20	3.392	0.998	0.439	0.277	0.205
30	2.368	0.670	0.293	0.185	0.137
40	1.797	0.503	0.220	0.139	0.102
50	1.441	0.403	0.176	0.111	0.082
α_0	6.340	3.305	9.579	6.936	3.777

[a] N_L is Loschmidt's number (2.69×10^{19} cm^{-3}), the number density at STP.
[b] Indicates peak value.

[1] For extensive bibliography, D.C. Lorents, *X International Conference on the Physics of Electronic and Atomic Collisions* (Dunod, Paris, 1977).
[2] M. Rokni, J.H. Jacob, J.A. Mangano, and R. Brochu, Appl. Phys. Lett. 30, 458 (1977).
[3] M.R. Flannery, in *Atomic Processes and Applications*, edited by P.G. Burke and B.L. Moiseiwitsch (North-Holland, Amsterdam, 1976), pp. 409—466.
[4] M.R. Flannery, in *Case Studies in Atomic Physics*, edited by E.W. McDaniel and M.R.C. McDowell (North-Holland, Amsterdam, 1972), Vol. 2, pp. 1—90.
[5] P. Langevin, Ann. Chim. Phys. 48, 433 (1903).
[6] J.J. Thomson, Philos. Mag. 47, 337 (1924).
[7] G.L. Natanson, Sov. Phys.-Tech. Phys. 4, 1263 (1959).
[8] D.R. Bates and M.R. Flannery, Proc. R. Soc. (London) A 69, 910 (1968).
[9] D.R. Bates and M.R. Flannery, J. Phys. B 2, 184 (1969).
[10] L. Loeb, *Basic Processes of Gaseous Electronics* (Univ. of California Press, Berkeley, 1955), Chap. 6.
[11] D.R. Bates, J. Phys. B 8, 2722 (1975).
[12] M.R. Flannery, Chem. Phys. Lett. (to be published).
[13] H.W. Ellis, R.Y. Pai, E.W. McDaniel, E.A. Mason, and L.A. Viehland, At. Data Nucl. Data Tables 17, 177 (1976).
[14] I. Dotan, D.L. Albritton, and F.C. Fehsenfeld, J. Chem. Phys. 66, 2232 (1977).
[15] I. Dotan and D.L. Albritton, J. Chem. Phys. 66, 5238 (1977).
[16] A. Dalgarno, Phil. Trans. R. Soc. A 250, 426 (1958).
[17] Benefited from discussion with J.H. Jacob. These states are the only ones with ionic character at intermediate separations and are well separated from other "covalent" states. [See Fig. 2 of P.J. Hay and T.H. Dunning, Jr., J. Chem. Phys. 66, 1306 (1977)]. Crossings with higher excited states are at relatively large separations where the probability of curve crossing is very small (Ref. 3). Indeed, one of the reasons that these states can lase so efficiently is that they are quite isolated from other "interfering" states.

APPENDIX C

Ionic Recombination of Rare-gas Molecular Ions X_2^+ with F^- in a Dense Gas X

This is a reprint of an anticle appeared in Applied Physics Letter, Vol 32, page 356-357, March 1978.

Ionic recombination of rare-gas molecular ions X_2^+ with F^- in a dense gas X[a]

M. R. Flannery[b]

Joint Institute for Laboratory Astrophysics, University of Colorado and National Bureau of Standards, Boulder, Colorado 80309

T. P. Yang

School of Physics, Georgia Institute of Technology, Atlanta, Georgia 30332
(Received 21 November 1977; accepted for publication 3 January 1978)

Rates for the recombination processes $X_2^+ + F^- + X \rightarrow [X_2F]^* + X$, ($X \equiv$ He,Ne,Ar,Kr,Xe) are calculated at 300 K for pressures of the background gas X up to 50 atm. We find rates as high as $(2\text{–}6)\times10^{-6}$ cm^{3}sec^{-1} for pressures of 1–8 atm as the gas is varied from Xe to He. The rates are somewhat smaller than those for the corresponding cases involving atomic ions.

PACS numbers: 34.50.Lf, 34.70.+e

The upper molecular states of RgF* in rare gas–fluorine (RgF) laser systems operating at high gas densities ($\frac{1}{2}$–5 atm) can be populated[1–3] by the three-body ionic recombination process

$$Rg^+ + F^- + Rg \rightarrow (RgF)^* + Rg \qquad (1)$$

involving positive ions produced by electron-impact ionization

$$\vec{e} + Rg^{(*)} \rightarrow \vec{e} + Rg^+ + e_s \qquad (2)$$

of rare-gas atoms in the ground and metastable states and negative ions F^- formed by dissociative attachment

$$e_s + F_2 \rightarrow F + F^- \qquad (3)$$

of the slow electrons e_s ejected in reaction (2). Theoretical rates for process (1) have already been presented[4] as a function of gas density N via various modifications of a treatment due to Natanson.[5]

However, the recombination also involves molecular ions Rg_2^+ formed by the three-body ion-atom association process

$$Rg^+ + Rg + Rg \rightarrow Rg_2^+ + Rg \qquad (4)$$

with the result that ions are neutralized via

$$Rg_2^+ + F^- + Rg \rightarrow [Rg_2^+F^-]^* + Rg \qquad (5a)$$

$$\searrow [RgF]^* + Rg, \qquad (5b)$$

where the brackets denote that the product may not remain bound. The branching ratios to the various dissociative channels are at present unknown, but RgF* may well be formed in reaction (5). A related source of production of RgF* involving the molecular ions is

$$Rg_2^+ + F^- \rightarrow RgF^* + Rg. \qquad (6)$$

Although this (mutual-neutralization type) process does not explicitly require a third body for its completion, its contribution is nevertheless acknowledged by the dissociative channel (5b).

By application of the theory already presented in a previous report,[4] we have obtained, for processes (5), recombination coefficients α (cm^3 sec^{-1}) defined in terms of the rate of ion loss by

$$\frac{dN^+}{dt} = \frac{dN^-}{dt} = -\alpha N^+ N^-, \qquad (7)$$

where $N^\pm$ are the number densities of the positive and negative ions.

In Fig. 1 are displayed the results α for the recombination of the rare-gas molecular ions with F^- in various background gases (He, Ne, Ar, Kr, Xe) as a function of neutral-gas density N at 300 K. (N is normalized to N_L, Loschmidt's number 2.69×10^{19} cm^{-3}, the number density at STP.) The coefficients α increase with N, exhibit maxima which decrease systematically with variation of the gas from He → Xe, from 6×10^{-6} to 1.8×10^{-6} cm^3 sec^{-1}, and which are located in the pressure range 1–8 atm. At much higher

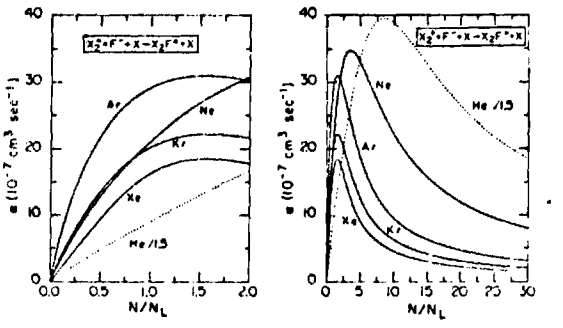

FIG. 1. Ionic recombination coefficients α (cm^3 sec^{-1}) for the processes $X_2^+ + F^- + X \rightarrow [X_2F]^* + X$ ($X \equiv$ He, Ne, Ar, Kr, Xe) as a function of neutral-gas density N (in units of Loschmidt's number N_L, 2.69×10^{19} cm^{-3}). The square brackets indicate that the molecule $[X_2F]^*$ may not remain bound. Gas X is as indicated on each curve. Note the rates for the He case have been divided by 1.5.

[a]Work supported by the U. S. Energy Research and Development Administration, Division of Laser Fusion, under contract E(40-1)-5002.
[b]Visiting Fellow, 1977–78 on leave from Georgia Institute of Technology.

 0003-6951/78/3206-0356$00.50

TABLE I. Mobilities ($cm^2/V\,sec$) of atomic and molecular ions in rare gases X. (Data without superscripts are from Ref. 6.)

X	F^-	X^+	X_2^+
He	29.5[a]	10.3	16.7
Ne	7.05[b]	4.08	6.16
Ar	3.33[a]	1.52	1.83
Kr	2.24[b]	0.823	1.22
Xe	1.69[b]	0.580[c]	0.79[c]

[a] From Refs. 7 and 8.
[b] From the Langevin formula, see Ref. 4.
[c] From Ref. 9.

gas densities N, α decreases as N^{-1} and is mainly determined by the sum of the mobilities of the positive and negative ions in the gas. The coefficients α therefore exhibit the systematic decrease with variation of the gas from He → Xe, in accord with the mobility data in Table I. In fact, the He case has somewhat special significance in that the sum of the mobilities in Table I of He_2^+ and F^- in He is much larger by between factors of 3 and 23 than the corresponding sums for the cases involving Ne-Xe. This characteristic becomes manifest in Fig. 1 by a much larger α for He at high N, and by the relatively higher and wider peak displaced to comparatively higher densities N.

At low densities, α is mainly controlled by the factors[4] involving the individual masses of the constituents and mean free paths of the ions in the gas. The variation with masses is quite complex but, at low densities, as the gas is varied from He → Xe, α increases, peaks for the Ar case, and then decreases.

Finally, we have tabulated the results in Table II in order that they be available for laser modeling. It is worth noting that these results are somewhat smaller at low and intermediate pressures (up to the locations of the maxima) and are higher at much larger pressures than the analogous cases[1] involving atomic ions alone. This behavior essentially arises from the greater masses of the molecular ions and from the larger mobilities of the molecular ions in the various gases, as indicated by Table I. We also note from Table II that the pure N^{-1} variation of α with N sets in for pressures greater than about 10 atm.

TABLE II. Three-body recombination rates α ($10^{-6}\ cm^3\,sec^{-1}$) for the processes $X_2^+ + F^- + X \rightarrow (X_2F)^* + X$ ($X \equiv He, Ne, Ar, Kr, Xe$) as a function of gas density N at 300 K. Low-density limit is $\alpha_0 N/N_L$ ($10^{-3}\ cm^3\,sec^{-1}$).

N/N_L[a]	He	Ne	Ar	Kr	Xe
0.1	0.154	0.315	0.683	0.350	0.192
0.2	0.302	0.593	1.195	0.649	0.384
0.4	0.583	1.070	1.925	1.147	0.762
0.6	0.851	1.471	2.407	1.535	1.114
0.8	1.107	1.815	2.725	1.825	1.409
1.0	1.356	2.113	2.924	2.024	1.627
1.2	1.597	2.370	3.038	2.147	1.765
1.4	1.833	2.593	3.089	2.209	1.832
1.6	2.065	2.783	3.096[b]	2.224[b]	1.845[b]
1.8	2.283	2.944	3.071	2.207	1.819
2.0	2.508	3.079	3.023	2.168	1.768
2.2	2.723	3.190	2.960	2.110	1.704
2.4	2.933	3.278	2.886	2.046	1.632
2.6	3.137	3.348	2.806	1.976	1.558
2.8	3.336	3.399	2.722	1.904	1.485
3.0	3.528	3.436	2.636	1.832	1.414
3.5	3.980	3.471[b]	2.421	1.659	1.252
4.0	4.383	3.445	2.216	1.502	1.114
4.5	4.746	3.379	2.028	1.363	1.000
5	5.055	3.287	1.859	1.242	0.902
6	5.519	3.064	1.576	1.046	0.754
7	5.795	2.829	1.358	0.898	0.646
8	5.914[b]	2.604	1.188	0.786	0.565
9	5.912	2.398	1.054	0.698	0.502
10	5.823	2.214	0.946	0.628	0.452
20	3.950	1.189	0.468	0.313	0.226
30	2.750	0.797	0.312	0.209	0.150
40	2.082	0.538	0.234	0.156	0.113
50	1.671	0.479	0.187	0.125	0.090
α_0	1.572	3.373	8.061	3.941	1.949

[a] N_L is Loschmidt's number ($2.69 \times 10^{19}\ cm^{-3}$), the number density at STP.
[b] Indicates peak value.

[1] M. Rokni, J. H. Jacob, J. A. Mangano, and R. Brochu, Appl. Phys. Lett. 30, 458 (1977).
[2] A. M. Hawryluk, J. A. Mangano, and J. H. Jacob, Appl. Phys. Lett. 31, 164 (1977).
[3] For extensive coverage see Proceedings of the 30th Annual Gaseous Electronics Conference, Palo Alto, 1977 (unpublished).
[4] M. R. Flannery and T. P. Yang, Appl. Phys. Lett. 32, 327 (1978).
[5] G. L. Natanson, Sov. Phys.-Tech. Phys. 4, 1263 (1959).
[6] H. W. Ellis, R. Y. Pai, E. W. McDaniel, E. A. Mason, and L. A. Viehland, At. Data Nucl. Data Tables 17, 177 (1976).
[7] I. Dotan, D. L. Albritton, and F. C. Fehsenfeld, J. Chem. Phys. 66, 2232 (1977).
[8] I. Dotan and D. L. Albritton, J. Chem. Phys. 66, 5238 (1977).
[9] L. M. Chanin and M. A. Biondi, Phys. Rev. 106, 473 (1957).

APPENDIX D

Ionic Recombination of Kr^+ and Kr_2^+ with F^- in a dense (but lighter) Buffer Rare Gases

This is a reprint of an article being scheduled to appear in Applied Physics Letter 33(7), 1 Oct 1978.

Ionic recombination of Kr^+ and Kr_2^+ with F^- in dense buffer rare gases[a)]

M. R. Flannery[b)]

Joint Institute for Laboratory Astrophysics, University of Colorado and National Bureau of Standards, Boulder, Colorado 80309

T. P. Yang

School of Physics, Georgia Institute of Technology, Atlanta, Georgia 30332
(Received 23 June 1978; accepted for publication 18 July 1978)

Rates, α, for the recombination of Kr^+ and Kr_2^+ with F^- in various buffer rare gases (He, Ne, Ar, Kr, Xe) at 300 K are calculated for a wide range of gas pressures. For pressures 1–5 atm, the population of KrF^* via recombination is greatest for Ne and Ar as third bodies, yielding $\alpha \sim 3\times10^{-5}$ cm^{3}sec^{-1}, while for pressures $\gtrsim$ 10 atm, He is to be preferred as a buffer gas.

PACS numbers: 34.50.Lf, 34.70.+e, 82.30.Fi

The laser action[1] observed in systems based on the excitation of rare gas Rg-fluorine F_2 mixtures at $\frac{1}{2}$–2 atm by high-energy electron beams originates on upper ($2^2\Sigma$, $2^2\Pi$) states of RgF^* populated mainly by the three-body *ion-ion recombination* process[2]

$$Rg^+ + F^- + M \rightarrow RgF^* + X, \tag{1}$$

where M is any third body, as, for example, a lighter rare-gas buffer, and terminates in the ground dissociative $X^2\Sigma^*$ states. The positive ions in process (1) are produced by electron-impact ionization

$$e + Rg^* \rightarrow e + Rg^+ + e_s \tag{2}$$

of rare-gas atoms (He, Ne, Ar, Kr, Xe) in the ground and metastable states, with the resulting ejection of slow electrons e_s which undergo dissociative attachment with F_2, as in

$$e_s + F_2 \rightarrow F + F^- \tag{3}$$

to form negative ions F^-. In the high gas pressures of interest, the atomic ions are rapidly converted to molecular ions by ion-atom association

$$Rg^+ + Rg + M \rightarrow Rg_2^+ + M \tag{4}$$

so that the upper state is also populated by[3]

$$Rg_2^+ + F^- + M \rightarrow [Rg_2^+F^-]^* + M \tag{5a}$$

$$\searrow [RgF]^* + Rg, \tag{5b}$$

where the square brackets denote that the reaction products may not remain bound. The above sequence (1)–(5) of processes is, by now, well known.

Previous reports[2,3] have presented theoretical recombination coefficients α (cm^{3}sec^{-1}) for processes (1) and (5) as functions of neutral-gas density N in cases for which the rare-gas buffer M is identical to the rare gas. In most lasers, however, the dominant positive ions are likely to be heavy rare-gas ions (e.g., Kr^+, Kr_2^+) which recombine with F^- in a lighter rare-gas buffer such as He, Ne, or Ar. The purpose of the present letter is therefore to furnish rates for these intercombinations, where the third body M is a different species from the positive ion, by application of our theory previously described,[2–4] and hence complete the series[2–4] on recombination.

Figures 1 and 2 display the rates α (cm^{3}sec^{-1}) at 300 K of recombination between Kr^+ and F^- in various rare

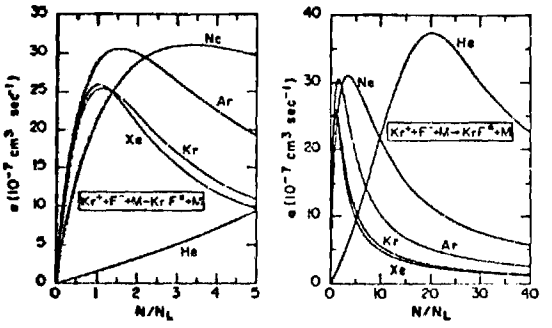

FIG. 1. Ionic recombination coefficients α (cm^3 sec^{-1}) at 300 K for $Kr^+ + F^- + M \rightarrow KrF^* + M$ ($M \equiv$ He, Ne, Ar, Kr, Xe) as a function of neutral-gas density N, in units of Loschmidt's number 2.69×10^{19} cm^{-3}. Buffer gas M as indicated on each curve.

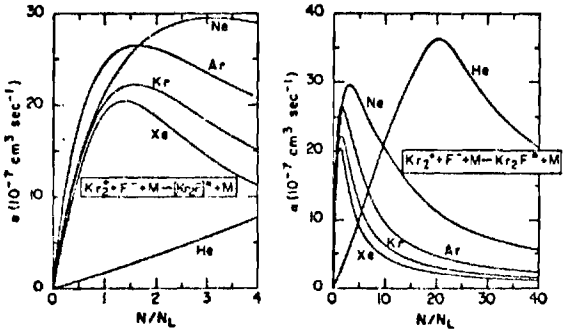

FIG. 2. As in Fig. 1 except for the process $Kr_2^+ + F^- + M \rightarrow [Kr_2^+F^-]^* + M$, where the brackets indicate that the product molecule may not remain bound.

a)Research sponsored by U. S. Department of Energy, Division of Laser Fusion, under contract EY-76-S-05-5002.
b)Visiting Fellow, 1977–1978, on leave from Georgia Institute of Technology.

 0003 6951/78/3307-0574$00.50

TABLE I. Mobilities ($cm^2/V\,sec$) of Kr^+, Kr_2^+ and F^- in various buffer rare-gases M. [Data without superscripts are theoretical values from Eq. (17), Ref. 2.]

M	Kr^+	Kr_2^+	F^-
He	20.2[a]	15.5	29.5[b]
Ne	5.47	5.20	7.05
Ar	2.30[c]	1.90	3.39[d]
Kr	0.823[e]	1.22[e]	2.24
Xe	0.964	0.804	1.69

[a]Expt. values from Ref. 5.
[b]Expt. values from Ref. 8.
[c]Expt. values from Ref. 6.
[d]Expt. values from Ref. 9.
[e]Expt. values from Ref. 7.

TABLE II. Three-body recombination rates α (10^{-6} $cm^3\,sec^{-1}$) for the processes $Kr^+ + F^- + RE \rightarrow KrF^* + RF$ (Rg ≡ He, Ne, Ar, Xe) for various gas densities N at 300 K. Low- and high-density limits are $\alpha_0(N/N_L)$ and $\alpha_\infty(N_L/N)$, respectively.

N/N_L[a]	He	Ne	Ar	Xe
0.1	1.400^{-2}[b]	3.618^{-1}	6.695^{-1}	5.896^{-1}
0.2	2.816^{-2}	6.678^{-1}	1.171	1.071
0.4	5.701^{-2}	1.165	1.856	1.806
0.6	8.657^{-2}	1.556	2.361	2.275
0.8	1.169^{-1}	1.873	2.676	2.517
1.0	1.479^{-1}	2.132	2.876	2.591[c]
1.2	1.797^{-1}	2.346	2.992	2.557
1.4	2.123^{-1}	2.522	3.046	2.462
1.6	2.457^{-1}	2.667	3.056[c]	2.338
1.8	2.799^{-1}	2.784	3.035	2.205
2.0	3.149^{-1}	2.877	2.991	2.072
2.2	3.508^{-1}	2.951	2.932	1.945
2.4	3.874^{-1}	3.008	2.864	1.827
2.6	4.248^{-1}	3.050	2.789	1.718
2.8	4.630^{-1}	3.079	2.711	1.618
3.0	5.021^{-1}	3.098	2.632	1.527
3.5	6.031^{-1}	3.108[c]	2.436	1.334
4.0	7.090^{-1}	3.079	2.250	1.181
4.5	8.194^{-1}	3.027	2.080	1.057
5	9.340^{-1}	2.959	1.925	9.551^{-1}
6	1.174	2.801	1.661	7.935^{-1}
7	1.427	2.632	1.449	6.866^{-1}
8	1.686	2.463	1.278	6.013^{-1}
9	1.947	2.300	1.140	5.346^{-1}
10	2.206	2.145	1.027	4.812^{-1}
20	3.746[c]	1.143	5.107^{-1}	2.406^{-1}
30	3.000	7.582^{-1}	3.400^{-1}	1.604^{-1}
40	2.255	5.676^{-1}	2.549^{-1}	1.203^{-1}
50	1.802	4.537^{-1}	2.039^{-1}	9.623^{-2}
α_0	1.391^{-1}	3.967	7.909	6.684
α_∞	9.004^{-1}	2.268^{-1}	1.019^{-1}	4.811^{-2}

[a]N_L is Loschmidt's number (2.69×10^{19} cm^{-3}), the number density at STP.
[b]The exponent denotes the power of 10 by which the entry is to be multiplied.
[c]Indicates peak value.

gases M ≡ He – Xe as a function of the buffer-gas density N (in units of Loschmidt's number $N_L = 2.69\times10^{19}$ cm^{-3}). As we see, the lighter gases Ne and Ar yield the highest $\alpha \approx 3\times10^{-6}$ $cm^3\,sec^{-1}$ for gas pressures of 1–5 atm, while α for He, the lightest gas, rises with N only relatively slowly to peak at 20 atm. This difference essentially arises from the much larger mobilities K^* for Kr^+ and F^- in He than in the remaining gases (cf. Table I). At low gas densities α is proportional[2] to the

TABLE III. Three-body recombination rates α (10^{-6} $cm^3\,sec^{-1}$) for the processes $Kr_2^+ + F^- + Rg \rightarrow [Kr_2F]^* + RG$ (Rg ≡ He, Ne, Ar, Xe), for various gas densities N at 300 K. The square brackets denote that the molecular Kr_2F^* may not remain bound. Low- and high-density limits are $\alpha_0(N/N_L)$ and $\alpha_\infty(N_L/N)$, respectively.

N/N_L[a]	He	Ne	Ar	Xe
0.1	1.675^{-2}[b]	3.755^{-1}	5.403^{-1}	2.795^{-1}
0.2	3.362^{-2}	6.890^{-1}	9.564^{-1}	5.408^{-1}
0.4	6.770^{-2}	1.190	1.566	1.020
0.6	1.023^{-1}	1.577	1.984	1.423
0.8	1.374^{-1}	1.884	2.268	1.727
1.0	1.731^{-1}	2.131	2.455	1.922
1.2	2.093^{-1}	2.331	2.568	2.021
1.4	2.461^{-1}	2.491	2.627	2.045[c]
1.6	2.836^{-1}	2.620	2.648[c]	2.017
1.8	3.216^{-1}	2.722	2.640	1.956
2.0	3.602^{-1}	2.800	2.612	1.877
2.2	3.994^{-1}	2.859	2.572	1.789
2.4	4.392^{-1}	2.902	2.522	1.699
2.6	4.796^{-1}	2.931	2.468	1.610
2.8	5.206^{-1}	2.948	2.411	1.525
3.0	5.621^{-1}	2.956[c]	2.353	1.445
3.5	6.682^{-1}	2.942	2.210	1.268
4.0	7.774^{-1}	2.895	2.073	1.122
4.5	8.893^{-1}	2.829	1.943	1.003
5	1.003	2.752	1.818	9.051^{-1}
6	1.236	2.587	1.562	7.552^{-1}
7	1.472	2.425	1.375	6.471^{-1}
8	1.705	2.278	1.205	5.659^{-1}
9	1.931	2.146	1.069	5.029^{-1}
10	2.148	2.027	9.596^{-1}	4.524^{-1}
20	3.622[c]	1.120	4.749^{-1}	2.261^{-1}
30	2.736	7.421^{-1}	3.162^{-1}	1.507^{-1}
40	2.043	5.553^{-1}	2.371^{-1}	1.130^{-1}
50	1.632	4.439^{-1}	1.896^{-1}	9.043^{-2}
α_0	1.670^{-1}	4.145	6.277	2.928
α_∞	8.152^{-1}	2.219^{-1}	9.481	4.522

[a]N_L is Loschmidt's number (2.69×10^{19} cm^{-3}), the number density of STP.
[b]The exponent denotes the power of 10 by which the entry is to be multiplied.
[c]Indicates peak value.

sum of the inverses of the ionic mean free paths λ^{-1} (and hence mobilities), while at high gas densities, a different (Langevin) mechanism for recombination yields[2]

$$\alpha \rightarrow \alpha_L = 4\pi e(K^+ + K^-). \tag{6}$$

Thus, at high N, α, in Figs. 1 and 2, decreases systematically as the buffer gas is varied from He → Xe, while at the low $N < N_L$, the combined effect of (decreasing) mobilities and of various (increasing) mass-ratio factors[4] yields little variation in α for all cases, except He. In conclusion, Ne and Ar are to be preferred for buffer gases at pressures of 1–5 atm, while for pressures ≥ 10 atm, He tends to be more efficient for excited-state production. Also, the molecular ions Kr_2^+ in general recombine less fast than the atomic ions Kr^+, as expected although the difference is not too significant.

The ion-ion recombination process populates the ionic excited states with near unit yield[7-10] for the efficient rare-gas halide laser systems. So that the rates α be available as data[11] for kinetic modeling of the KrF laser at high pressures, representative values are presented in Tables II and III, together with the associated limits at low and high gas densities.

[1]For extensive coverage of references see J. J. Ewing, Phys. Today 31, 32 (1978); C. A. Brau, in *Excimer Lasers*, edited by C. K. Rhodes (Springer, Berlin, to be published).
[2]M. R. Flannery and T. P. Yang, Appl. Phys. Lett. 32, 327 (1978).
[3]M. R. Flannery and T. P. Yang, Appl. Phys. Lett 32, 356 (1978)
[4]M. R. Flannery, Chem. Phys. Lett. 56, 143 (1978).
[5]C. L. Chen, Phys. Rev. 131, 2550 (1963).
[6]K. B. McAfee, D. Sipler, and D. Edleson, Phys. Rev. 160, 130 (1967).
[7]H. W. Ellis, R. Y. Pai, E. W. McDaniel, E. A. Mason, and L. A. Viehland, At. Data Nucl. Data Tables 17, 177 (1976).
[8]I. Dotan, D. L. Albritton, and F. C. Fehsenfeld, J. Chem. Phys. 66, 2232 (1977).
[9]I. Dotan and D. L. Albritton, J. Chem. Phys. 66, 5238 (1977).
[10]M. Rokni, J. H. Jacob, and J. A. Mangano, Phys. Rev. A 16, 2216 (1977).
[11]E. W. McDaniel, M. R. Flannery, H. W. Ellis, F. L. Eisele, W. Pope, and T. G. Roberts, in U.S. Army Missile Research and Development Command High Energy Laser Laboratory Technical Report H-78-1, 1978, Vols. 1 and 2 (unpublished).

REFERENCES

Bates, D. R.

1975, J. Phys., B8, 2722

1950, Phy. Rev., 77, 718 (B2)

Bates, D. R. and Flannery, M. R.

1968, Proc. Roy.Soc. (London), A302, 367 (BF1)

1969, J. Phys. B (Proc. Roy. Soc.) (2), 1, 1145

Bates, D. R. and Massey, H. S. W.

1943, Phil. Trans. Roy. Soc.(London), A239, 269

Bates,D. R. and McKibbin, C. S.

1973, J. Phys., B6, 2485

1974, Proc. Roy. Soc. (London), A339, 13

Bates, D. R. and Mendas, I.

1978, Proc. Roy. Soc. (London), A359, 287

Bates, D. R. and Moffett, R. J.

1966, Proc. Roy. Soc. (London), A281, 1

Beaty, E. C. and Patterson, P. L.

1965, Phy. Rev., 137, 346

Bekefi, G. (e.d.) (BE1)

1976, Principle of Laser Plasmas,

Wiley Interscience, N. Y.

Biondi, M. and Chanin, L. M. (BIC)

1954, Phy. Rev., 94, 910

Bohme, D. K., Dunkin, D. B., Fehsenfeld, F. C. and Ferguson, E. E.

1969, J. Chem. Phys., 51, 863

Braw, C. A. and Ewing, J. J.

1975, App. Phys. Lett., 27, 435

Chen, C. L. (CH)

1963, Phy. Rev., 131,2550

Cooper, J.

1966, Rept. of Prog. In Phys. Vol. 29, Part 1, 35

Dargano, A. (DA)

1958, Phil. Tras. Roy. Soc. (London), A250, 426

Dotan, I., Albriton, D. L. and Fehsenfeld, F. C.

1977, J. Chem. Phys., 66, 2232 (DAF1)

1977, J. Chem. Phys., 66, 5238 (DAF2)

Ellis, H. W., Pai, R. Y., McDaniel, E. W., Mason, E. A. and Viehland, L. A. (EL)

1976, At. Data & Nucl. Data, Table 17,177

Ewing, J. J., 1978, Phy. Today, May, 32 (EW)

Flannery, M. R.,

1972, Case Studies in Atomic Collisions, Vol 2, Chap .1, eds., McDaniel, E.W. and McDowell, M.R.C. (N.Holland, Amsterdam) (FM1)

1976, Atomic Processes and Applications, Chap. 12 eds., Burke, P.G. and Moiserwitsch, B.L. (N. Holland, Amsterdam) (FM2)

1978, Chem. Phy. Lett. 56, 143 (FM3)

Fowler, R. H.

1936, Statistical Mechanics 2nd ed p.161 (London, Cambridge Univ. Press)

Ganer, J. P. and Chanin, L. M.

1969, Phy. Rev. 182, 167

Goldstein, H.

1950, Classical Mechanics, Chap 3, Addison-Wesley

Harper, W. R.

1932 Proc. Camb. Phil. Soc. 28, 219

1935 Proc. Camb. Phil. Soc. 31, 429

Jeffé G.

1940, Phy. Rev. 176, 141

Landau, L. D. and Lifshitz, E. M.

1960, Mechanics, Chap IV

Langevin, P., (LA)

1903, Ann. de Chin. et de Phy., 28, 433

Loeb, L. B.

1955, Basic Processes of Gaseous Electronics

(U. of Calif. Press, Berkerly, L.A., 2nd ed.)

Lorents, D. C.

1976, Physica, 82C, 19

1977, Xth ICAC (Paris)

Mächler, W.

1936, Z. Phy. 104, 1

McAfee, K. B. Sipler, D. and Edleson, D.

1967, Phy. Rev. 160, 130 (MCSE)

McDaniel, E. W.

1964, Collisional Phenomena in Ionized Gases,

Wiley & Sons Inc., N. Y.

McDaniel, E. W. and Mason, E. A.

1973, The Mobility and Diffusion of Ions in Gases,

Wiley Interscience, N. Y. (MM)

Natanson, G. L.

1959, Soviet Phy.-Tech. Phy. 4, 1263

Stickley, C. M.

1978, Phy. Today, May, 50

Thomson, J. J.

1924, Phil. Mag., 47, 337

Wadehra, J. M. and Bardsley, J. N.

1978, App. Phy. Lett. 32, 76

Werner, C. W. and George, E. V.

1976, Chap 10 of Laser Plasmas (BE1)

VITA

Ting-Pin Yang was born on May 12, 1943, in Tainan Taiwan, R.O.C.. He is the fifth son of Dr. and Mrs. Liu-Ho Yang.

From 1961 to 1965 he attended National Taiwan University in Taipei and got his B.S. in physics. He then went to study in National Tsing-Hua University and got his M.S. in physics in 1967.

After one year of stay in the same university as a research assistant for the equivalent military service, he came to this country. He spent several years in C.C.N.Y. of N. Y. C. where he got married with the former Jo-Lien Hwang. In 1976 he came to Georgia Tech. to finish up his career of graduate study.

He likes classical music and is a member of the American Physical Society.